

**International  
Progress Report**

**IPR-03-35**

# **Äspö Hard Rock Laboratory**

## **Update of the hydrogeological model 2002**

Patrik Vidstrand  
Bergab

December 2003

**Svensk Kärnbränslehantering AB**

Swedish Nuclear Fuel  
and Waste Management Co  
Box 5864  
SE-102 40 Stockholm Sweden  
Tel 08-459 84 00  
+46 8 459 84 00  
Fax 08-661 57 19  
+46 8 661 57 19



**Äspö Hard Rock  
Laboratory**



Report no.	No.
IPR-03-35	F117K
Author	Date
Patrik Vidstrand	Dec.2003
Checked by	Date
Rolf Christiansson	2005-03-10
Approved	Date
Christer Svemar	2005-03-30

# Äspö Hard Rock Laboratory

## Update of the hydrogeological model 2002

Patrik Vidstrand  
Bergab

December 2003

*Keywords:* Äspö descriptive model, GeoMod, Hydrogeology, Characterisation, Hydraulic conductors, Groundwater flow model

This report concerns a study which was conducted for SKB. The conclusions and viewpoints presented in the report are those of the author(s) and do not necessarily coincide with those of the client.





# Preface

The main purpose of the GeoMod project, which initiated in the beginning of 2002, was to update the previous geoscientific model of Äspö (Äspö96), mainly by incorporating additional data collected after 1995. The updated model (Äspö02) was meant to, as far as possible, be integrated in a three dimensional digital model and to be documented in a single technical report.

The geoscientific disciplines: geology, rock mechanics, hydrogeology and hydrogeochemistry, were supposed to be integrated into a common understanding of the site. However it became obvious, during the spring 2003, that the necessary integration efforts far exceeded the expected. As a result of this, the GeoMod project was temporarily terminated in May 2003.

The result obtained within hydrogeology, when the project was terminated, is presented in this report. The other progress reports are:

- IPR-03-34  
Äspö Hard Rock Laboratory  
Update of the geological model 2002
- IPR-03-36  
Äspö Hard Rock Laboratory  
Update of the hydrogeochemical model 2002
- IPR-03-37  
Äspö Hard Rock Laboratory  
Update of the rock mechanical model 2002

Recommendations of further work are presented in the reports.

The helpful comments, suggestions and reviewing from Johan Andersson, Mel Cascoyne, Richard Everitt, John A Hudson, Bill Lanyon and Anders Winberg are acknowledged. The support and help from: Mansueto Morosini, Tommy Olsson and Roger Taringer are acknowledged.

Rolf Christiansson



# Abstract

The GeoMod project was aiming at updating the existing model by integrating new data collected since 1995. The major part of the new data has been produced in the lower part of the Äspö tunnel spiral. The updated model is contained in a 1 km<sup>3</sup> cube with focus on a volume including the tunnel spiral volume from about 200 to 500 metres. Before the integration of the models was completed the GeoMod project was temporarily terminated in May 2003.

As part of an integrated descriptive model the hydrogeological 3D site descriptive model was established. This progress report presents the information gathered concerning hydrogeology.

The Äspö02 model does in many parts differ significantly from the Äspö96 model. Unfortunately many of the indications that support these differences have not been possible to validate due to project limitations. However, the indications are strong and also the suggested changes are complex developments of the conceptual model compared to the Äspö96 model.

Much of the primary data is stored in the database SICADA. SICADA contains data on transmissivity, storage, yield, etc.; however nothing on how the data earlier has been interpreted. Further it has been observed that even though the treatment and sorting of primary data were performed in the same way for Äspö02 as for Äspö96, the results turn out different. The reason/reasons for this discrepancy is hard to specify. However, the most likely reason is that all data has not been stored in SICADA. Also the treatment of truncation limits and similar statistical problems are not well documented in the different reports.

Additional problems in site descriptions come from the scale dependent definitions of a structure. For a larger scale model such as Äspö02 a deterministic structure is of the scale of tens to hundreds of metres, while a smaller scale model such as one corresponding to the size of an experimental site, defines structures of the scale metres to tens of metres.

Further, the older conceptual model, Äspö96, is presented with hydrostatic boundary conditions under the Baltic Sea. However, there are now at least some indications that a hydrostatic boundary condition, caused by the presence of the Baltic Sea, is not a realistic assumption. Also the NNW trending drawdown behaviour was in the Äspö96 model interpreted as the results of deterministic NNW hydraulic conductors crossing over the tunnel spiral. In Äspö02 these structures are recognised along local tunnel sections within the spiral as clusters of hydraulic fractures. However, the extension and also the direction of the individual fractures within these clusters could not be vindicated as belonging to NNW hydraulic conductors but are instead viewed as a part of the dominant hydraulic NW fracture set. This fracture set may be interconnected by either splays within the set or by a less dominant fracture set trending NE. Either way the NW trending fracture set, together with inter-connective structures would create drawdown behaviour much like the one recognised in both the Äspö96 model, as well as in the new Äspö02 model.

The treatment of these conceptual uncertainties introduces uncertainty in prognoses of both flow and concentrations as well as in many other areas of interest. This is clearly illustrated by the importance of deterministic structures in the flow descriptions that are results from individual numerical groundwater flow models. If these kinds of models are used for predictions of e.g. hydraulic pressures at an unknown location in the bedrock; it is crucial to the results if this region of the bedrock coincides with a deterministic structure or not.

# Sammanfattning

GeoMod projektets syfte var att uppdatera den existerande modellen genom att integrera data som tagits fram efter 1995. Huvuddelen ny data kommer från den nedre tunnelspiralen från Äspö HRL. Den uppdaterade modellen begränsas av en 1 km<sup>3</sup> stor kub med fokus på en volym som inkluderar tunnelspiralen, ungefär -200 till -500 meter. Innan projektet var avslutat avbröts det tillsvidare i maj 2003.

Som en initial del i det integrerade arbetet upprättades en hydrogeologisk 3D platsbeskrivande modell. Denna rapport presenterar den information som insamlats inom ämnesområdet hydrogeologi.

Äspö02 modellen skiljer sig i flera punkter från den äldre Äspö96 modellen. Tyvärr har många av de hydrologiska indikationerna inte kunnat valideras på grund av projektets begränsningar och att projektet ej slutförts enligt de ursprungliga planerna. De hydrologiska indikationerna är signifikanta och dessutom oftast utvecklingar av de konceptuella modellerna som funnits tidigare.

Den stora datavolymen är lagrad i SICADA. SICADA innehåller data om transmissivitet, magasinskoefficienter, specifikt flöde mm. Emellertid kan man inte få information om hur data är utvärderad och vilka antaganden som gjorts. Det har dessutom observerats att trots likvärdig behandling av data nås ej samma resultat. Orsaken till detta är inte möjlig att fastställa men kan bero på att all data inte har lagrats i SICADA. Dessutom kan mätgränsvärden och andra statistiska trunkeringar påverka resultaten, behandling av dessa faktorer är inte tydligt beskriven i befintliga rapporter.

Ytterligare problem för platsbeskrivning uppstår på grund av storleksberoende definitioner. I en stor modell såsom Äspö02 är en deterministisk geologisk struktur i storleksintervallet tiotals till hundratals meter; emedan en lokal experimentplats kan beskrivas av deterministiska strukturer i skalan meter till tiotals meter.

I den äldre modellen, Äspö96, antogs att Östersjön kunde betraktas som en hydrostatisk rand. Nu finns emellertid information som indikerar att ett sådant antagande inte är realistiskt. Dessutom antogs NNV-avsänkningen bero på ett fåtal deterministiska hydrauliska strukturer som skär tvärs igenom tunnelspiralen. I den nya Äspö02 modellen är dessa strukturer inte längre att betrakta som deterministiska utan beskrivs som ett kluster av vattenförande sprickor med obekant utsträckning. Dessa sprickor har i huvudsak en strykning åt NV och binds troligen ihop av NÖ sprickor för att på så sätt ge upphov till den aktuella avsänkningen.

Hur man väljer att behandla dessa konceptuella osäkerheter introducerar prognososäkerheter vad avser bl.a. flöde och koncentrationer m.fl. Denna prognososäkerhet illustreras tydligt av flödesdominansen längs deterministiska strukturer. Därmed är det av stor vikt att man gör en korrekt bedömning huruvida en bergvolym som skall prognostiseras tillhör en struktur eller inte.



# Contents

<b>1</b>	<b>Introduction</b>	<b>13</b>
1.1	The GeoMod project	14
1.1.1	Objectives	14
1.1.2	GeoMod related reports	15
1.1.3	Reviewing	15
<b>2</b>	<b>Site location and overview of existing data</b>	<b>17</b>
2.1	Overview	17
2.2	Coordinate system	18
2.3	Geoscientific investigations and experiments	19
2.3.1	The data used in the modelling	20
2.3.2	Experiments in Äspö HRL	20
<b>3</b>	<b>Previous hydrogeological models over Äspö</b>	<b>21</b>
<b>4</b>	<b>Evaluation of primary data – surface hydrogeology</b>	<b>23</b>
4.1	Baltic Sea	23
4.1.1	Sea level	23
4.1.2	Salinity	23
4.1.3	Shore level elevation	23
4.2	Hydrological setting of Äspö	25
4.2.1	General boundary conditions	25
4.2.2	Temperature	25
4.2.3	Precipitation	25
4.2.4	Evapotranspiration	29
4.3	Quaternary deposits	31
4.4	Water table and piezometric levels	31
4.5	Groundwater recharge	35
<b>5</b>	<b>Evaluation of primary data – hydraulic interpretation</b>	<b>37</b>
5.1	Available data and test designs	37
5.2	Hydraulic properties	38
5.2.1	Transmissivity of hydraulic conductors	38
5.2.2	Hydraulic conductivity of the rock mass	39
5.2.3	Storage coefficient (storativity) of the hydraulic conductors and of the rock mass	47
5.2.4	Specific storage of the hydraulic rock domains	48
5.3	Tunnel water inflows	50
5.4	Hydraulic fracture statistics	53
5.4.1	Hydraulic feature intensity	53
5.4.2	Fracture transmissivity	55

<b>6</b>	<b>Three-dimensional site descriptive hydrogeological modelling</b>	<b>57</b>
6.1	General modelling assumptions	57
6.2	Modelling strategy	58
	6.2.1 Rock	58
	6.2.2 Quaternary deposits	59
6.3	Definition of HCDs and HRDs based on primary data and the geological 3D site descriptive model	59
	6.3.1 Hydraulic Conductor Domains	59
	6.3.2 Hydraulic Rock Domains	62
	6.3.3 Correlation with geological characteristics	64
	6.3.4 Hydraulic connectivity pattern	64
	6.3.5 Hydraulic Soil Domains	65
6.4	Hydrogeological simulation approach	65
6.5	Numerical code	66
6.6	Numerical modelling approach	66
	6.6.1 Hydraulic conductivity domains (HCD)	67
	6.6.2 Hydraulic conductivity domains HRD	68
	6.6.3 Boundary conditions	69
	6.6.4 Results	71
	6.6.5 Uncertainties	73
<b>7</b>	<b>The Äspö HRL site hydrogeological descriptive model results</b>	<b>77</b>
7.1	Hydraulic Conductor Domains (HCD)	77
7.2	Hydraulic Rock Domains (HRD)	77
	7.2.1 SC description of HRD	77
	7.2.2 DFN approach for HRD description	78
7.3	Hydraulic Soil Domains (HSD)	79
7.4	Boundary Conditions	79
	7.4.1 Air temperatures and precipitation	79
	7.4.2 Drainage basins	79
	7.4.3 Recharge and discharge	79
	7.4.4 Water table	80
	7.4.5 Baltic Sea level variation and salinity	81
	7.4.6 Vertical boundaries	81
	7.4.7 Bottom boundary	81
	7.4.8 Tidal effects	81
7.5	Groundwater flow pattern according to numerical simulations	82
<b>8</b>	<b>Concluding remarks and overall assessment of uncertainties in the hydrogeological description</b>	<b>83</b>
8.1	Uncertainties in the primary data	83
8.2	Uncertainties due to scale dependant descriptions	84
8.3	Over-all dependence in the result on conceptual boundary conditions	84
8.4	Over-all dependence in results on conceptual deterministic structures	85
<b>9</b>	<b>References</b>	<b>87</b>
	<b>Appendices</b>	<b>91</b>



# Foreword and acknowledgement

The first two chapters are based on draft versions of introduction chapters by Tommy Olsson, partly edited by Roger Taringer.

The intension of the author has been to fit this report into the frame developed in a site descriptive methodology report /Andersson et al. 2002a/. This intension has not at all times been easily conducted nor has the report an optimal structure. This mainly due to the fact that the GeoMod project aims at reviewing and compiling previously reported material and does as such a project not follow the typical paths of an on-going site investigation.

It should be stressed that the report does not report on any new numerical groundwater modelling however, a major effort has been put into a critical review of the older numerical model results. Substantial parts of this critical review have been done by Sven Follin and reported to the author.

The author acknowledges:

- the work done by Mansueto Morosini, Tommy Olsson, and Ioanna Gurban as partners within the hydrogeological working group.
- The work done by project partners, Rolf Christiansson, Marcus Laaksoharju, Hussein Hakami, Johan Berglund, Philip Curtis and Roger Taringer.
- Helpful comments and explanations by Ingvar Rhén, Anders Winberg, Urban Svensson, and Thomas Eliasson.
- And not least the reviewing and supporting work by Bengt Åhlén, Bill Lanyon and Sven Follin.



# 1 Introduction

The Swedish Nuclear Fuel and Waste Management Company (SKB) established the Äspö Hard Rock Laboratory in late 1980th in order serve as a test area for SKB's work to design and construct a deep geological repository for spent fuel and to develop and test methods for characterization of selected repository site.

The role of the Äspö Hard Rock Laboratory is to provide input to the performance assessments that have to be supplied as part of each license application and to develop, test, and evaluate methods for site investigations, detailed investigations, repository construction as well as disposal and backfilling of tunnels before they are applied within the deep repository programme. The work with the Äspö HRL has been divided into three phases: the Pre-investigation phase, the construction phase, and the operating phase.

During the Pre-investigation phase, 1986–1990, studies were made to provide background material for the decision to locate the laboratory to a suitable site. The natural conditions of the bedrock were described and predictions made of geological, hydrogeological, geochemical etc. conditions to be observed during excavation of the laboratory. This phase also included planning for the construction and operating phases.

During the Construction phase, 1990–1995, comprehensive investigations and experiments were performed in parallel with construction of the laboratory. The excavation of the main access tunnel to a depth of 450 m and the construction of the Äspö Research Village were completed. Excavation started on October 1st, 1990 after approval had been obtained from the authorities concerned, and was completed in February 1995.

At the end of the construction stage, the different models used during the site characterization were compiled and evaluated as a first attempt to establish a multidisciplinary site descriptive model, where the results were published in a series of technical reports:

- Stanfors, R, Erlström, M, Markström I. Äspö HRL – Geoscientific evaluation 1997/1. Overview of site characterization 1986 – 1995. SKB TR 97-02.
- Rhen, I (ed), Bäckblom G., Gustafson, G, Stanfors, R, Wikberg, P. Äspö HRL – Geoscientific evaluation 1997/2. Results from pre-investigations and detailed site characterization. Summary Report. SKB TR 97-03.
- Stanfors, R, Olsson, P, Stille, H. Äspö HRL – Geoscientific evaluation 1997/3. Results from pre-investigations and detailed site characterization. Comparison of predictions and observations. Geology and Mechanical stability. SKB TR 97-04.
- Rhen, I, Gustafson, G, Wikberg, P. Äspö HRL – Geoscientific evaluation 1997/2. Results from pre-investigations and detailed site characterization. Comparison of predictions and observations. Hydrogeology, Groundwater chemistry and Transport of solutes. SKB TR 97-04.

- Rhen, I (ed), Gustafson, G, Stanfors, R, Wikberg, P. Äspö HRL – Geoscientific evaluation 1997/2. Models based on site characterization 1986 – 1995. SKB TR 97-05.
- Almén K-E (ed), Olsson P, Rhen I, Stanfors R, Wikberg P. Äspö Hard Rock Laboratory. Feasibility and usefulness of site investigation methods. Experience from the pre-investigation phase. SKB TR 94-24.

The Operating phase began in 1995. A preliminary outline of the programme for the Operating phase was given in SKB's Research, Development and Demonstration (RD&D) Program 1992. Since then the programme has been revised and the basis for the current programme is described in SKB's RD&D Program 1998.

During the operating stage a number of different experiments and studies have been executed in Äspö HRL, which provides additional information compared to the experience obtained and presented in the previous reports. In order to update the geoscientific models, SKB initiated the project GeoMod to compile the results from the operating period 1995-2002.

## **1.1 The GeoMod project**

### **1.1.1 Objectives**

The GeoMod project was aiming at updating the existing model by integrating new data collected since 1995. The major part of the new data has been produced in the lower part of the Äspö tunnel spiral. The updated model is contained in a 1 km<sup>3</sup> cube with focus on a volume including the tunnel spiral volume from about 200 to 500 metres depth.

The specific objectives in the GeoMod project were to:

- Describe the geoscientific properties of a prescribed rock volume containing the tunnel spiral.
- Identify relevant processes to explain the geoscientific properties.
- Define the boundary conditions of importance to the rock volume processes.
- Develop methodology to integrate the knowledge from the different geoscientific disciplines.
- Develop a coherent integrated geoscientific model of Äspö.

The project started January 2002. Before the integration of the models finished the GeoMod project was temporarily terminated in May 2003. Finally, SKB decided to reduce the content of the project by omitting the fully integration between the different geoscientific disciplines. It was decided that the work with the completed integration was postponed until 2005.

As a consequence, the different geoscientific models; i.e. the geological, hydrogeological, rock mechanics and hydrogeochemical, are published in four separate reports, one for each discipline.

The objectives of this report are to present the result within hydrogeology.

### 1.1.2 GeoMod related reports

This report presents the updating of the hydrogeological part of the GeoMod project.

Three other reports are produced with in GeoMod:

- IPR-03-34  
Äspö Hard Rock Laboratory  
Update of the geological model 2002  
Johan Berglund, Philip Curtis, Thomas Eliasson, Tommy Ohlsson, Peter Starzec, Eva-Lena Tullborg  
December 2003
- IPR-03-36  
Äspö Hard Rock Laboratory  
Update of the hydrogeochemical model 2002  
Marcus Laaksoharju, Ioana Gurban  
December 2003
- IPR-03-37  
Äspö Hard Rock Laboratory  
Update of the rock mechanical model 2002  
Hossein Hakami  
December 2003

### 1.1.3 Reviewing

Although, a complete integration between the disciplines have not been accomplished in the current version of the geoscientific modelling, the relation and interaction between the disciplines have been addressed with respect to the scientific content. The Scientific Content Issues are:

- Is the scientific content complete, given the objectives and current level of the work?
- Is the science clearly explained?
- Is the model adequate, given the current state of play?
- Is it clear how updating can be accomplished?
- Is the presented information traceable?
- Are the conclusions justified and adequate?
- Confidence in the model and robustness

The evaluation and it's robustness for the different disciplines have been in focus and the statements put forward in the individual reports are not contradictive unless this is clearly stated.



## 2 Site location and overview of existing data

### 2.1 Overview

The Äspö HRL is located on the Äspö Island which is located near to the Simpevarp nuclear site. A great number of investigations have been made both on Äspö and in adjacent areas, such as Laxemar and Ävrö, c.f. Figure 2-1.

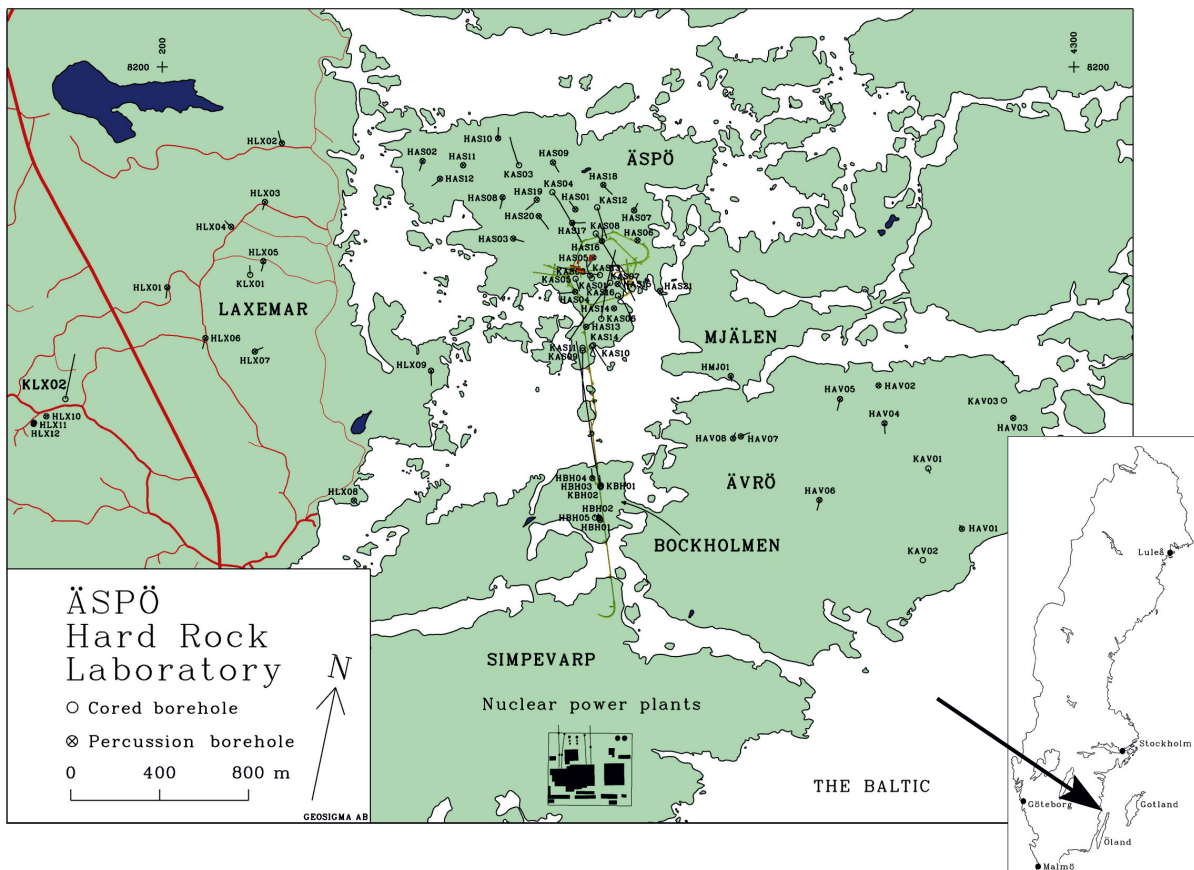


**Figure 2-1.** Overview of the Äspö Island and the adjacent areas. The selected model domain is shown in Figure 2-2.

The GeoMod-project will update the existing model by integrating new data collected since 1995. Most new data have been collected during the operational phase for different experiments conducted in the tunnel. The majority of the new information originates from the experimental sites in the lower part of the Äspö HRL. The updated model will focus on a volume including the tunnel spiral (c.f. Figure 2-2.).

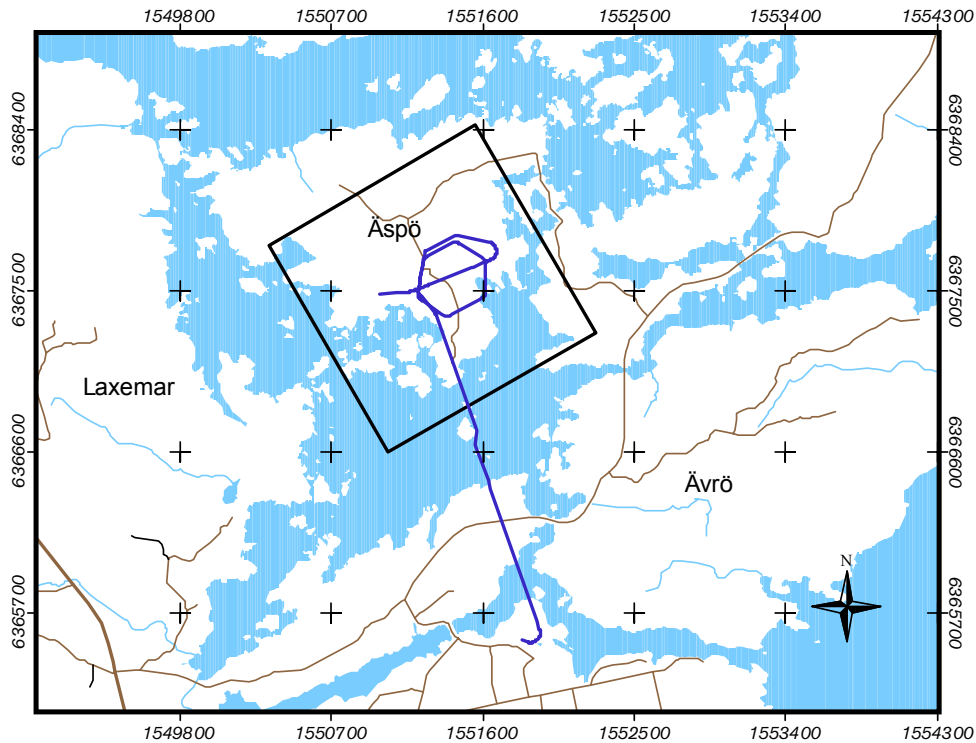


**Figure 2-2.** Map showing the GeoMod model area along with the horizontal projection of the Äspö tunnel (RT90 coordinate system).

## 2.2 Coordinate system

The corner coordinates of the model volume are defined by a virtual cube with the corner coordinates presented in Table 2-1.

**Table 2-1. Model volume coordinates.**

Äspö 1km Cube Coordinates			
RT90-RHB70			
	Easting	Northing	Elevation
	[m]	[m]	[mamsl]
Top square			
1	1551200.046	6367099.181	50
2	1550700.046	6367965.206	50
3	1551566.071	6368465.206	50
4	1552066.071	6367599.181	50
Bottom square			
5	1551200.046	6367099.181	-1000
6	1550700.046	6367965.206	-1000
7	1551566.071	6368465.206	-1000
8	1552066.071	6367599.181	-1000

The modelling is contained within a common virtual cube with 1 km side length extending from +50 m to -1000 mamsl (meter above mean sea level) in elevation to which appropriate boundary conditions have to be set. This volume is to be tied to its regional context based on the previous model, Äspö96.



## 2.3 Geoscientific investigations and experiments

The underground part of the laboratory consists of a tunnel from the Simpevarp peninsula to the southern part of Äspö where the tunnel continues in a spiral down to a depth of 450 m (Figure 2-3). The total length of the tunnel is 3600 m where approximately 400 m at the end have been excavated by a tunnel boring machine (TBM) with a diameter of 5 m. The first part of the tunnel has been excavated by conventional drill and blast technique. The underground tunnel is connected to the ground surface through a hoist shaft and two ventilation shafts. Äspö Research Village is located at the surface on the Äspö Island and it comprises office facilities, storage facilities, and machinery for hoist and ventilation (Figure 2-3).

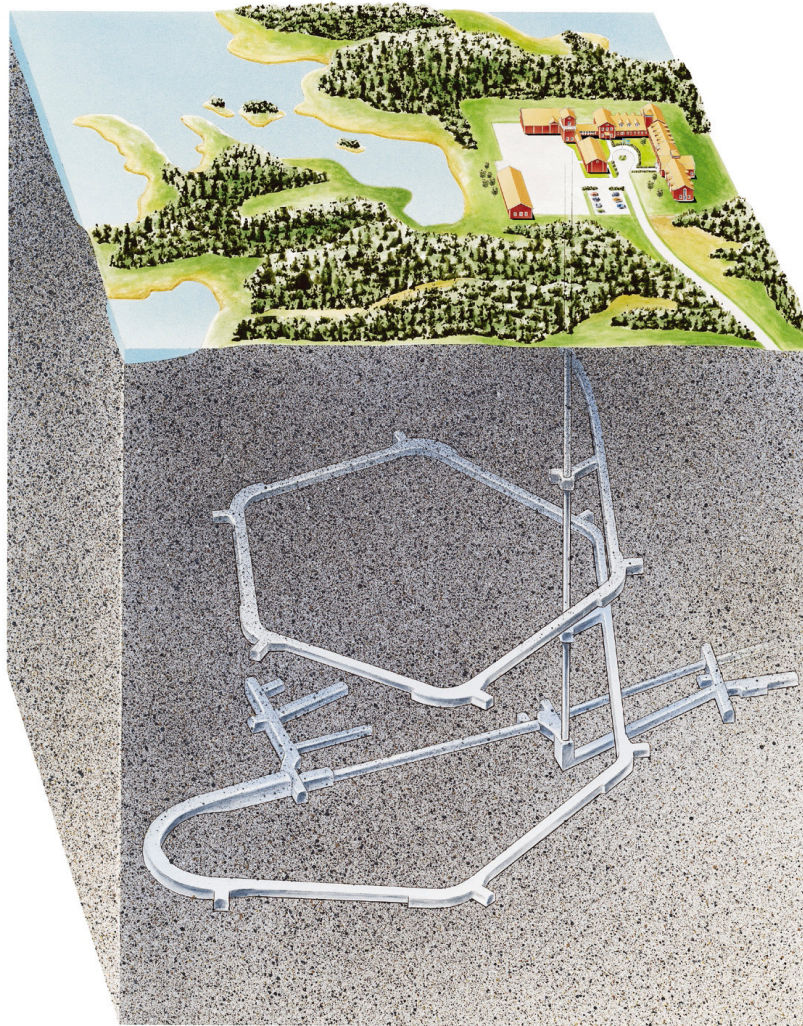


*Figure 2-3. Overview of the Äspö Hard Rock Laboratory Facilities within GeoMod's virtual volume.*

### **2.3.1 The data used in the modelling**

All data used for the modelling where quality assured data, received from SKB:s databases Site Characterisation Data base (SICADA) and Hydro Monitoring System (HMS). The databases contain all tests, sampling and analyses obtained from percussion and core drilled boreholes at surface or in the underground experimental areas of Äspö HRL.

### **2.3.2 Experiments in Äspö HRL**

A great number of experiments have been executed in Äspö HRL since the start of the operating phase. Examples of experiments where relevant data was collected are, REX, TRUE, TRUE BS, HQ, ZEDEX, JADE, MICROBE, COLLOID, PROTOTYPE REPOSITORY, and MATRIX.

### 3 Previous hydrogeological models over Äspö

The results from modelling of the borehole and surface measurements have been reported in numerous reports and scientific papers. For the operational stage of the Äspö HRL the Äspö96 model was constructed /Rhén et al., 1997b/. Interested readers are referred to this reference.

Below the Äspö96 model over deterministic hydraulic conductors is presented as being a valuable comparison with the new model presented herein.

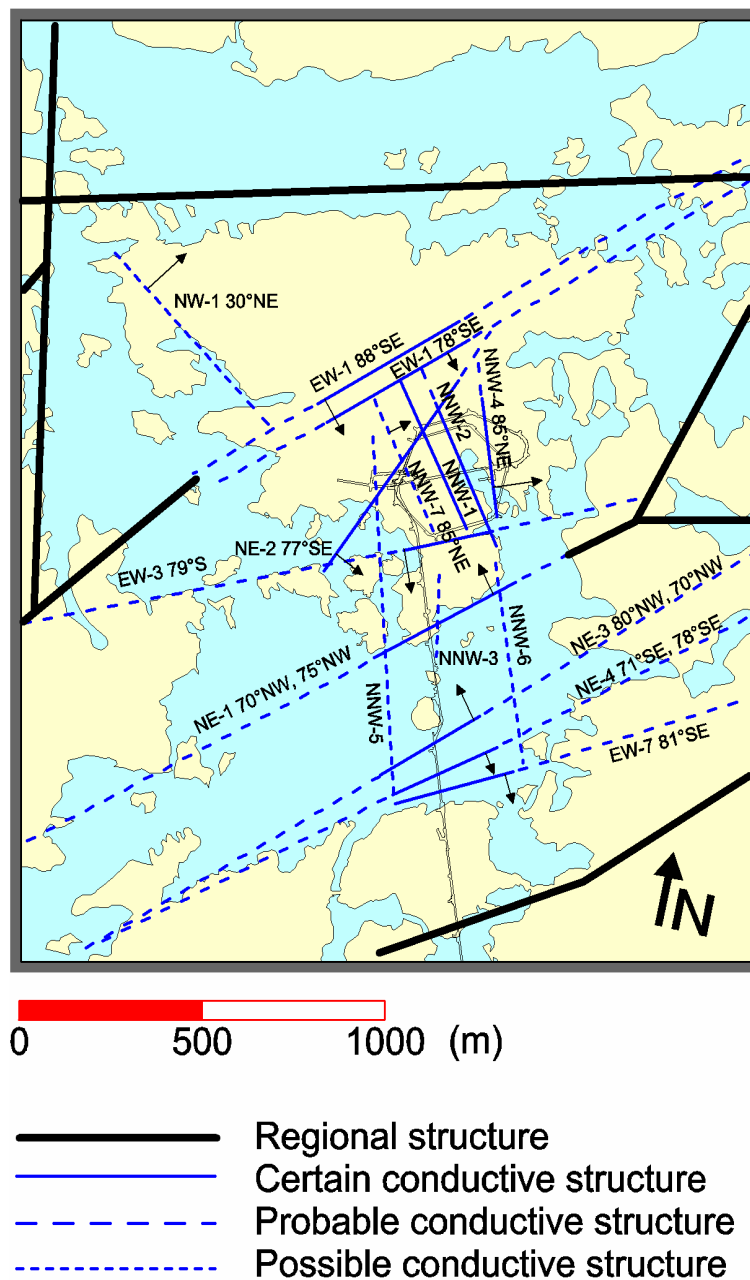


*Figure 3-1 Model of hydraulic conductors on the site scale /Rhén et al., 1997b/.*



## **4 Evaluation of primary data – surface hydrogeology**

This section summaries the main elements of the Äspö characteristics, which may be used as top surface boundary conditions in the Äspö02 Model domain. Information herein is mainly based on the below stated references but also presents additional comments and figures concerning the Äspö02 Model domain. Descriptions of the hydrology, meteorology, and oceanography in the municipally of Oskarshamn, with a focus on the coastal vicinity of Simpevarp peninsula and Äspö, are found in /Graffner, 2003/, /Andersson et al., 2002a/, /Larsson-McCann et al., 2002/, /Follin et al., 1998/, and /Rhén et al., 1997a/.

### **4.1 Baltic Sea**

#### **4.1.1 Sea level**

The Swedish Meteorological and Hydrological Institute (SMHI) records the sea level at the city of Oskarshamn on an hourly basis and with an accuracy of one centimetre. In Figure 4-1 the monthly mean sea level is shown, values refer to the national Swedish datum level RH70. Further statistics on sea temperature, salinity, chemical composition, etc. are presented in /Larsson-McCann et al., 2002/.

For a shorter period of time, quick changes in weather conditions can cause a deviation, on the scale of centimetres, in the sea level between the Oskarshamn station and local sea level around Äspö.

#### **4.1.2 Salinity**

The Baltic Sea around Simpevarp peninsula has good water exchange and is strongly affected by coastal processes due to local wind and stratification conditions /Larsson-McCann et al., 2002/. The salinity of the Baltic Sea in the vicinity of Äspö is about 6 grams per litre /Larsson-McCann et al., 2002/. However, a variation both in time and space is found and values down to 4 grams per litre have been observed /Rhén et al., 1997a/. These salinity values are somewhat less than the offshore value of around 7 grams per litre in this area of the Baltic Sea /Larsson-McCann et al., 2002/.

#### **4.1.3 Shore level elevation**

The sea level of the Baltic Sea has changed its value due to isostatic and eustatic processes all since the last glaciation. Figure 4-2 shows the modelled shore level elevation from the last deglaciation and extrapolated 10 000 years into the future. Modelled past and predicted future shore level location according to present day datum is further described and presented in /Morén & Pålsson, 2001/. A visualisation of the Baltic Sea development around Äspö is shown in /Rhén et al., 1997a/.

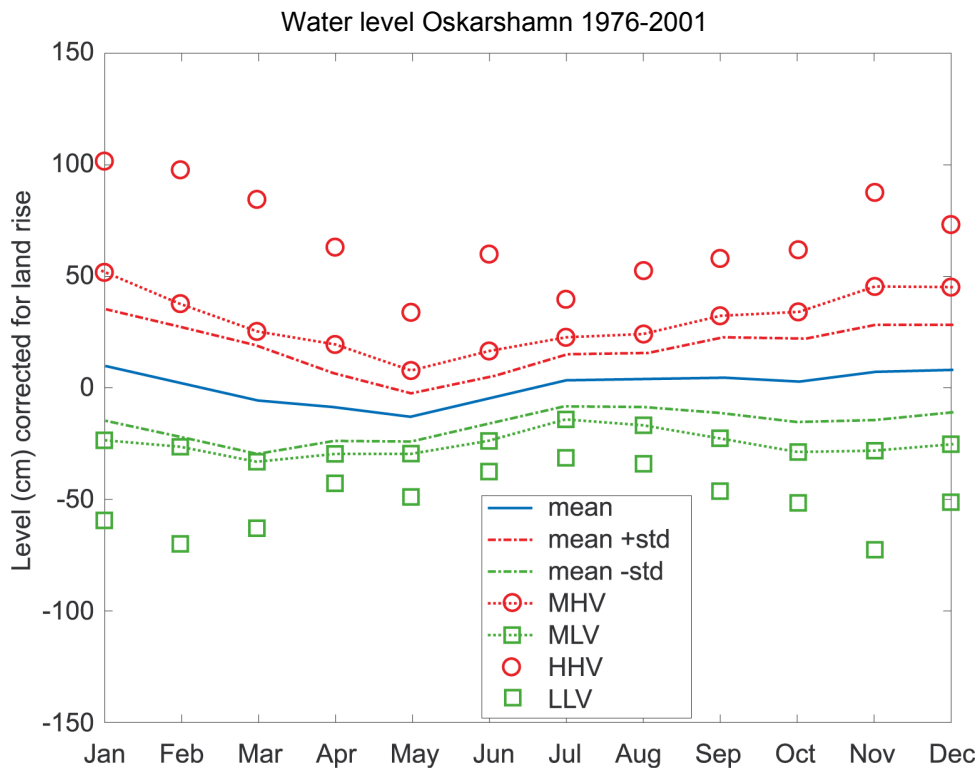


**Figure 4-1** Monthly sea water level [cm] statistics at Oskarshamn 1976-2001. Monthly mean water level and its corresponding one standard deviation are shown. MHV/MLV signifies mean high/low water level, i.e. mean of all years 1976-2001. HHV/LLV signifies highest/lowest water level ever during 1976-2001. Taken from /Larsson-McCann et al., 2002/. Figure is based on hourly measurements. To obtain correct extreme value statistics, levels have been corrected for land rise.

**Shore level, Oskarshamn, 14000 B.P. - 10000 A.P.**

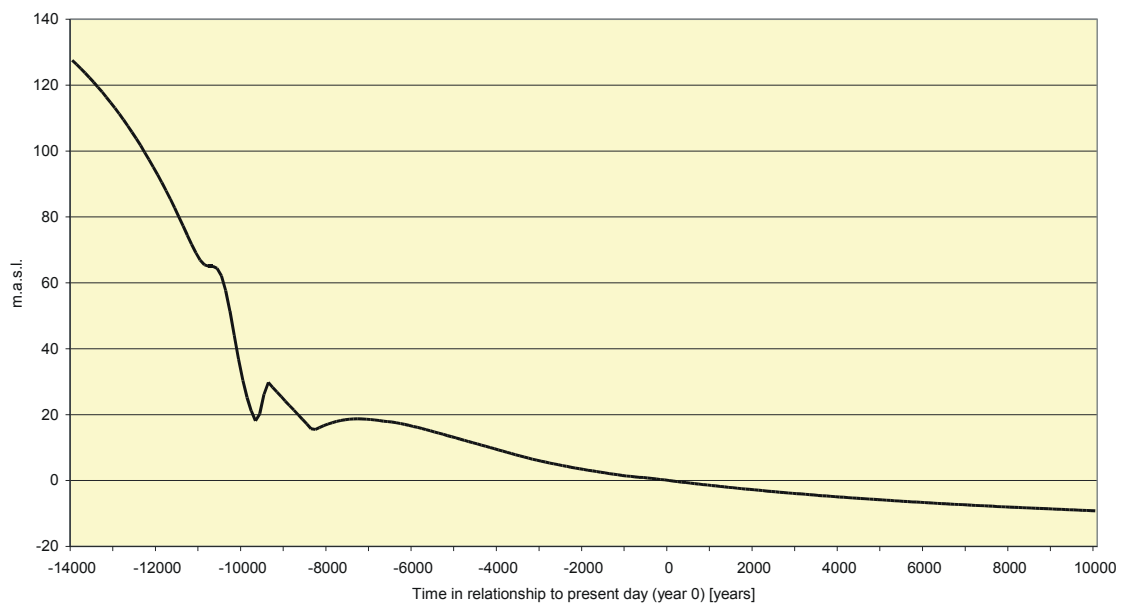


**Figure 4-2** Relative shore level location in the Oskarshamn region of the Baltic Sea. Data from /Pässe, 2001).

## **4.2 Hydrological setting of Äspö**

### **4.2.1 General boundary conditions**

Figure 4-3 to Figure 4-5 illustrate the setting of the isle of Äspö and hence show the surface boundary for the Äspö02 Model domain including drainage basins, rivers, and ponds. At the chosen scale a total number of twelve drainage basins have been identified for the Isle of Äspö. In general the low-lying grounds are covered with peat and other organic sediments. /Follin et al., 1998/ show the large-scale drainage basins in Oskarshamn County.

### **4.2.2 Temperature**

/Larsson-McCann et al., 2002/ present results from 1961 - 2000 for a couple of different measurement sites at the coast of Småland. /Graffner, 2003/ presents results from a local measurement station at Äspö at which data was collected between 1997 and 2002. According to /Graffner, 2003/ the mean air temperatures on Äspö varies between 0°C in January to 16°C in July (Figure 4-6). Figure 4-7 shows the yearly mean air temperatures. Äspö mean air temperatures are in good agreement with the lengthier measurement series by SMHI presented in /Larsson-McCann et al., 2002/. Mean air temperature values for Oskarshamn and Ölands norra udde from these latter measurement series are included in Figure 4-6 and Figure 4-7 as references.

### **4.2.3 Precipitation**

The corrected annual mean precipitation in Oskarshamn is 633 mm/year for the period 1961-1990, with approximately 20% as snow. For the period 1991-2000 the equivalent value is somewhat higher (681 mm). A measurement series by /Graffner, 2003/ for 1998-2000 from Äspö has been corrected with the correction series for Oskarshamn /Larsson-McCann et al., 2002/. With this correction series the Äspö annual mean precipitation is 687 mm/year. In Figure 4-8 the monthly sum of precipitation for Äspö is corrected both with the correction series for Ölands norra udde and Oskarshamn /Larsson-McCann et al., 2002/. Values from these two latter sites are used as references. The yearly sum of precipitation for Äspö is somewhat more erratic than the comparative sites of Oskarshamn, Ölands norra udde, and Kråkemåla but fits well in-between the low trend-line for Ölands norra udde and the high trend-line of Kråkemåla (see Figure 4-9).

In /Larsson-McCann et al., 2002/ the relative humidity, calculated global radiation, air pressure and wind information are presented also. Further, characteristics such as specific discharge for Forshultesjön, Gerseboån, and Laxemarån on the fringing mainland are presented.



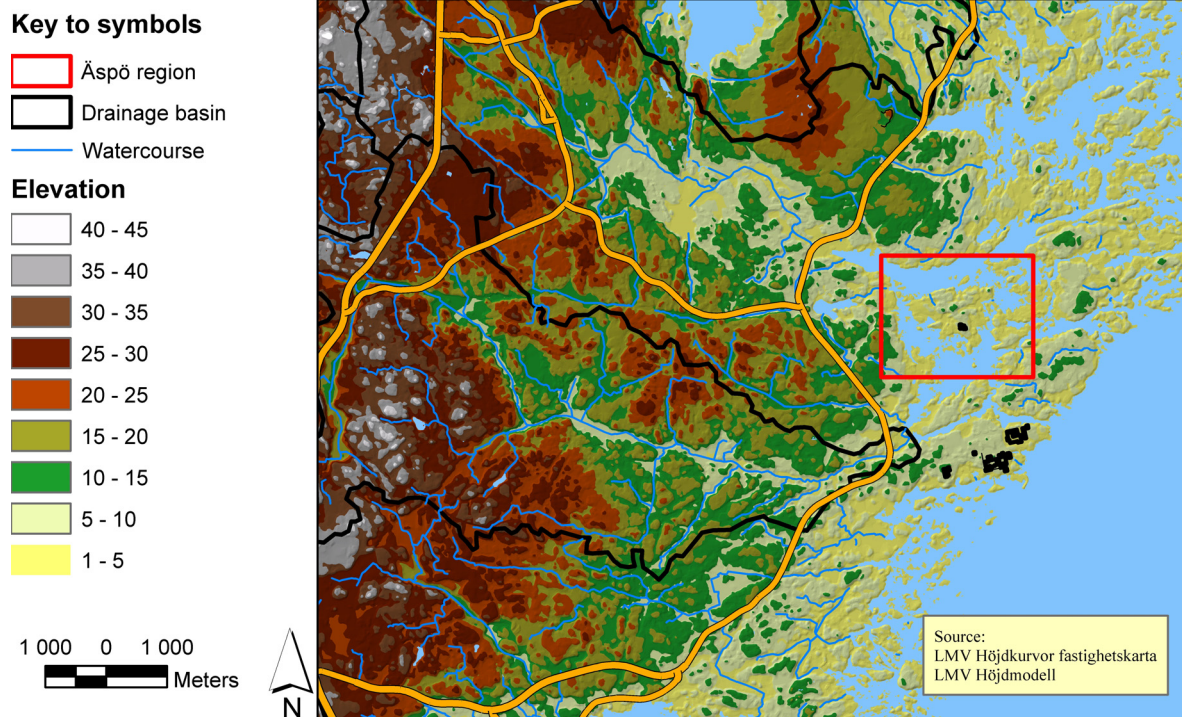


*Figure 4-3 Large-scale drainage basins, rivers, and streams in the Simpevarp area.*

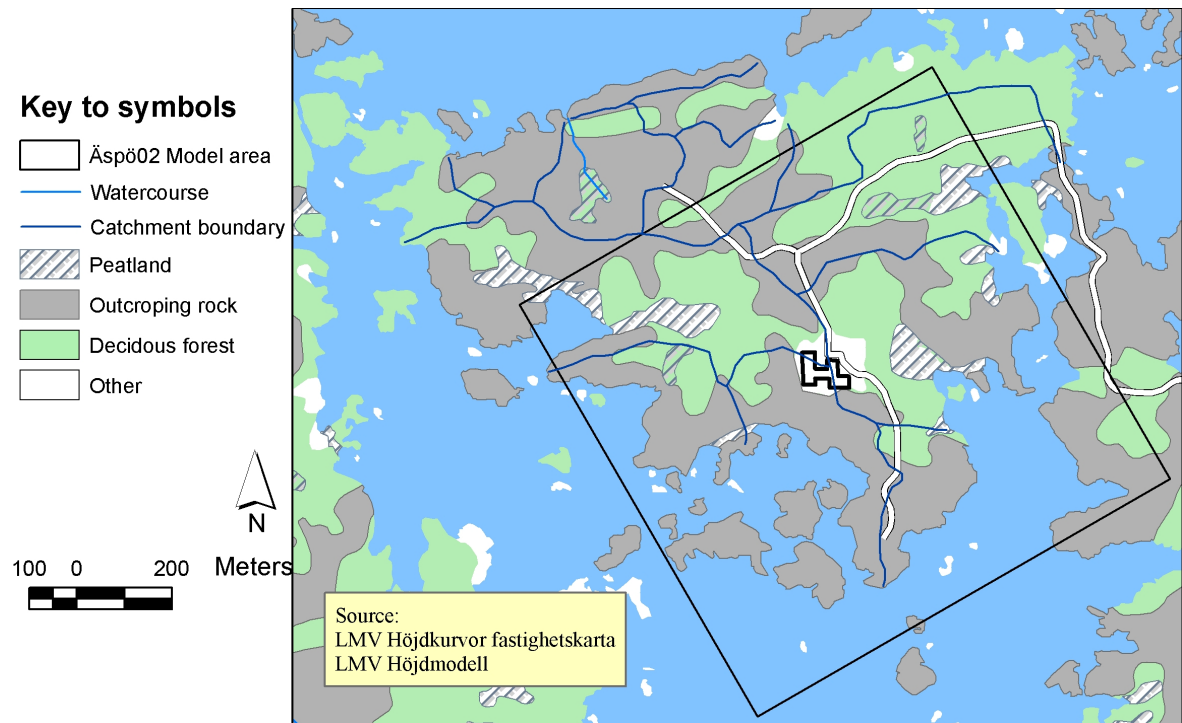


*Figure 4-4 Surface characteristics, drainage basins and streams on Äspö.*



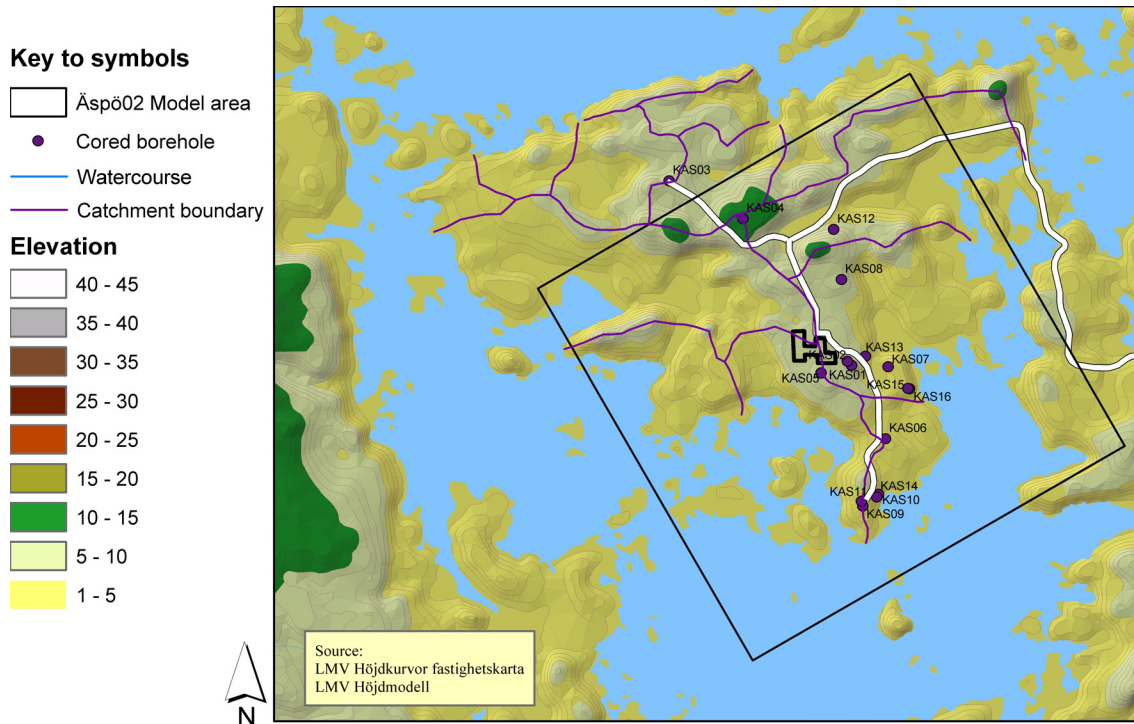


**Figure 4-5** Topography, drainage basins and cored boreholes on Äspö.

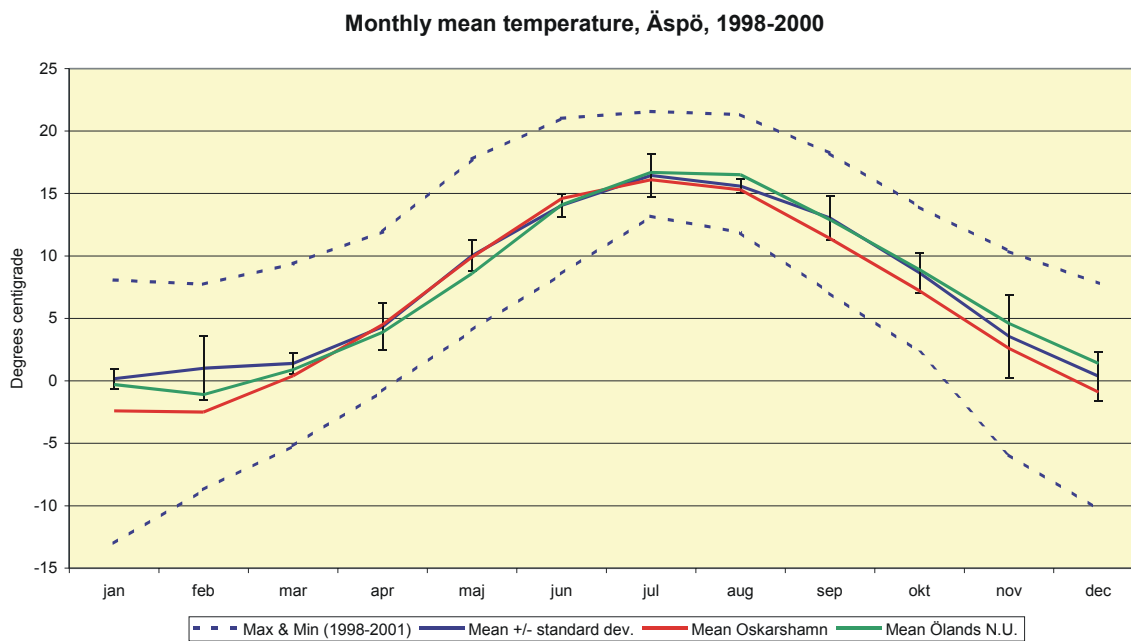


**Figure 4-6** Monthly mean max an min temperatures for Äspö. The mean values for Äspö are based on the years between 1998 and 2000. The reference sites are based on the standard normal period<sup>1</sup> 1961-1990 (Data from /Larsson-McCann et al., 2002/ and /Graffner, 2003/).

<sup>1</sup> According to SMHI a standard normal period is a chosen 30 years period during which the statistic results of climate characteristics is believed to be representative for a specific area.

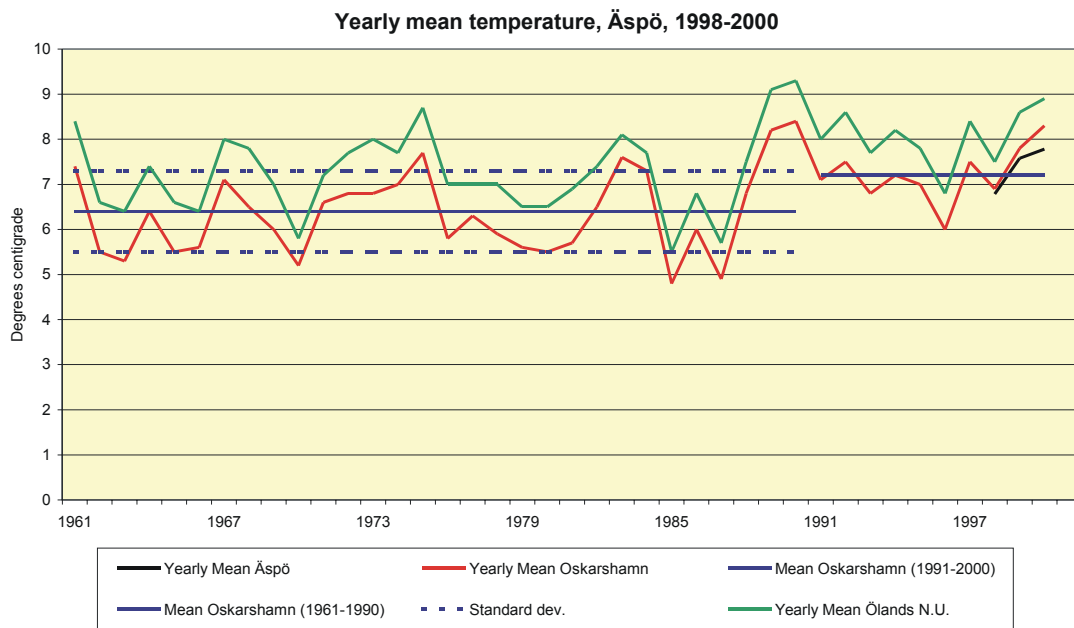


**Figure 4-7** Yearly mean temperature for Äspö and the reference sites. The Äspö values are based on the years between 1998 and 2000. The reference sites are presented for the period 1961-2000. 1961-1990 is a standard normal period, hence a mean value for this time interval and another for 1991-2000 (Data from /Larsson-McCann et al., 2002/ and /Graffner, 2003/).

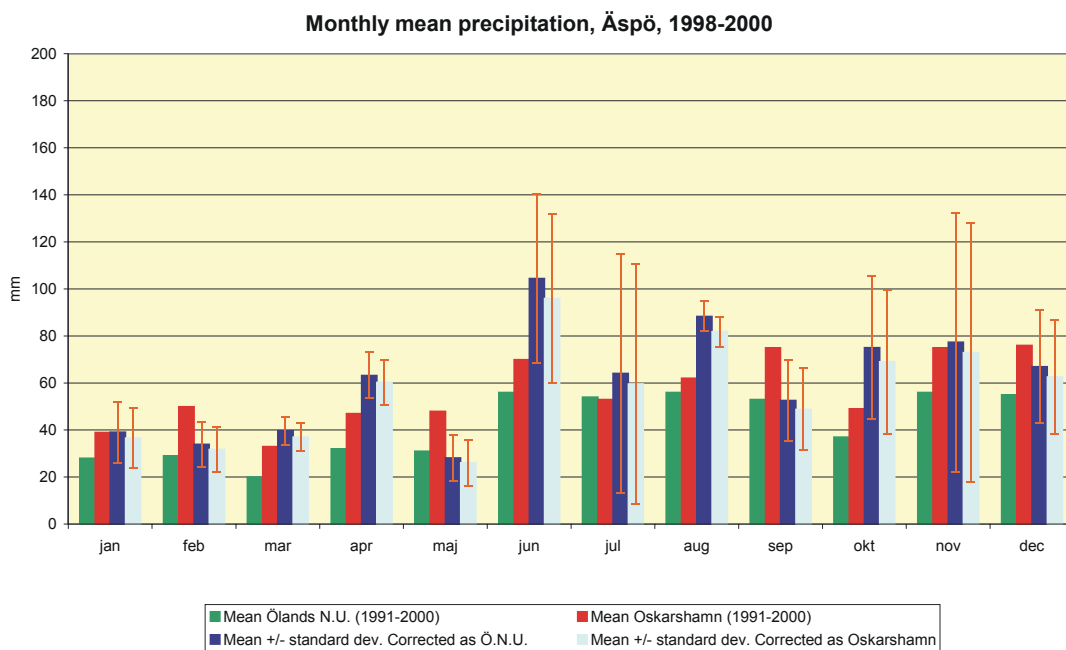


**Figure 4-8** Average of the monthly sum of precipitation for Äspö and the reference sites. The mean value is for Äspö and is based on the years between 1998 and 2000. The reference sites are for the standard normal period 1961-1990. Äspö data is corrected both as Ölands norra udde (Ölands N.U.) and Oskarshamn (Data from /Larsson-McCann et al., 2002/ and /Graffner, 2003/).

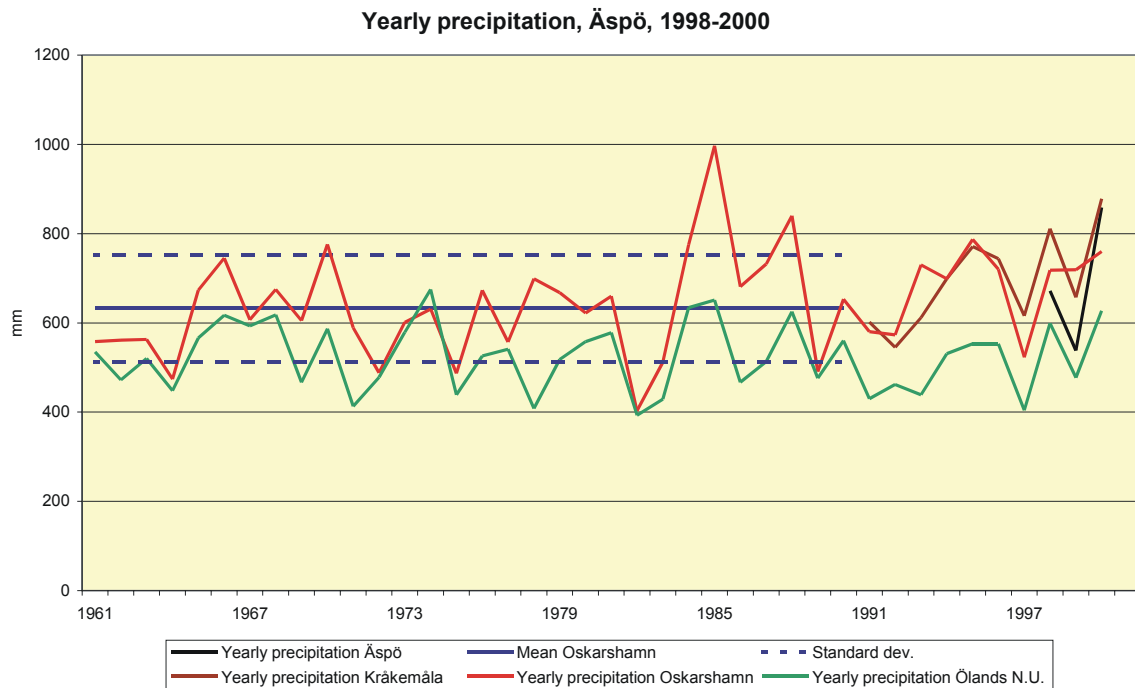


**Figure 4-9** Yearly sum of precipitation for Äspö and reference sites. The yearly sum value at Äspö is based on the years between 1998 and 2000. The mean value is based on the standard normal period 1961-1990 for Oskarshamn (Data from /Larsson-McCann et al., 2002/ and /Graffner, 2003/).

#### 4.2.4 Evapotranspiration

Using the Penman formula /Larsson-McCann et al., 2002/ has calculated the potential evapotranspiration for Västervik/Gladhammar and Ölands norra udde; and /Graffner, 2003/ has calculated the potential evapotranspiration for Äspö. In Figure 4-10 and Figure 4-11 results from Västervik/Gladhammar and Ölands norra udde are used purely as reference values, further information on these sites is found in /Larsson-McCann et al., 2002/. The expected potential evapotranspiration, based on values for Ölands norra udde, is around 590 mm/year for the entire measurement series from 1961-2000. The mean value based on the three year values by /Graffner, 2003/ indicate a somewhat higher value (610 mm/year). The same three years for Ölands norra udde average to 560 mm/year. One important difference between /Graffner, 2003/ and /Larsson-McCann et al., 2002/ is the global radiation. This variable is measured directly by /Graffner, 2003/ but calculated by /Larsson-McCann et al., 2002/.

/Graffner, 2003/ have measured the specific discharges from two local, but representative, drainage areas of northern Äspö. Based on the precipitation values presented in section 4.2.3 and the measured specific discharge from these two areas a value for the actual annual evapotranspiration is evaluated to approximately 450 mm/year.

Monthly sum of Potential Evapotranspiration, Äspö, 1998-2000

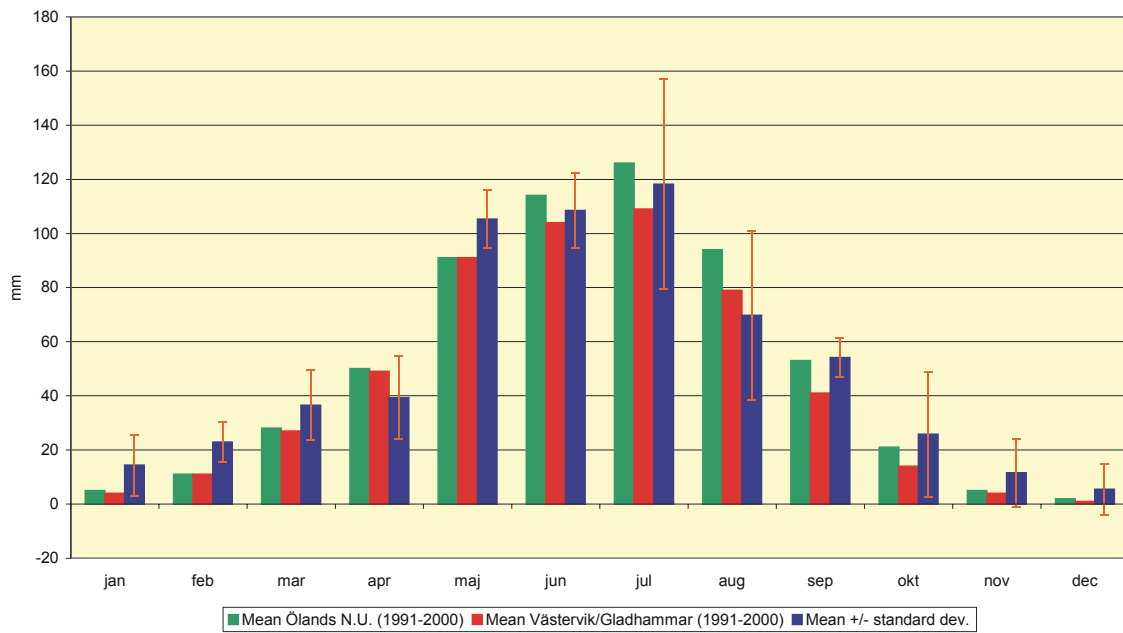


Figure 4-10 Average monthly sum of potential evapotranspiration in [mm] for Äspö (1998-2000) and the reference sites. The reference sites are based on the standard normal period 1961-1990 (Data from /Larsson-McCann et al., 2002/ and /Graffner, 2003/).

Yearly sum of Potential Evapotranspiration, Äspö, 1998-2000

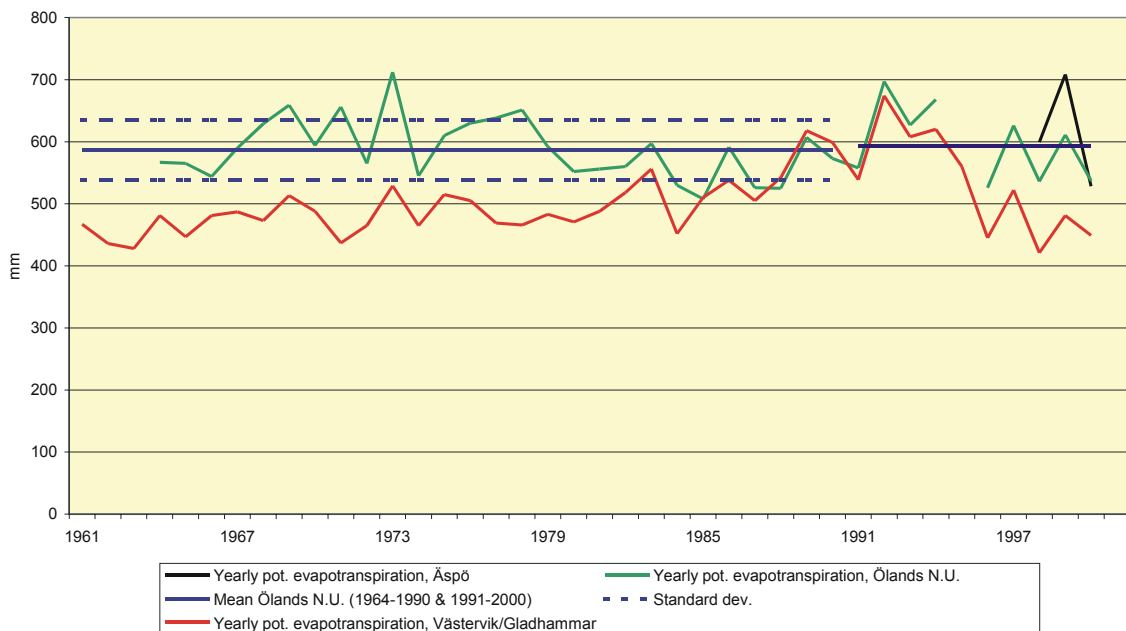


Figure 4-11 Yearly sums of potential evapotranspiration for Äspö (1998-2000) and the reference sites. The reference sites include data from the period 1961-2000 (Data from /Larsson-McCann et al., 2002/ and /Graffner, 2003/).

### 4.3 Quaternary deposits

The mapped Quaternary deposits are schematically shown in Figure 4-4. Much of the surface characteristics are bedrock outcrops and till. On Äspö the soil cover is thin - thicknesses between 0 and 5 metres - and mainly of a boulderly till character; which on low areas are covered with fluvial deposits such as clay, sand, and gravel. The highest water level after the latest deglaciation was approximately 100 metres above the present level in this part of the Baltic Sea /Påsse, 1997/. Due to the land uplift, most parts of Äspö have successively been exposed to wave energy. This process has revealed the bedrock on local summits, which sometime are encircled by gravel and boulders.

In some low areas, which often resemble small valleys, a peat layer is found at the surface. Beneath this peat layer are sometimes sheets of out-washed material, mainly gravel, found. However, profiles containing clayey gyttja instead of the out-washed material are also found /Sundblad et al., 1991/ and /Landström et al., 1994/. Below these intermittent layers of out-washed material or gyttja, a layer of glacial clay covers a possible bottom layer of till.

### 4.4 Water table and piezometric levels

Groundwater occurs in the porous soils and within the bedrock fracture network. Hydraulic properties of soil and especially rock are extremely heterogeneous. Therefore the description of some variables, such as the water table, are scale dependent. Variations in time and space cause a large uncertainty in the variable description at the small scale. As a result of the fracture network the water table is highly irregular and sometimes even representative of a locally isolated flow system. With depth below the water table such irregular pressure distributions are smoothed and also less effected by annual water table variations.

A maximum water table elevation is found during late autumn to spring and a minimum in late summer /Andersson et al., 2002a/. /Svensson, 1987/ placed the main recharge event in conjunction with the snow melt period in early spring. The water table level is known from the boreholes at Äspö, however the measurement locations have become less dense and sometimes adjusted during the second half of the nineties and the beginning of 21st century.

The development of a smoothed and continuous water table between 1991 and 2000 were established based on a kriging interpolation of available measurement sections from surface boreholes (HAS and KAS boreholes). It is important to keep in mind that this kind of treatment misses the erratic behaviour of the water table caused by the heterogeneous hydraulic conductivity field.

In order to be able to compare measurement values from different years the total amount of available sections where examined and it was concluded that 41 sections meet the necessary criteria. Figure 4-12 shows the development of the hydraulic head situation from year 1991 up to year 2000. In the plot for 1991 it is important to note that the face of the tunnel had not reached the first kilometre chainage. That is, the tunnel advance had not reach the subsurface of the isle of Äspö.

There are some characteristics between year 1995 and year 2000 that need further comment. As compared to year 1995, year 2000 seems to have a significant extension of the drawdown cone periphery towards north-west. This is only partially true; the included measurement sections have a small decrease in the measured pressure for this time period and the drawdown has not reached a steady-state condition. However, most of the visual effect shown in Figure 4-12 is an interpolation bias due to a pumping experiment on northern Äspö indicated by the orange points in north-west in year 2000. Further the extensional shrinking in the north-east part of the drawdown cone periphery may be the result of the removal and later on change into a single-packer system of a measurement section in borehole HAS18; indicated by the green point in the year 1995 plot.

Given the changes in the monitoring systems and disturbance from pumping tests it is not possible to make detailed statements about changes in the lateral extent of the drawdown however it is clear that between 1995 and 2000 the drawdown extended to greater depths. Hence based on the presented results and additional comments it seems as the drawdown is still transient and it is still valid that the geological structure EW1 acts as a semi-permeable barrier for flow across its boundaries as were concluded in /Rhén et al., 1997a/.

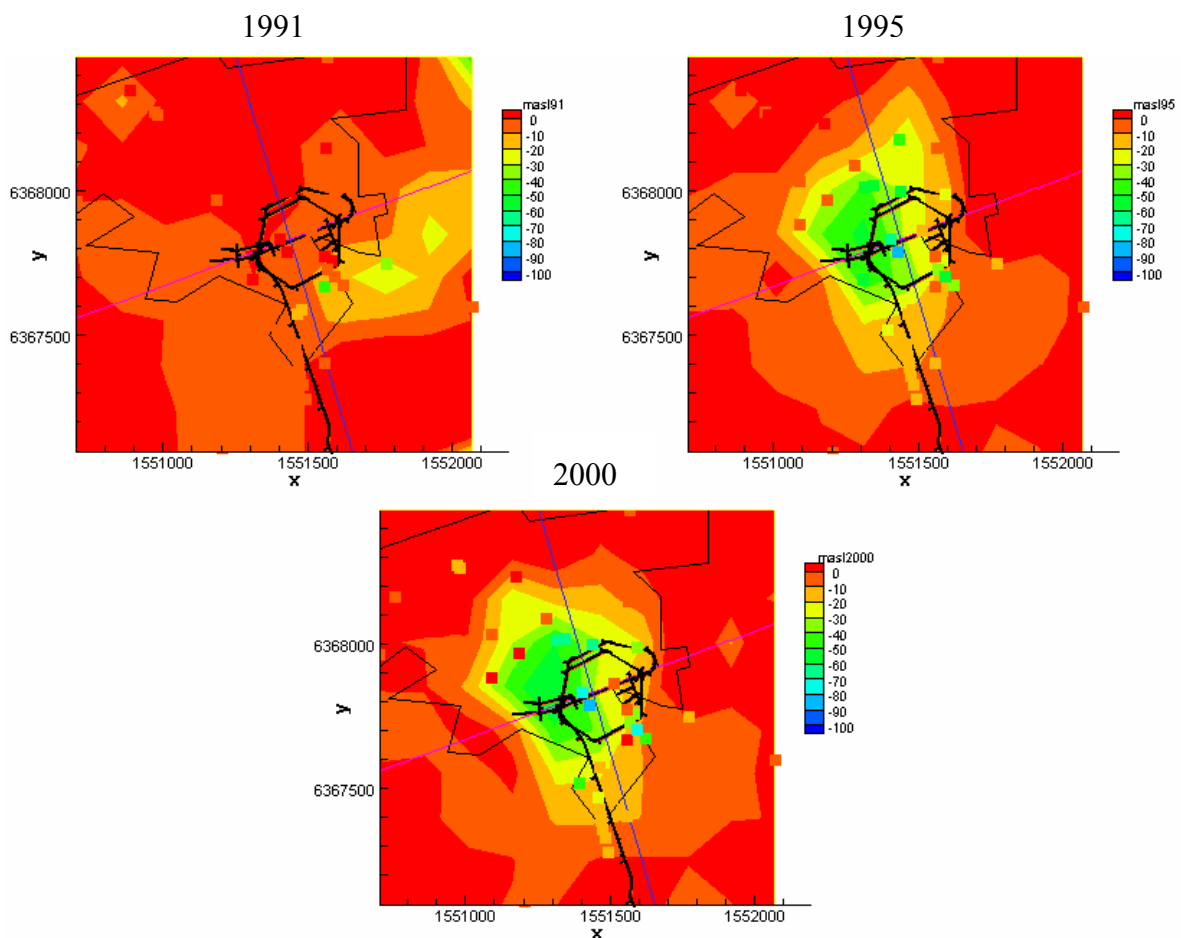


**Figure 4-12** Development of the hydraulic head with time. Upper left - 1991; upper right 1995; and lower - 2000.

Figure 4-13 shows the hydraulic head distribution for year 2000. Noteworthy in this figure is the extensive drawdown in the southern part of the tunnel spiral. The location of this deep drawdown region coincide with the geological structure EW3 and also most likely the NE1 structure. Both these structures are hydraulic conductors with high transmissivity values. If these geological structures are responsible for the deep drawdown in this southern Äspö region it should be expected to find a significant effect along the structures strike directions. The measurement data is however located along the tunnel chainage and the interpolation is unable to capture such drawdown behaviour.

The resulting drawdown, from the different numerical groundwater flow models built on the Äspö96 model, see /Rhén et al., 1997a/, indicates a drawdown much more related to the hydraulic conductors that are defined within the model domain than the interpolation. Personal communication, on the results of the Task 5<sup>2</sup> modelling, with /Svensson, 2003/ and /Laaksoharju, 2003/ suggest that more "new" meteoric waters exist within the Äspö domain than possible from solely Äspö surface recharge. Therefore it must be concluded that meteoric waters are collected from other areas such as the mainland on Laxemar. These waters could only find their ways through a permeable hydraulic conductor with a drawdown extending under the Baltic Sea into the mainland or fringing isle.

On the finer scale the interpolation shown in Figure 4-13 indicates a small change, compared to the natural conditions, in the hydraulic head in the deeper parts of the spiral centre. As stated above results from numerical groundwater flow models indicate more variation in the water table compared to the continuous interpolation shown in Figure 4-12 and Figure 4-13, with the deep drawdown concentrated along major hydraulic conductors. If a measurement section was located within a rock block it would most likely turn out with a smaller drawdown compared to regions with a connection to a hydraulic conductor even within the spiral centre.

---

<sup>2</sup> Task 5 is the fifth exercise of an international co-operation on different numerical modelling issues.

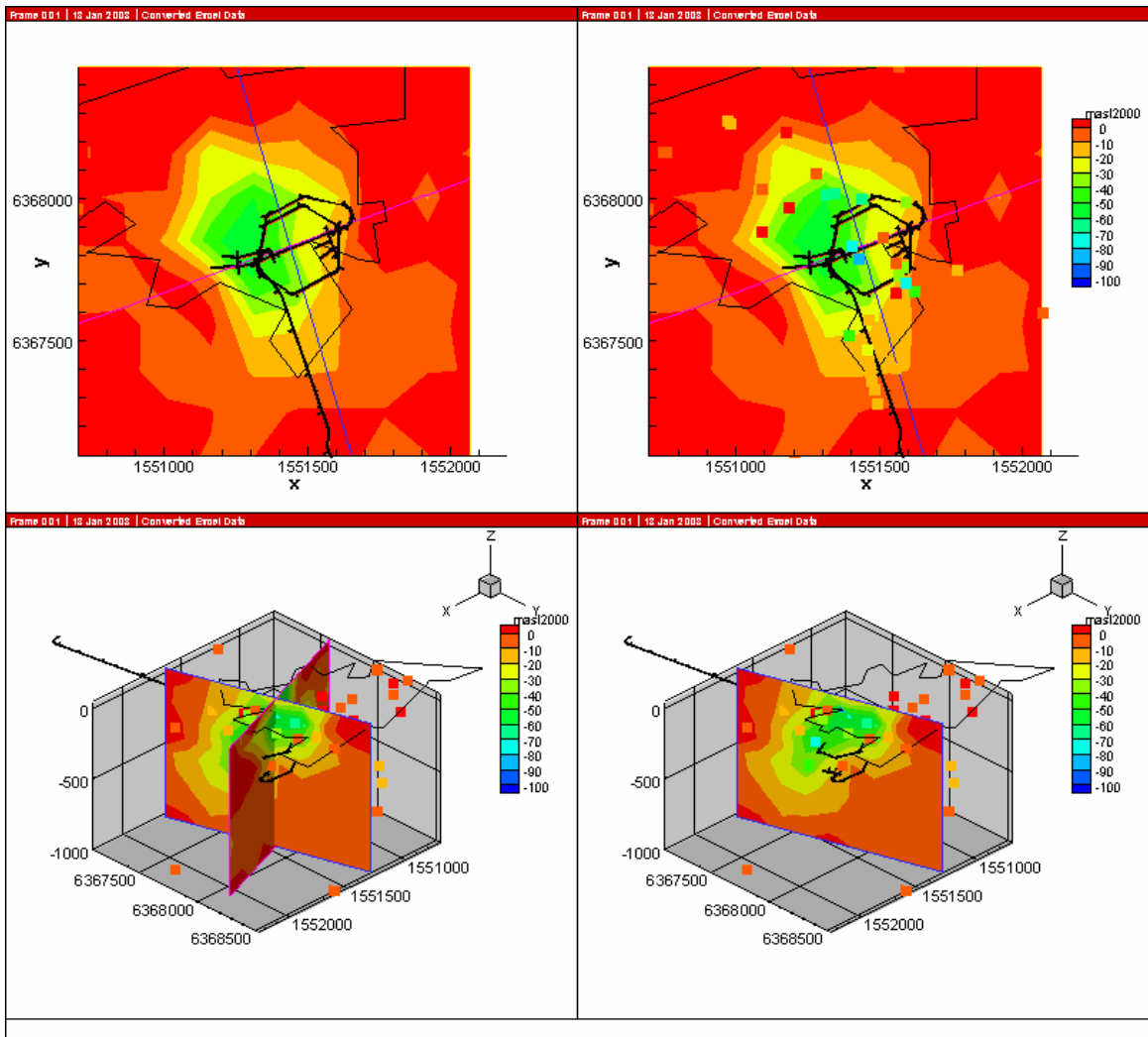


**Figure 4-13** The hydraulic head distribution at year 2000. Interpolated values.

The piezometric levels are influenced by a number of factors. Close to the water table, effects of precipitation events and sea water level fluctuations can be observed, especially in conjunction with highly connective fracture zones. With depth these localised effects are smoothed out however replaced by a short time fluctuation on the diurnal scale caused by the earth tide. A calculation of the earth tide at Äspö indicates a relative movement no larger than approximately  $\pm 0.25$  metres but in general confined within  $\pm 0.1$  metres /Rhén et al., 1997a/. A general description of earth tides and illustration of the calculated tidal effect at Äspö can be found in /Rhén et al., 1997a/.



## 4.5 Groundwater recharge

As indicated in Figure 4-4 and Figure 4-5 Äspö is composed of a large number of small drainage basins. This implies small areas of recharge and discharge. The recharge available for deep groundwater should be small in relation to the total amount of annual recharge.

/Svensson, 1997a/ studied the groundwater recharge by means of a numerical groundwater flow model. This study concluded on a net deep (5 metres below ground surface) groundwater recharge of 0.5 mm/year on Äspö under natural conditions, that is before the tunnel was excavated. Since 1997, a pumping experiment has been ongoing at the almost undisturbed northern parts of Äspö. Here /Graffner, 2003/ has been able to maintain a steady drawdown depth of approximately 45 metres with a discharge of 15 mm/year. This later figure is based on an assumption that the discharge is feed with water from the entire drainage basin (approximately 49 000 m<sup>2</sup>). According to /Graffner, 2003/ it is conclusive that no drawdown occur outside the boundary of this drainage basin. However, the actual drawdown area within the drainage basin has not been possible to assign, hence the conservative use of the entire drainage basin area. The discharge caused by the described pumping experiment has not indicated a significant change of the surface flows. This suggests a deep groundwater recharge of at least 15 mm/year under natural conditions.

The additional drainage utilised by the presence of Äspö HRL, is believed to cause a larger recharge to deep groundwater than would be under natural conditions. /Svensson, 1997a/ concluded on an average net deep groundwater recharge of 134 mm/year with the tunnel present (front at 3600 metres). However, the above described experiments on the northern part of Äspö have not been able to indicate that the deep groundwater recharge increases due to an additional deep drainage /Graffner, 2003/. As the deep groundwater recharge is believed to be mainly concentrated to fracture zones. /Graffner, 2003/ suggests that an increased infiltration is inhibited by the presence of clayey layers found in the Quaternary deposits of the low areas of Äspö.



## **5 Evaluation of primary data – hydraulic interpretation**

This section summarizes the characteristics for the main part of the primary hydraulic data compiled from the SICADA and HMS databases. The chapter presents data in a general manner and data is only sub-divided into hydraulic conductor or hydraulic rock mass domains. The data valid for hydraulic conductors are mainly compiled from /Rhén et al., 1997a/. The data presented in the chapter on hydraulic conductivity of the rock mass are in reality a mixture between hydraulic conductor data and rock mass data. This is due to the construction of the database, SICADA, which contain data of position by coordinates and additional parameter values (evaluated permeability, hydraulic conductivity, or transmissivity). Since the geological zone description and the hydrogeological conductor description have discrepancies in defined width as well as in inferred position; it has been impossible to establish the tests defined as belonging to hydraulic conductors from available data. Such division could only be established by a complete re-work on the data from both geology and hydrogeology.

The parameters considered are for the hydraulic rock domain: effective hydraulic conductivity and specific storage or storativity; and for the hydraulic conductor domain: transmissivity and storativity. Statistics of inflows to the laboratory tunnels and additional information on fracture flow will also be presented.

### **5.1 Available data and test designs**

Hydraulic tests of different kinds have been performed during the lifespan of the Äspö HRL. Data have been compiled from the SICADA and HMS databases together with additional data from reports documenting individual experiments at HRL.

The data in SICADA have been analysed and all data defined as measurements from transient hydraulic tests have been compiled into a large data set containing approximately 3300 unique hydraulic tests that each yield a site and scale specific hydraulic conductivity value. Sometimes the hydraulic tests in addition have yielded values for specific storage and information on connectivity.

The hydraulic test designs are different due to experimental objectives but also due to the fact of being performed either from the surface or at depth within the tunnel. For specific descriptions of test designs individual experiment reports are referred. General descriptions of test designs could be found in e.g. /Andersson et al., 2002a/.

## 5.2 Hydraulic properties

### 5.2.1 Transmissivity of hydraulic conductors

For most of the geological defined zones, but also for some clusters of hydraulic fractures assumed to be connected over a large region /Rhén et al., 19997/, different hydraulic tests have been performed both for local measurements, e.g. single-borehole tests, and tests of spatial responses, e.g. interference tests. However, in general, only one or a few tests have been performed on each conductor; therefore no spatial variability has been possible to assign to any of the conductors.

Figure 5-1 shows the distribution of the estimated transmissivity values for all deterministic hydraulic conductors defined by /Rhén et al., 1997a/. The geometric mean transmissivity of all hydraulically tested conductors is  $1.4E-05$  [ $m^2/s$ ] with a standard deviation of 1.55 for the logarithm of the transmissivity. No significant depth trend was observed and the statistics presented above are assumed to be valid down to a depth of 500 metres. At depths below 500 metres only a few tests have been performed on hydraulic conductors and therefore no statistics are available. The few tests performed do not differ significantly in estimated values. However, /Rhén et al., 1997a/ suggest a probable decrease to approximate 20 per cent of the mean value presented above. The absence of depth trend presented above may, with care, be used also at deeper levels /Rhén et al., 1997a/.

During the construction phase continuously probe holes were classified belonging to either hydraulic conductors (fracture zones) or rock mass. The hydraulic tests of the probe hole defined as hydraulic conductors yielded a mean hydraulic conductivity of  $2.0E-08$  [ $m/s$ ]. Since most of the hydraulic conductor domains are assumed having a thickness around 10 metres, this hydraulic conductivity value is much lower than the transmissivity estimate presented above. This discrepancy is due to the fact that the deterministic hydraulic conductors are based on wide geological structures and the probe hole conductors may be defined based only on a single highly water conducting fracture as a hydraulic conductor.

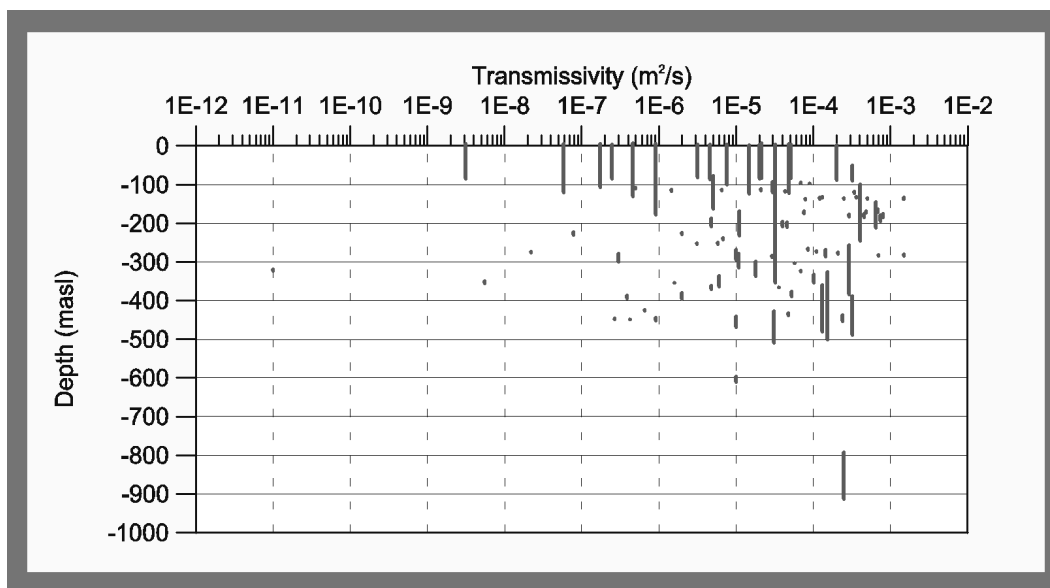


**Figure 5-1** Distribution of transmissivity values of hydraulic conductors at the Äspö area /Rhén et al., 1997a/.

## 5.2.2 Hydraulic conductivity of the rock mass

The evaluated hydraulic conductivity values for the rock mass are mainly based on different single-borehole tests. These tests represent values from the entire model domain. Hence some of the upper bound hydraulic conductivity values are likely to contain information on rock volumes defined as hydraulic conductors.

The evaluated results of hydraulic tests are known to show a scale dependency. A deeper discussion on this scale dependency applied on hydraulic conductivity values from Äspö HRL can be found in /Rhén et al., 1997a/, /Holmén, 1997/, and /Vidstrand, 1999/.

The majority of hydraulic tests performed after 1996 are performed within the scope of some specific experiment and are therefore, in general, of a relative small scale (c.f. Figure 5-2). Series of hydraulic tests performed at the same scale are few and no tests performed after 1996 can be used to validate the statistics presented in /Rhén et al., 1997a/ based on tests in the scales of 3-, 30-, and 100-metres. This since no new test series has been performed for these scales. The La Scala experiment<sup>3</sup> produced a systematic series of data from the scales 2-, 10-, 30, 90, and 270-metres. This data set have no noteworthy effect on the previous result, but the La Scala data sample is small and therefore have little effect on most combined regression; even though regression on the La Scala data produce a significant different result. Table 5-1 presents the average values for the three scales, 3-, 30-, and 100-metres.

**Table 5-1 Hydraulic conductivity of hydraulic rock mass domains, based on tests performed at the test scale of 3 metres. Statistics for hydraulic tests are compiled from data presented in /Rhén et al., 1997a/.**

Test scale [m]	K [m/s] (geometric mean)	Standard dev.	Data origin
3	1.2E-09	1.74	Hydraulic tests in KAS02-08
30	2.3E-09	1.53	Hydraulic tests in KAS02-03
50-200 (100)	4.1E-08	0.92	Hydraulic tests in defined hydraulic rock domains on Äspö

A compilation of evaluated transient tests stored within SICADA produced a number of 3310 unique hydraulic conductivity values from a variety of test scales. Figure 5-2 shows the results of the compilation of transient tests. One problem associated with an analysis on a compiled data set such as this is the fact that most values are representatives of a unique experiment with unique objectives. But also the spatial position and extension of the tests may include both predefined hydraulic rock and conductor domains. In Figure 5-2 the important experiments are illustrated in different colours. The specific objectives of an experiment could yield a bias toward e.g. high conductivity values. As an example, the TRUE experiments focused on understanding the fractures and performed tests over known structures. Interestingly, however, the

<sup>3</sup> The La Scala experiment is short for Laborative hydraulic testing to Approach SCALing LAws. The experiment was performed during spring 1998 and is reported in /Vidstrand, 1999/.

outcome does not seem to yield a bias, but are instead well distributed within the entire scatter of the compiled data set. On the other hand the ZEDEX experiments, with its focus on the excavation disturbed zone (EDZ), surprisingly yielded a bias towards the low end of the compiled hydraulic conductivity values. This bias may be due to an unsaturated condition within a more permeable fringing zone around the excavation. However, the Plug and Backfill experiment was also performed within the same rock volume but also extending further away from the tunnel wall. This experiment also yielded information supporting a hydraulically tight rock mass. Hence this rock volume is likely to be less permeable than the average value for Äspö HRL.

Due to the bias from experimental objectives all these hydraulic conductivity values should be treated with a conceptual care. Care should be used analysing all tests performed at a small scale, in a crystalline hard rock site. This because the concept of hydraulic conductivity - on which the evaluation methods are built - is only valid for a porous media continuum.

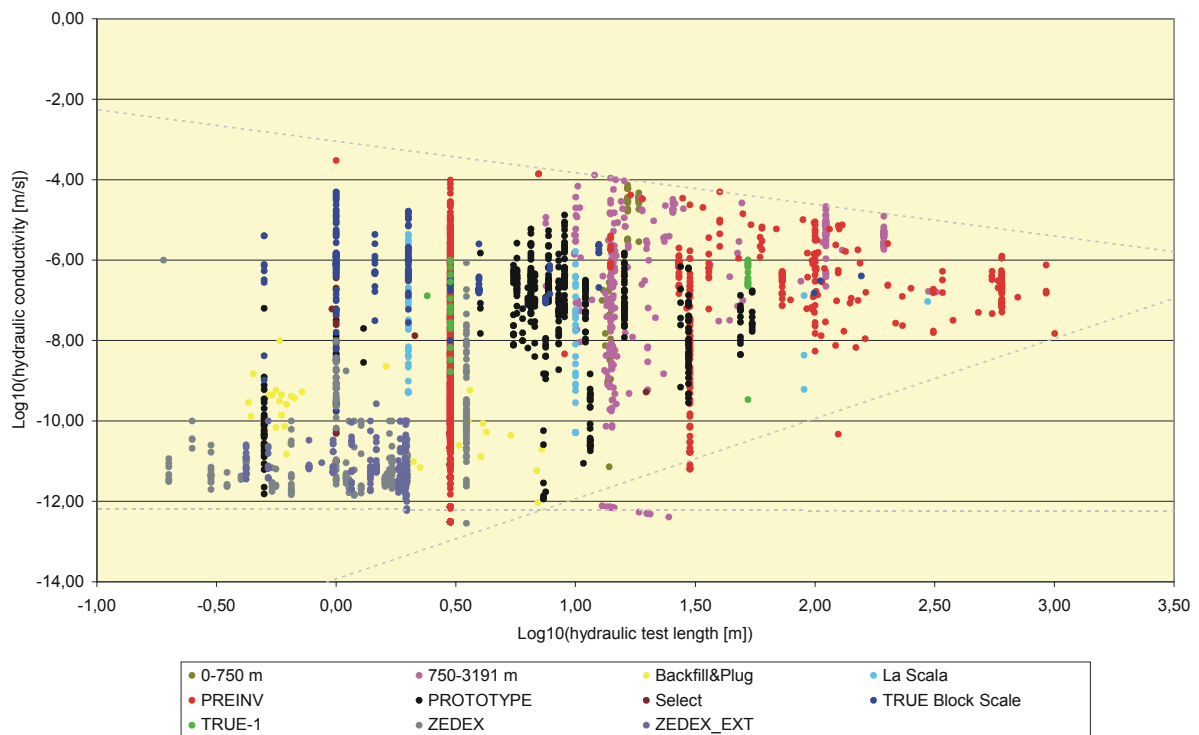


**Figure 5-2** Distribution of hydraulic conductivity values with scale. Different experiments are illustrated with different colours in order to visualise bias due to experimental issues. The following experiments were performed after 1996: Prototype Repository, Backfill & Plug, ZEDEX\_EXT, La Scala, and True Block Scale.

Figure 5-2 illustrates a couple of interesting characteristics. Firstly the hydraulic conductivity values seem bounded by an upper and a lower boundary, shown in Figure 5-2 as two inclined dashed lines. These boundaries appear to converge towards a hydraulic conductivity value of approximately  $1.0E-07$  [m/s] at a scale in the order of one to ten kilometres. Secondly, there seems to be a lower boundary at an evaluated hydraulic conductivity value somewhere between  $1.0$  to  $10.0E-13$  [m/s]. For many of the hydraulic tests this hydraulic conductivity value is well below the measurement limit, however for other tests and this especially for the small scale tests the theoretical limit is lower and therefore it should have been possible to establish lower hydraulic conductivity values. Some core samples of Äspö diorite have been tested using the Helium gas method /Laajalahti et al. In Gustafsson, 2001/. These tests yielded an average hydraulic conductivity value of  $3.0E-13$  [m/s] for these cores. /Maaranen et al. preprint/ presents the tabulated results of above presented core analyses. From this table it is conclusive that the scatter of evaluated core hydraulic conductivities is in the order of 1.5 orders of magnitude. Within the ZEDEX experiment laboratory measurement of core permeability values further suggest a matrix hydraulic conductivity between  $1$  and  $6E-13$  [m/s] /Emsley et al., 1997/. It is therefore possible that the rock matrix hydraulic conductivity at Äspö HRL is approximately  $1.0E-12$  [m/s].

Scoping flow calculations performed within the Matrix Fluid experiment at Äspö HRL suggest a rock matrix hydraulic conductivity between  $1.0$  and  $6.0E-14$  [m/s] /Gustafsson, 2001/. These flow calculations were based on established inflow and pressure measurements performed in a borehole; believed located in the centre of a rock matrix block. However, the calculations were also dependent of steady-state assumptions and a rather simplified conceptual model. Hence the result should be viewed carefully but are important since they in a way illustrate the field; which may include effects such as Faraday's cage<sup>4</sup> and engineered pressure fields due to the proximity of the tunnel.

The use of the 3-, 30-, 100-metre, and borehole scales in /Rhén et al., 1997a/ resulted in a proposed scaling by regression. Viewing the entire data set in Figure 5-2 it is clear that the used 30-metre scale data is somewhat dislocated towards the lower boundary. This dislocation together with the fact that the small-scale tests have a possible bias towards the lower hydraulic conductivity boundary may suggest that alternative scaling methods may be used.

The compiled data set was scaled into a representative scale, which for the Äspö02 model was set to 30 metres. This scaling was performed using regression with different formulas for upscaling and downscaling. This kind of scaling by regression transforms the value linearly along the regression trend line. This treatment also superimposes the variance in the small-scale data onto the larger scale. Figure 5-3 presents the statistics for the compiled data set, viewed as unscaled, scaled, and scaled data from hydraulic tests from a test scale of 10 metres and larger presents the regression formulas used together with the regression formula presented in /Rhén et al., 1997a/.

---

<sup>4</sup> In hydrogeology Faraday's cage effects refer to a conceptual idea that the flow within the fracture network surrounding a low-permeable rock block, at least, under transient situations will inhibit some of the flow over the rock block. Hence create an artefact of lower permeability of a rock block than that would be the result of a hydraulic test.

An alternative approach to scaling for the entire dataset shown in Figure 5-2 is one based on stochastic upscaling methods. Figure 5-2 indicates a smaller increase with scale than proposed by the regression. For scales larger than 10 metres the centre line (the mean value) of the hydraulic conductivity values increases from around 1.0E-08 [m/s] up to a value of approximately 1.0E-07 [m/s]. Based on interpolation of specific capacity of wells in the county of Kalmar the latter value represents a regional hydraulic conductivity /Rhén et al., 1997a/. Along the same scale transformation the scatter (the variance) in the data goes from a value for  $s(\text{Log}_{10}(K))$  of 4 towards a zero amplitude.

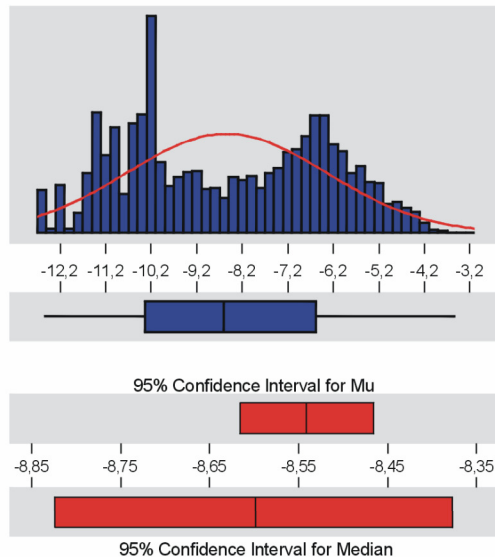
This slight increase of the hydraulic conductivity is in better agreement with the theoretical behaviour of a normally distributed parameter in a stochastic porous media. However, these stochastic theories should be treated with care since the nature of fractured rock is unlikely to be well described by a statistical homogeneous material, especially when the variance is this large.

The sub-sample of data for scales smaller than 10 metres are too small to indicate significant statistics for porous media approaches. For these smaller scales it is recommended that fracture statistics be used. This fact can partly be concluded due to the statistics presented in Figure 5-3. Herein the Anderson-Darling normality test is strongly rejecting the statistics for the entire data sample being normally distributed. However, eliminating sub-samples smaller than 10 metres results in successively increasing the acceptance up to the level seen in the bottom illustration of Figure 5-3. This Anderson-Darling normality test is still in a statistical manner far from a normal distribution but compared to historical hydrogeological comparison acceptable.

**Table 5-2 Regression formulas on the form  $Y=a+b \cdot \text{Log}_{10}(\text{scale})$**

<b>Y</b>	<b>a</b>	<b>b</b>	<b>Formula origin and usage criteria</b>
Log <sub>10</sub> (Ka)	-6.119	-0.466	/Rhén et al., 1997a/
Log <sub>10</sub> (Kg)	-9.411	0.817	/Rhén et al., 1997a/
s(Log <sub>10</sub> (K))	2.089	-0.758	/Rhén et al., 1997a/
Log <sub>10</sub> (Kg)	-9.860	2.164	Used on data from hydraulic tests with scale smaller than 30 metres.
Log <sub>10</sub> (Kg)	-5.724	-0.289	Used on data from hydraulic tests with scale larger than 30 metres.





Log10(Hydraulic conductivity [m/s])  
Unscaled data

Anderson-Darling Normality Test

A-Squared: 63,175  
P-Value: 0,000

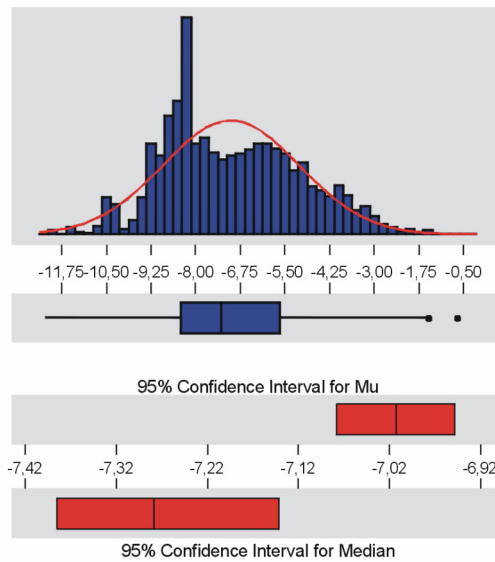
Mean -8,54120  
StDev 2,20181  
Variance 4,84797  
Skewness 7,72E-02  
Kurtosis -1,25430  
N 3310

Minimum -12,5441  
1st Quartile -10,3372  
Median -8,5982  
3rd Quartile -6,5790  
Maximum -3,5229

95% Confidence Interval for Mu  
-8,6162 -8,4662

95% Confidence Interval for Sigma  
2,1500 2,2562

95% Confidence Interval for Median  
-8,8239 -8,3768



Log10(Hydraulic conductivity [m/s])  
Data scaled to 30 metre scale

Anderson-Darling Normality Test

A-Squared: 26,892  
P-Value: 0,000

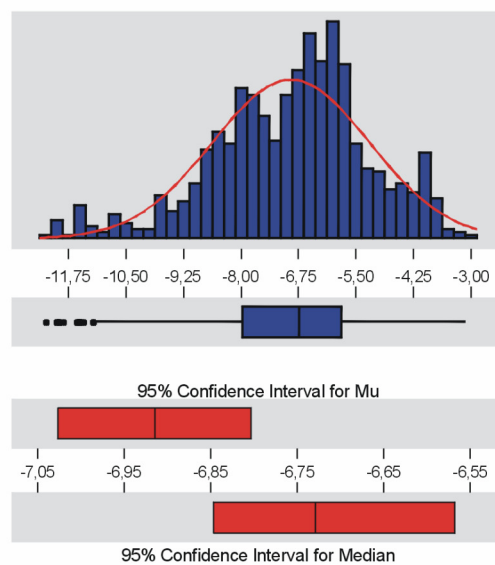
Mean -7,01312  
StDev 1,90896  
Variance 3,64413  
Skewness 0,314350  
Kurtosis -4,2E-01  
N 3310

Minimum -12,2198  
1st Quartile -8,4117  
Median -7,2785  
3rd Quartile -5,6371  
Maximum -0,6785

95% Confidence Interval for Mu  
-7,0782 -6,9481

95% Confidence Interval for Sigma  
1,8641 1,9561

95% Confidence Interval for Median  
-7,3850 -7,1414



Log10(Hydraulic conductivity [m/s])

Test scale larger than 10 metres  
Data scaled to 30 metre scale

Anderson-Darling Normality Test

A-Squared: 3,685  
P-Value: 0,000

Mean -6,91531  
StDev 1,70274  
Variance 2,89933  
Skewness -4,9E-01  
Kurtosis 0,346534  
N 887

Minimum -12,2198  
1st Quartile -7,9707  
Median -6,7290  
3rd Quartile -5,8247  
Maximum -3,1198

95% Confidence Interval for Mu  
-7,0275 -6,8031

95% Confidence Interval for Sigma  
1,6270 1,7859

95% Confidence Interval for Median  
-6,8470 -6,5677

Figure 5-3 Statistics for the entire data sample of hydraulic conductivity values.

The anisotropy of the hydraulic conductivity was analysed in /Munier et al., 2001/. /Munier et al., 2001/ assumed that surface boreholes are approximately vertical and therefore primarily test sub-horizontal structures; and that tunnel probe boreholes are approximately horizontal and uniformly distributed in direction along the tunnel spiral. These assumptions yielded the possibility to establish sets of different statistical sub-samples, which gave the statistical result presented in Table 5-3. The resulting hydraulic conductivity values are extremely anisotropic which can only be explained by a direct correlation with the structural geology. Analyses on the wet geological structures have concluded that there exist three hydraulically active fracture sets /La Pointe et al., 1995; Stigsson et al., 2001; Berglund et al., 2003/, however the strong dominance of the NW striking fracture set yields the strong anisotropical behaviour that are displayed in hydraulic tests.

**Table 5-3 Geometric mean of hydraulic conductivity values (m/s) based on surface boreholes and tunnel probe holes. Horizontal degrees are expressed in Äspö local coordinate system. Original transmissivity data taken from /Munier et al., 2001/, the presented values are representatives of a 30 metre scale.**

Direction for a plane (as in a fracture plane) orthogonal to the boreholes.				
Domain	Vertical plane, horizontal 120-140°	Vertical plane, horizontal 20-80°	Horizontal plane	Ratio
Äspö96	1.1E-07	4.2E-10	4.0E-09	260:1:10

Figure 5-4 and Figure 5-5 show the distribution of hydraulic conductivity values with depth. An effective stress dependant trend in hydraulic conductivity values with depth is frequently discussed in the literature and many relationships have been proposed, both empirical e.g. /Carlsson & Olsson, 1993/ and /Gustafson et al., 1989/ and more theoretical e.g. /Oda et al., 1989/ and /Wei et al., 1995/. However, based on the available data sample (Figure 5-4) it is impossible to conclude on a specific depth trend. For depth below 500 metres few hydraulic tests are performed. The data compiled and visualised in Figure 5-4 indicate a slight decreasing trend for hydraulic conductivity below 500 metres, however the statistical significance of such a trend can not easily be validated.

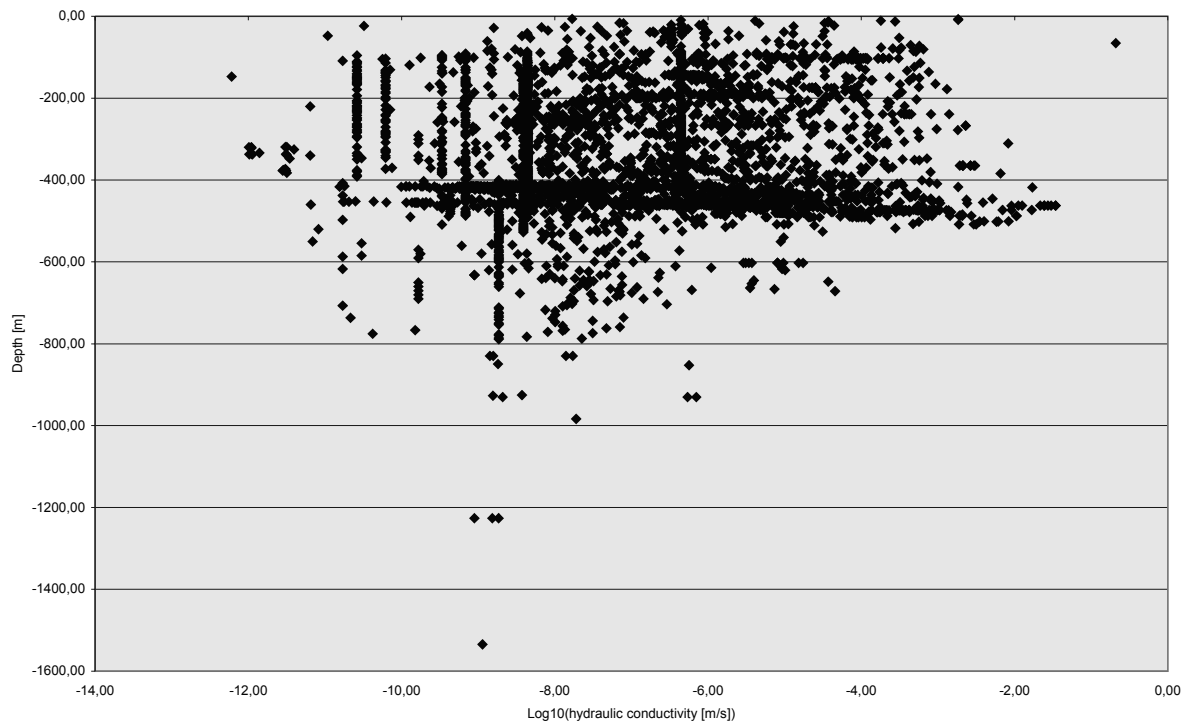


**Figure 5-4** Distribution of the scaled hydraulic conductivity values with depth. All available data in SICADA are used.

Figure 5-5 illustrates the hydraulic conductivity distribution with depth if analysed on the same data sub-samples as for the analysis on anisotropy. The surface boreholes, which indicate the hydraulic conductivity values of horizontal structures within the bedrock do, as the distribution showed in Figure 5-4, indicate that there are no significant depth trends. However, analysis on the results from tunnel probe holes yields a weak decreasing trend with depth (Table 5-4). This depth trend is mostly visible if only the low hydraulic conductivity direction is analysed. As a result a depth dependency seems valid for vertical structures. However, as seen in Figure 5-5 the differences in relationship with depth may be an artefact of a difference between different geological rock blocks.

**Table 5-4** Regression formulas on the form  $Y=a+b(\text{depth})$  for the hydraulic conductivity depth trend in vertical structures (based on probe holes).

Y	a	b	Formula origin and usage criteria
Log10(Kg)	-5.84	0.00725	Depth trend while including all data.
Kog10(Kg)	-6.50	0.00194	Depth trend while excluding outliers (measurement limit values).

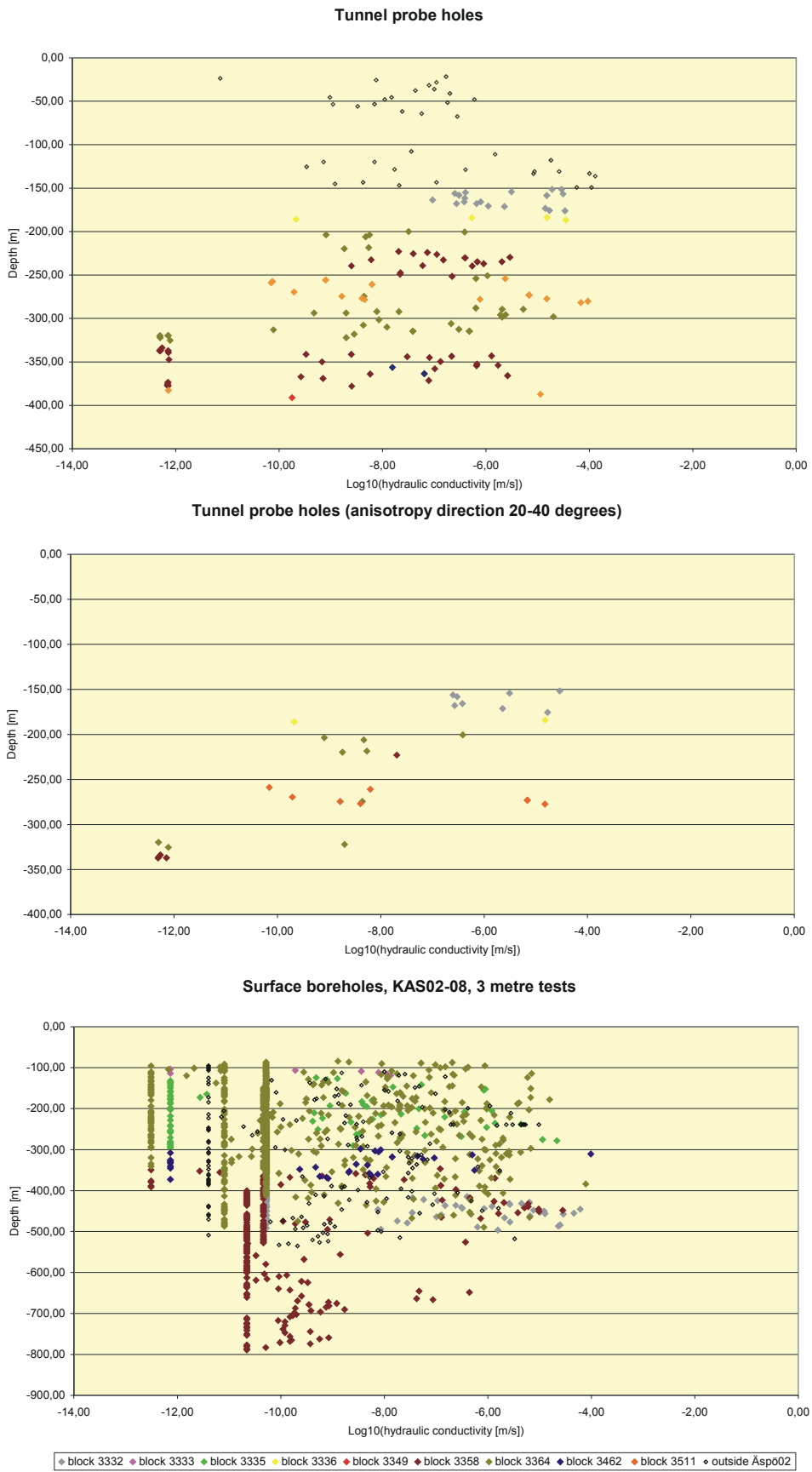


**Figure 5-5** Distribution of hydraulic conductivity values with depth displayed for different rock blocks and based on the sub-samples used for anisotropy estimations in the hydraulic conductivity.

### 5.2.3 Storage coefficient (storativity) of the hydraulic conductors and of the rock mass

As described in /Rhén et al., 1997a/ there are few interference tests at Äspö useful for direct evaluation of the storage coefficient. /Rhén et al., 1997a/ reports on some interference tests on hydraulic conductors, which were assumed to represent radial flow regimes. These test results were used to establish a linear relationship between the logarithms of the transmissivity and the storage coefficient. This established relationship is presented in Table 5-5 approximated to a power law relationship. However, /Rhén et al., 1997a/ argue that the linear regression should probably have a lesser slope than the slope presented.

**Table 5-5 The relationship between transmissivity and storativity in water conductive geological zones. The linear relationship between  $\text{Log}_{10}(T)$  and  $\text{Log}_{10}(S)$  on the form  $S=aT^b$ .**

a	b	n (sample size)
9.22E-03	0.785	5

Mechanical estimates based on Rock Mass Rating (RMR) values indicate a storage coefficient around  $1.0E-05$  [-] /Rhén et al., 1997a/ for a 10-20 metres wide fracture zone. This value is in good accordance with the results from the linear regression presented in Table 5-5.

As a part of the Prototype Repository experiment the storage coefficient for the rock was estimated on the basis of the diffusivity value. As for the hydraulic conductors a linear relationship for the rock mass in the Prototype Repository area was established. This latter established relationship is presented in Table 5-6 approximated to a power law relationship. The estimates of the storage coefficient from this experiment is transformed to specific storage values and further discussed in the next section.

**Table 5-6 The relationship between evaluated transmissivity and estimated storativity in water conductive rock. The linear relationship between  $\text{Log}_{10}(T)$  and  $\text{Log}_{10}(S)$  on the form  $S=aT^b$ .**

a	b	n (sample size)
2.18	0.919	14 interference tests

#### 5.2.4 Specific storage of the hydraulic rock domains

As for the storage coefficient there are few interference tests at Äspö useful for direct evaluation of the specific storage. Based on measures on some mechanical properties and estimates of the porosity of the rock at Äspö, a value on the minimum specific storage was set to be around  $1.0E-07 [m^{-1}]$  /Rhén et al., 1997a/.

Some interference tests on southern Äspö were used to establish an approximation of the specific storage /Rhén et al., 1997a/. These tests resulted in an evaluated specific storage, on the order of one magnitude larger than the minimum estimate,  $2.0E-06 [m^{-1}]$ .

Based on the two sets of values described above /Rhén et al., 1997a/ established a linear relationship between the logarithms of the hydraulic conductivity and the specific storage. This relationship is presented in Table 5-7 approximated to a power law relationship.

**Table 5-7 The relationship between evaluated hydraulic conductivity and estimated specific storage in water conductive rock. The linear relationship between  $\text{Log}_{10}(K)$  and  $\text{Log}_{10}(S_s)$  on the form  $S_s = a \cdot K^b$ .**

a	b	n (sample size)
6.037E-05	0.2312	3

In the La Scala experiment the specific storage was evaluated based on single-borehole tests with Hantush methodology. A common estimated flow dimension at Äspö HRL is somewhere in between 2.2 and 2.8. These kinds of flow dimensions indicate that a leaky-aquifer method may be valid for evaluation of hydraulic conductivity of the rock mass. The diagnostic results from the La Scala evaluation indicate higher values for the specific storage than presented by /Rhén et al., 1997a/. Figure 5-6 shows the specific storage in relationship with hydraulic conductivity and scale.

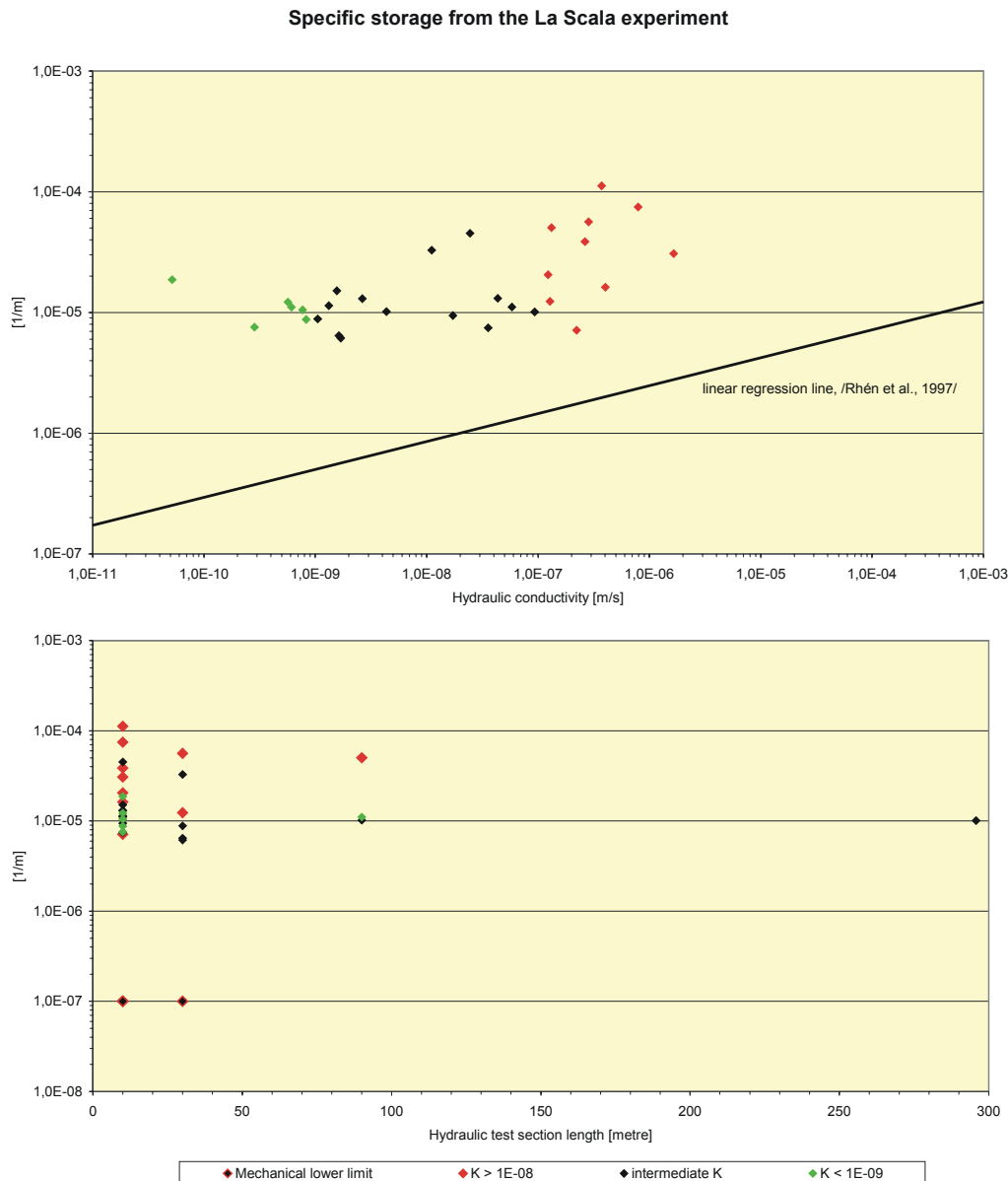


**Figure 5-6** Estimated specific storage from the La Scala experiment. Previously unpublished data by /Vidstrand, 1998/.

Estimates for the rock storage coefficient from the hydraulic tests performed in the Prototype Repository experiment (Figure 5-7) indicate a much lower limit for the specific storage than the previously suggested by rock mechanical properties. A specific storage values around 1.0E-08 correspond to theoretical specific storage values for a case with fresh water, where the compressibility of the rock is 1.0E-11 [m<sup>2</sup>/N], and the porosity is one percent.

The result from La Scala rely on the validity of the Hantush methodology and the representability of the La Scala rock volume; and the results from the Prototype Repository experiment rely on the validity of a transformation of a diffusivity value. However, both experiments indicate on a large scatter along the regression line for the estimated specific storage values. And further states that it may not be that easy to estimate the specific storage based on hydraulic conductivity information only.

### Specific storage from the Prototype Repository experiment

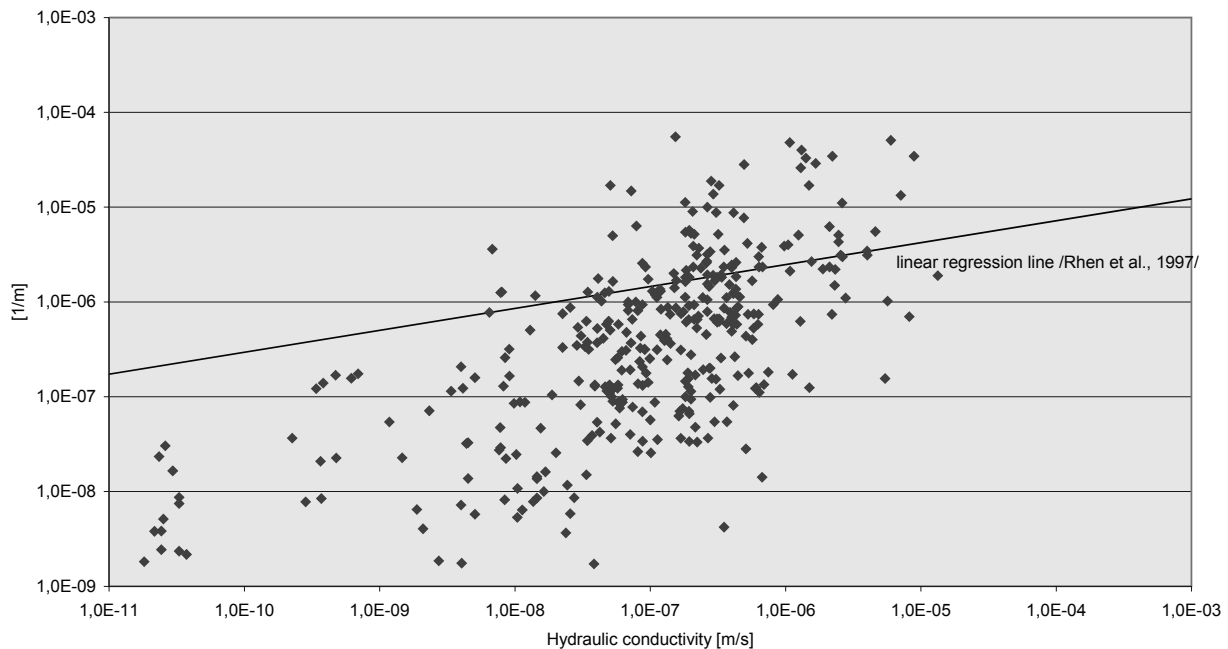


*Figure 5-7 Estimated specific storage from the Prototype Repository experiment.*

### 5.3 Tunnel water inflows

All through the Äspö HRL project the tunnel water inflow has been measured. The development of the tunnel water inflow during the construction phase was presented in /Rhen et al., 1997a/.

After the finalised construction work it is observable that the tunnel water inflow have become less with time (Figure 5-9). There are presently indications that this slow decrease has come to an end. Between 1996 and 2001 the decrease in inflow was approximately 10 litres per second. Compared with the maximum values of tunnel water inflow measured in 1994 and 1995 the flow has decreased to a stable value at approximately 65 per cent after year 2000.

The tunnel chainage from 0 to 1372 metres (Figure 5-8) is alone responsible for approximately 65 per cent of the total tunnel water inflow. The decreasing trend in the total tunnel water inflow is also apparent in this upper section of the tunnel chainage. Figure 5-10 presents the yearly average value of the tunnel water inflow for the tunnel chainage 1372 down to the bottom. A decreasing trend is apparent for the length interval between 1883 and 2496 metres. Tunnel chainage 0-1372 metres are intersected by the hydraulically active geological zones NE1, NE3 and NE4 together with a NW to NNW trending cluster of hydraulically active fractures, previously denoted as the hydraulic conductor NNW3 /Rhen et al., 1997a/. For the tunnel chainages 1883-2496 and 2994-3600 the dominating inflow relates to the geological zone NNW4 for the first part and the NW to NNW trending hydraulically active clusters of fractures, that previously were defined as NNW1 and NNW2 /Rhen et al., 1997a/, for the last part of the interval. For the reminding tunnel chainage little or no decreasing trend is apparent.



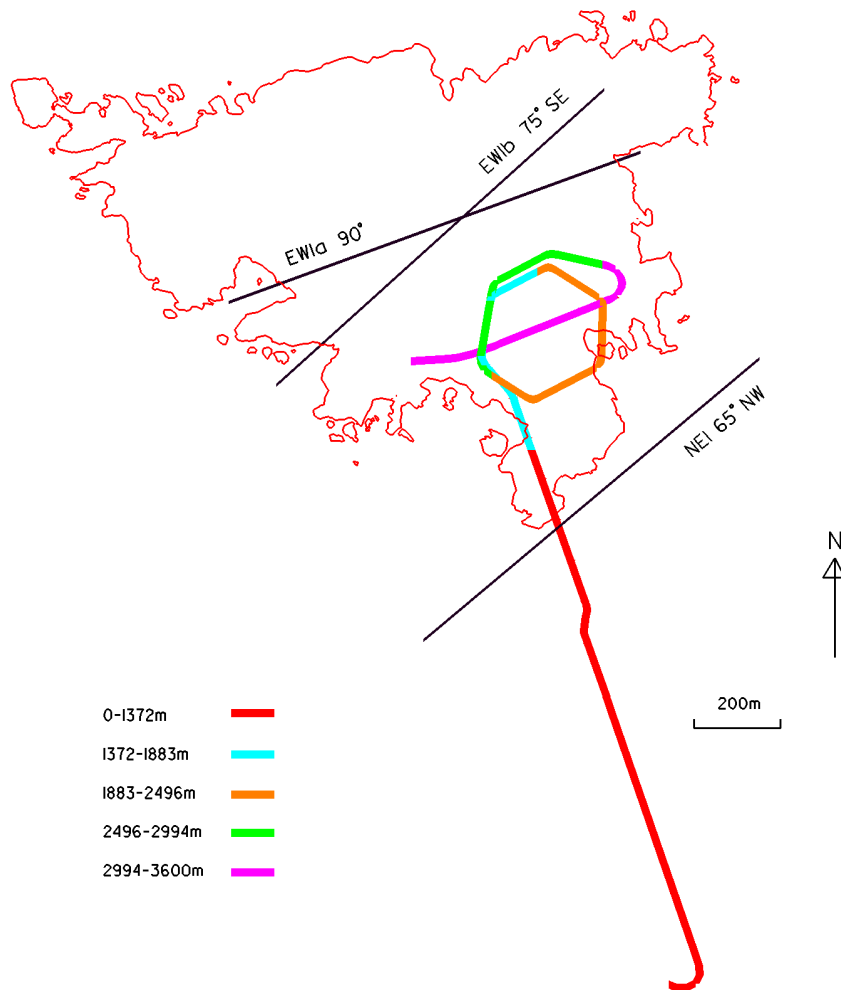


**Figure 5-8** Different sections along the tunnel chainage used in dividing the tunnel water inflow.

Although precipitation of fracture minerals may be the most likely explanation for decreasing tunnel water inflow, an alternative and plausible hydraulic reason for this observed decrease in tunnel water inflow is a, with time, smaller driving potential pressure from above. The extensive drawdown, for tunnel chainage 0-1372 metres, illustrated in Figure 4-13 does support this hypothesis. And the same is most probable for tunnel chainage 1883-2496 metres, which is located close to the centre of tunnel spiral drawdown.

Further, the accumulation of soil particles, from the geological zones, in the grout injected rock surrounding the tunnel may also contribute to a tightening of the seal in tunnel sections where the fringing rock has been grouted. Additional effects may arise from two-phase flow and degassing due to pressure changes in the rocks that fringe the tunnel e.g. /Jarsjö and Gale, 2001/.

Assuming that a decreasing potential pressure is at least partly responsible for the decreasing inflow. The lack of a decreasing trend in the other tunnel chainage sections than the ones described in the paragraphs above, indicate less hydraulic connectivity for some of the hydraulically active clusters of fractures defined along the tunnel spiral than what was previously defined by /Rhén et al., 1997a/ as hydraulic conductors (e.g.

NNW1 and NNW2). This since a well-connected conductor should show a decrease in flow at all positions if the main reason for the decrease inflow is a decreasing driving potential pressure.

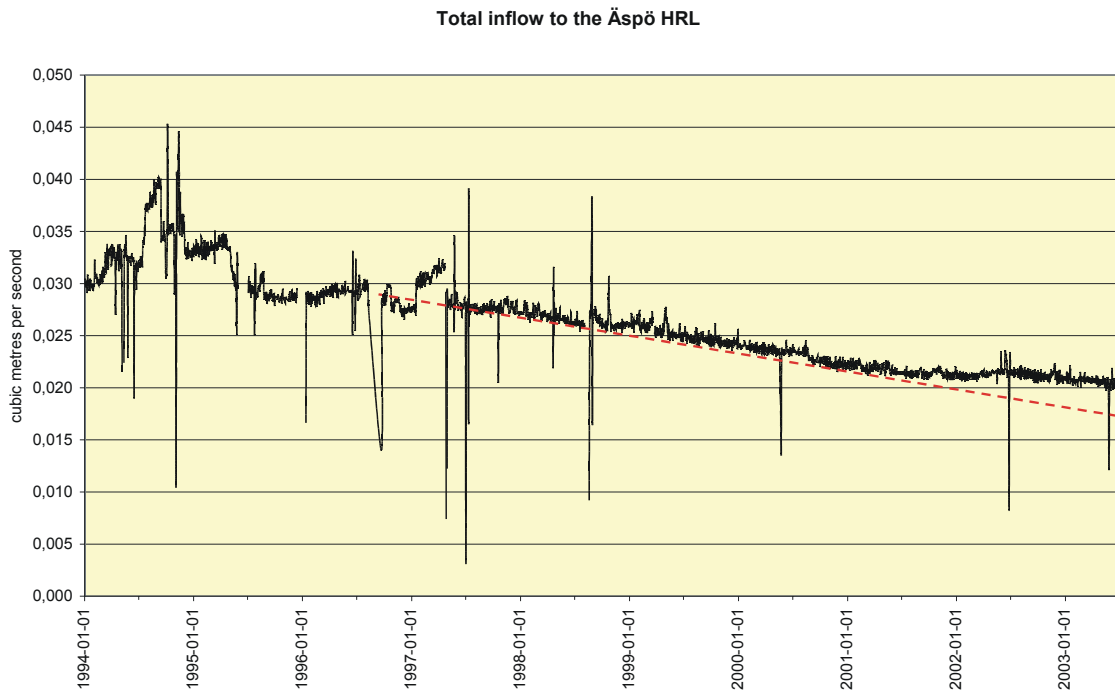


**Figure 5-9** Calculated tunnel water inflow from the bedrock, based on measured supplied and discharged water volumes within the entire Äspö HRL.

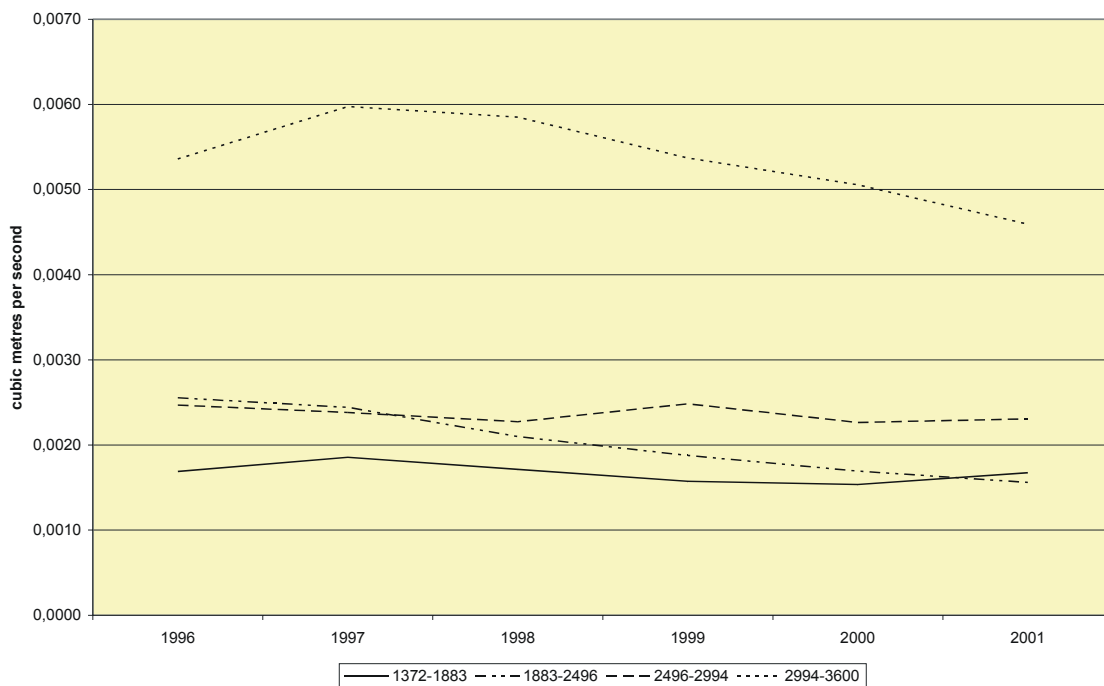


**Figure 5-10** Yearly average of measured tunnel water inflow for the tunnel chainage, 1372 - 3600 metres, divided into four different intervals.

Figure 5-11 presents year 2000 average tunnel water inflow along the different tunnel chainage sections.

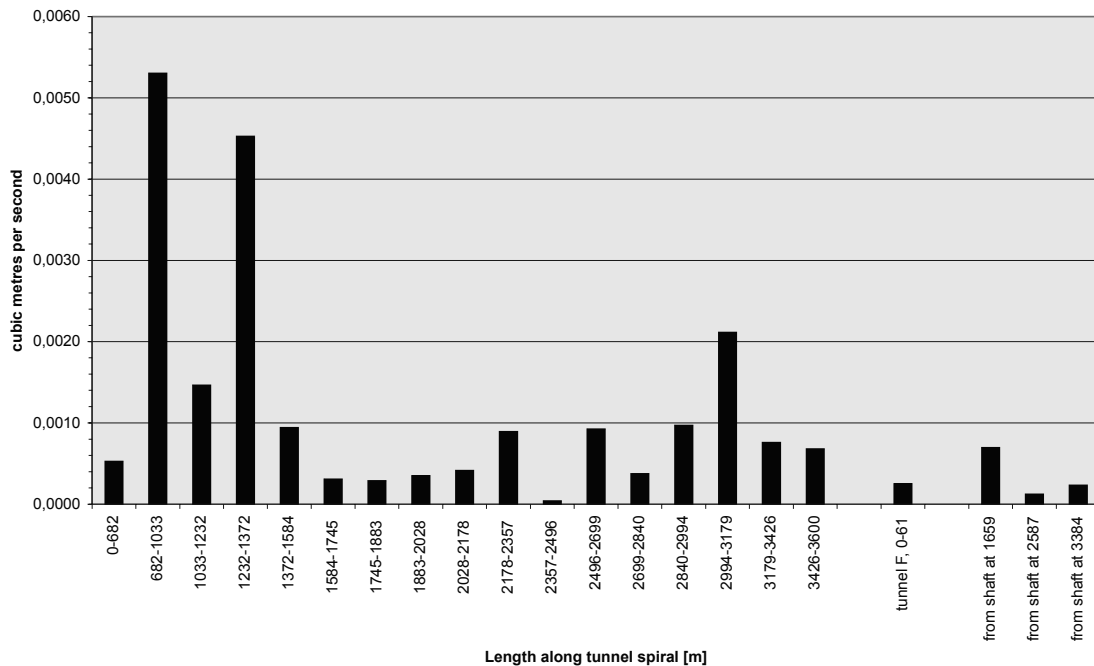


*Figure 5-11 Yearly average (for year 2000) of tunnel water inflow for all measurement sections.*

## 5.4 Hydraulic fracture statistics

### 5.4.1 Hydraulic feature intensity

Fracture statistics for dry as well as hydraulic features at Äspö is to be presented in /Berglund et al., 2003/. Therefore only a brief summary of results from the TRUE- and the Prototype Repository experiments and from the high-permeability study are presented below.

The intensity of conductive background fracturing has for a few sub-domains been derived directly from the POSIVA flow logs. This has been done by direct counting of flowing fractures and dividing that number with the measured length of the borehole. For estimates of the pure background fracture intensity the deterministic defined fractures are eliminated. The TRUE Block Scale project derived background fracture intensity,  $P_{10}$  [ $m^{-1}$ ] (number of fractures per unit length of the borehole), for the experimental volume denoted the TTV region. Based on measurements in four boreholes /Andersson et al., 2002b/ presents a mean value for the background fracture intensity of  $0.19 [m^{-1}]$ . For modelling purposes the fracture volumetric intensity,  $P_{32}$  [ $m^2/m^3$ ] (area of fractures per volume of rock mass), is more useful than the fracture intensity. The fracture volumetric intensity was calculated to  $0.29 [m^2/m^3]$  by use of the ratio,  $C$ , of the simulated values for  $P_{32}$  and  $P_{10}$  /Andersson et al., 2002b/.

Both in /Rhén & Forsmark, 2000/ and / Rhén & Forsmark, 2001/ results of fracture intensity is presented. The first is a high-permeability feature (HPF) study over the entire Äspö domain and the latter presents results from the Prototype Repository experiment. In both these studies the results are based on evaluated hydraulic tests with different length extension. This creates a probable decrease in the estimated values for the fracture intensity. Table 5-8 and Table 5-9 show results from these two studies, respectively. As a comparison to the TRUE Block Scale data presented above, /Andersson et al., 2002b/ present deterministically defined features with transmissivity values higher than  $1.0E-10$  [ $m^2/s$ ].

**Table 5-8 Distance between hydraulic conductors with a transmissivity (T) greater than a specified value of the transmissivity ( $T_j$ ). Data compiled from tables presented in /Rhén & Forsmark, 2000/.**

$T_j$ [ $m^2/s$ ]	Surface boreholes		Cored tunnel boreholes		Tunnel boreholes, probe holes*	
	Mean distance (arithmetic)	$P_{10}$	Mean distance (arithmetic)	$P_{10}$	Mean distance (arithmetic)	$P_{10}$
1.0E-11	3.27	0.31			18.93	0.05
1.0E-10	4.11	0.24			19.86	0.05
1.0E-09	7.57	0.13			20.88	0.05
1.0E-08	9.82	0.10	14.18	0.07	24.41	0.04
1.0E-07	13.79	0.07	14.15	0.07	32.51	0.03
1.0E-06	20.88	0.05	14.36	0.07	36.62	0.03
1.0E-05	44.88	0.02	27.21	0.04	73.25	0.01

- The tunnel probe holes are evaluated with an alternative method where the boreholes are stochastically combined creating a lengthier borehole than the original.

**Table 5-9 Distance between hydraulic conductors with a transmissivity (T) greater than a specified value of the transmissivity ( $T_j$ ). Data compiled from tables presented in /Rhén & Forsmark, 2001/.**

All boreholes in the Prototype Repository experiment**		
$T_j$ [ $m^2/s$ ]	Mean distance (arithmetic)	$P_{10}$
1.0E-11	1.89	0.50
1.0E-10	4.00	0.45
1.0E-09	5.99	0.20
1.0E-08	8.63	0.11
1.0E-07	17.02	0.06
1.0E-06	63.73	0.02

\*\* These tests are evaluated with an alternative method where the boreholes are not only stochastically combined to create a lengthier borehole, but the start and end point of the lengthier borehole is counted as a relevant feature.

## 5.4.2 Fracture transmissivity

Within the TRUE Block Scale experiment background fracture transmissivity values were established based on the flow values derived during the POSIVA flow logging. Based on these fracture transmissivity values /Andersson et al., 2002b/ present a fracture transmissivity distribution, reproduced in Figure 5-12.

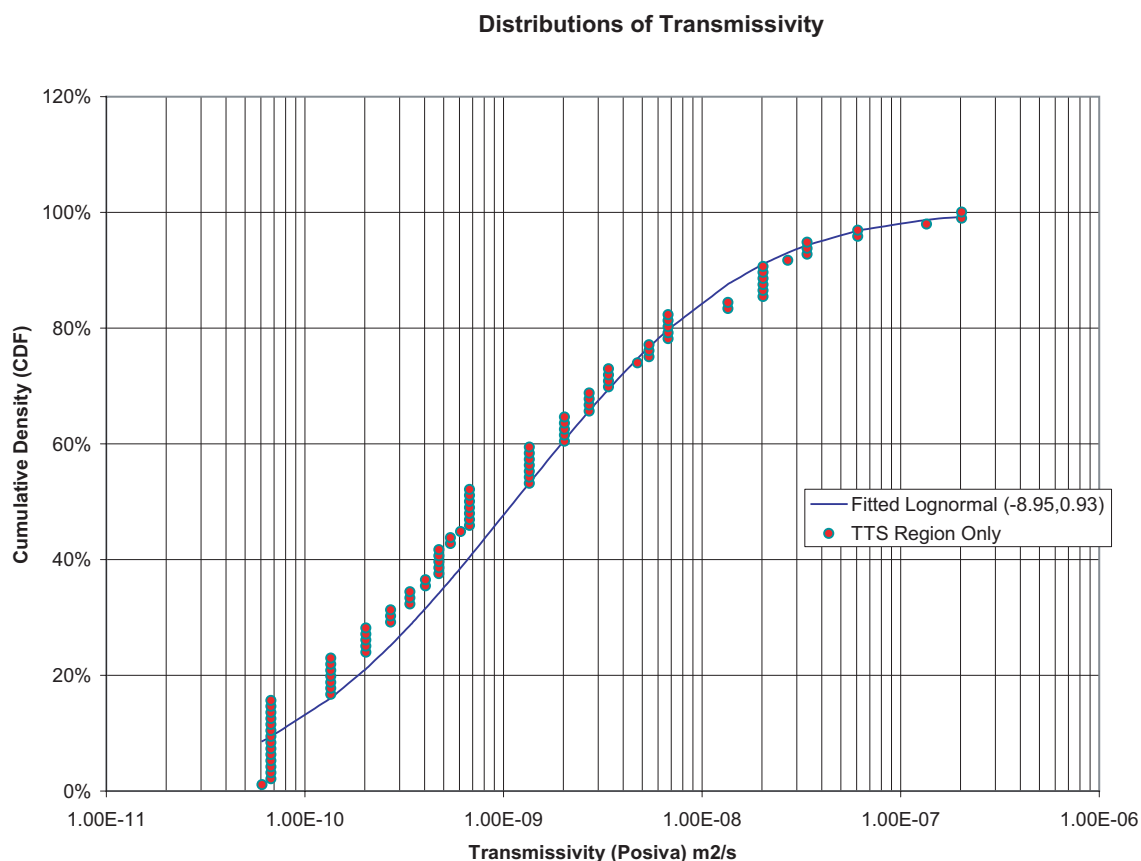


**Figure 5-12** Fit of a lognormal distribution to the TTV region data from the TRUE Block Scale experiment. The presented fit passes a Kolmogorov-Smirnov test at the 10 percent level. Figure taken from /Andersson et al., 2002b/.

The fracture transmissivity distribution established in the TRUE Block Scale experiment shows a good agreement with distributions based on numerical fracture simulation and hydraulic tests within specific length intervals, inferred from e.g. /LaPointe et al., 1995/ and /Uchida et al., 1994/ and also for the Laxemar area /Andersson et al., 2002a/.

Further, results from the Prototype Repository experiment suggests a highly skewed distribution, which is evaluated as lognormal and suggests mean values for the hydraulic conductivity around  $1\text{E}-10$  [m/s]. Based on these measurements /Stigsson et al., 2001/ concluded on fracture transmissivity values between  $1\text{E}-12$  and  $1\text{E}-10$  [ $\text{m}^2/\text{s}$ ] and standard deviations between 1.5 and 2.5 on the logarithmic values. The Prototype Repository region is, in general, a low-permeable region in the Äspö2 volume.

Contradictory to the evaluated results above, results from in-situ and laboratory tests on single fractures, e.g. /Hakami, 1995/ (laboratory aperture measurements), /Rutqvist, 1995/, and /Alm, 1999/ (in-situ hydraulic testing), indicate a higher mean fracture transmissivity around  $1.0\text{E-}6$  [ $\text{m}^2/\text{s}$ ]. None of these tests were performed at Äspö. Some of the fracture statistics used by Hakami were however based on a fracture replica from the Äspö HRL. The studies by /Rutqvist, 1995/ and /Alm, 1999/ also state the strong relationship between the estimated fracture transmissivity and normal stress. This fact indicates a clear anisotropy and depth dependency, which however concerning the depth dependency has not been significantly illustrated in the hydraulic field data compiled for the Äspö HRL.

## 6 Three-dimensional site descriptive hydrogeological modelling

Site descriptive modelling of the hydrogeology requires an integrated approach with inputs from several other disciplines. This section concerns the three-dimensional site descriptive hydrogeological modelling. Essential tools in hydrogeology are different kinds of hydraulic tests and numerical groundwater flow modelling. Both these kinds of tools are blunt, especially in a hard rock, and should be treated with care. Especially the latter tends to be used as a visualisation of the reality.

One objective with this project was to update the older Äspö96 hydrogeological model /Rhén et al., 1997a/. The Äspö96 model is based on performed work and collected data from the site characterisation and construction phases during the time period 1986-1995. The Äspö96 model was found to be a rigid model especially concerning the underlying treatment and evaluation of primary data; therefore it was decided, and a project prerequisite, to use the old results and not to rework the data. However, due to integrated results in this project it was impossible to adopt all of the hydraulic domain descriptions defined in the Äspö96 hydrogeological model. Still, due to the existing Äspö96 model the site descriptive modelling work in this project has both the advantage and disadvantage of using an older model as a part in the modelling work.

### 6.1 General modelling assumptions

The bases for the hydrogeological modelling are the identified objects within the geological model. Essential objects are *Deformation Zones*, *Rock Units*, and *Soil Units*. Deformation zones may be brittle deformation zones (fracture zones) or ductile deformation zones. Rock units as well as soil units can be combined into domains to illustrate parts of the rock or soil with similar characteristics but geometrical separated.

The evaluation results from hydraulic tests together with a geometrical description of the geological model gives as result parameters and properties of the *Hydraulic Conductor Domains (HCD)* and *Hydraulic Rock Domains (HRD)* that in general coincide with the defined deformation zones and rock domains respectively (Figure 6-1). However, if the hydraulic properties significantly vary within the defined geological zone or domain, these may be subdivided into two or more HCD or HRD respectively.

## Hydrogeological description

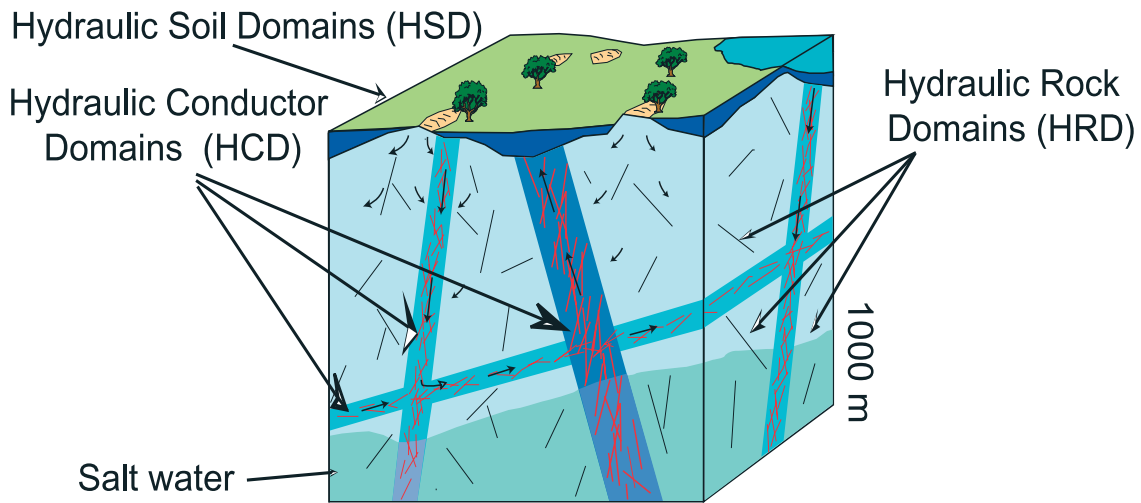


*Figure 6-1* Principal illustration of features in a hydrogeological model. Taken from /Andersson et al. 2002a/.

## 6.2 Modelling strategy

### 6.2.1 Rock

The first step in the development of the site descriptive hydrogeological model is to use the geometrical geology model and hydraulic tests to analyse the different geological units. These analyses give valuable information for assigning properties and boundaries to the defined units.

Measured pressure responses in surrounding boreholes gives valuable information about the connectivity pattern within the model domain. Both the information from geometrical descriptions and hydraulic tests and the observed pressure responses give information for assignment of anisotropic properties and behaviour.

A subsequent step is the implementation of primary information into a numerical groundwater flow model. By the use of explorative simulations the natural conditions can be exemplified in three dimensions. Hydraulic responses can sometime be explained and also predicted. These types of explorative simulations are used to validate both the geometrical descriptions of different hydraulic units and the assigned properties. For the Äspö02 model it was due to economical and time aspects decided to use an older numerical groundwater simulation, the Laboratory Scale model /Svensson, 1999/, which geometrical boundaries fit into those of the Äspö02 model domain.

At Äspö a massive amount of hydraulic tests have been performed and herein the results are compiled and used as input in the assigning process. Further, previous performed model exercises both the Äspö96 model and local-scale modelling for experimental sites are used in the development of the Äspö02 model.



### **6.2.2 Quaternary deposits**

For most modelling cases grain size distribution curves and hydraulic tests in the soil layers is the base for the assigning of properties to the geological soil units. Only limited tests of the soil characteristics at Äspö have been performed. Further the Quaternary deposits are thin and in general localised in the low areas of Äspö (Figure 4-4). Therefore, and due to the focus on the tunnel spiral depth interval, no Hydraulic Soil Domains (HSD) have been assigned for the Äspö02 model.

## **6.3 Definition of HCDs and HRDs based on primary data and the geological 3D site descriptive model**

Several geological and hydrogeological observations have been used to test different geological alternatives of possible deformation zones. In this Section the chosen geometrical descriptions of hydraulically essential geological domains are compiled and given hydrogeological characteristics.

### **6.3.1 Hydraulic Conductor Domains**

Figure 6-2 illustrates the location of the defined hydraulic conductors. Table 6-1 presents a condensed set of hydrogeological information about each of the defined hydraulic conductors. The defined hydraulic conductors coincide with geological zones, however, neither the exact position nor the width is an absolute prerequisite between the hydraulic conductor and the geological zone. Further, there are geological zones that have no hydraulic significance and hence are not defined as a hydraulic conductor.

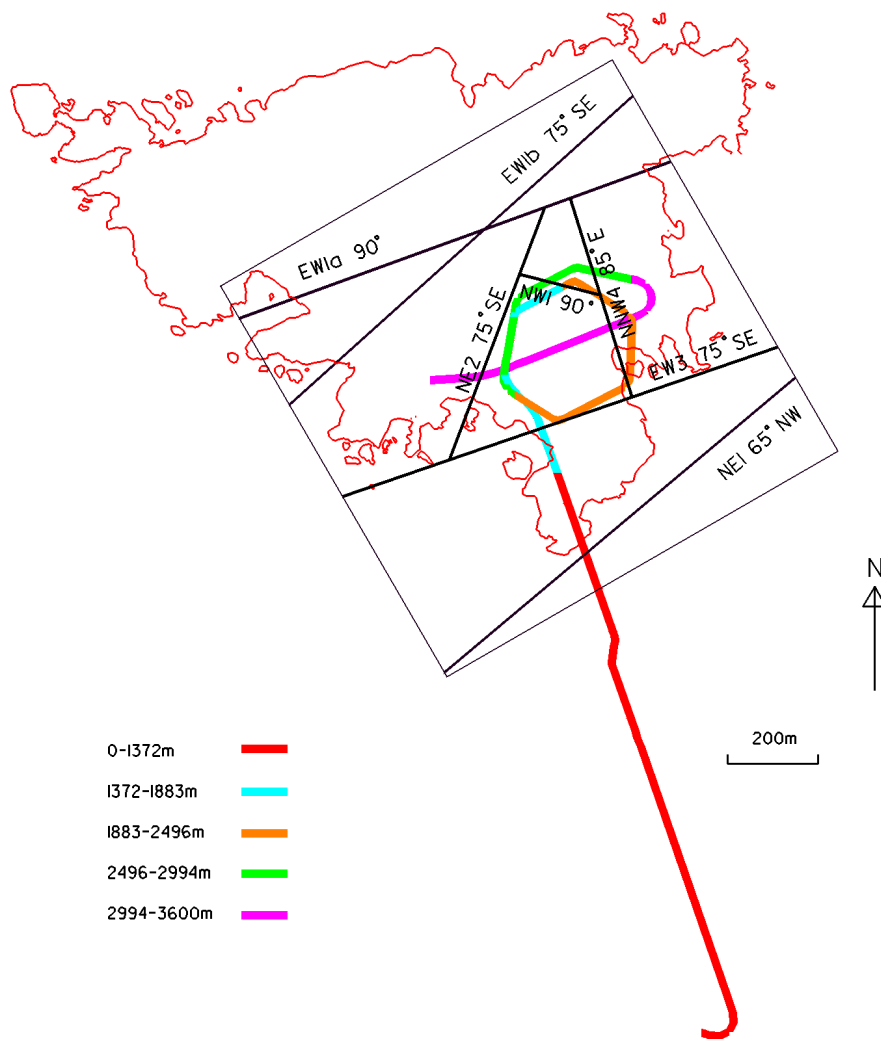


Figure 6-2 Hydraulic conductors defined within the Äspö02 model.

Table 6-1 Hydraulic conductor domains defined within the Äspö02 model.

HCD	Idcode	Hydraulic conductivity [m/s]	Barrier	Hydraulic width at z=0 [m]	Depth dependent thinning	Terminating at...
EW-1(a)	ZAS0001A0	2.6E-08*	SEMI*	20*	yes	
EW-1(b)	ZAS0001B0	6.0E-07*	SEMI*	20*	yes	
NE-2	ZAS0004A0	1.2E-08*		10*		
NNW-4	ZAS0005A0	6.5E-06*		10*	yes	
NW1	ZAS0007A0	5.0E-07**		10**		
EW-3	ZAS0003A0	1.7E-06*		10*		NE1
NE-1	ZAS0002A0	2.2E-05*		10*		

\* /Rhen et al., 1997a/

\*\* Based on analyses of compiled data which are specified in a zone ATLAS<sup>5</sup> (in prep.).

<sup>5</sup> The Atlas refers to zone descriptions, which compile essential information from geology, hydrogeology, and hydrogeochemistry.

The EW1 zone is a fairly wide and complex structure, which based on geological information is believed getting thinner with depth reference. In the geological model, EW1 is considered having a more fractured structure in the northern and southern parts of the zone /Rhén et al., 1997/. Therefore EW1 is considered as two hydraulic conductors. Hydraulic interference tests have confirmed that the core of the EW1 zone shows a behaviour of a semi-permeable barrier /Rhén et al., 1997a/, even though some single-borehole tests in KAS04 indicate a couple of high water conductive sections through the EW1 zone. The EW1 zone is one of two zones with a regional extent within the model domain. The recognition of EW1 as a major weakness zone /Berglund et al., 2003/ yields that the EW1 zone together with NE1 probably have played an important role in the development of faults in between these zones. These two zones may be viewed as the southern and northern geological boundaries for the laboratory. As such a boundary EW1 can be defined as a no-flow boundary.

The NE2 zone is a fairly low conductive structure at all locations where it is intersected by the tunnel /Rhén et al., 1997/. Further the geological information suggests that the zone is undulating (possibly splaying) and is getting thinner with depth and towards north /Berglund et al., 2003/. The chemical signature of tunnel inflow water in this structure suggests a increasing meteoric water content, all while the Baltic Sea water and the glacial water decrease in content proportions /Rhén et al., 1997b/.

The NNW4 zone is located along many high leakage positions in the tunnel. Further the geological information suggests that the zone change character with depth. NNW4 is expected to intersect the tunnel at tunnel chainage 3130-3165. This does not occur, however a number of individual fractures with a similar strike as NNW4 suggests that the zone has been ended into several sub-parallel fractures /Berglund et al., 2003/.

The NW1 zone is from a geological view thin, but hydraulic information suggests a conductive domain of approximately 10 metre thickness.

The EW3 zone is believed to terminate at its contact with the NE1 zone /Berglund et al., 2003/, which on average happens at an approximate depth of 200 metres below the ground surface. The interpretation by /Rhén et al., 1997a/ is that the core of the EW3 zone has on average a low hydraulic conductivity. The geological characteristics of this zone indicate a partly clay altered core /Berglund et al., 2003/. /Rhén & Stanfors, 1995/ concluded that this structure is fairly wet and pre-grouted on the southern side but dry with no pre-grouting on the northern side. It is therefore a plausible conclusion that this hydraulic conductor is located along the edge of the structure at the southern side of the zone /Rhén et al., 1997a/.

The NE1 zone is one of two zones with a regional extent within the model domain. The recognition of NE1 as a major weakness zone /Berglund et al., 2003/ yields that the NE1 zone together with EW1 probably have played an important role in the development of faults in between these zones. These two zones may be viewed as the southern and northern geological boundaries for the laboratory. Based on graphs presented in /Rhén et al., 1997b/ the tunnel water inflow from the NE1 zone showed an increase in Baltic Sea water - and decreasing proportions of the other available waters - during the first two years after the tunnel crossed the structure. /Rhén et al., 1997a/ refer to several hydraulic tests that indicate a good hydraulic connectivity between hydraulic responses in the NE1 zone and the eastern parts of the rock domain named Block 3 and the NNW4 zone. This fact, together with the experiences from grouting of the NE1 zone suggests that the zone is permeable for flow across its extension even though a completely clay-altered core is described /Rhén et al., 1997a/.

### **6.3.2 Hydraulic Rock Domains**

The statistical information presented in Figure 6-3 can be used to estimate hydraulic properties of the rock mass between the deterministic fracture zones. This statistical information is however strongly biased from experimental objectives, strike and dip of geological structures, amount of tests, etc., which to a large degree make the information inappropriate. However, used quantitative together with geological descriptions of the blocks it is conclusive that no significant difference exist between the different blocks and that all block may be viewed as one Hydraulic Rock Domain (HRD). Hence assigning the anisotropic results of the Äspö02 domain for hydraulic conductivity (Table 6-2 and c.f. Table 7-1)

Spatial assignment for the specific storage is hard to assess in a fractured media. However estimates from the Äspö HRL suggest a minimum specific storage around  $1.0E-09 [m^{-1}]$ . A weak relationship between hydraulic conductivity and the specific storage has been observed. Based on linear regression (Appendix 3) of the data illustrated in Figure 5-7 anisotropic values corresponding to respectively hydraulic conductivity value may be assigned (c.f. Table 7-3).

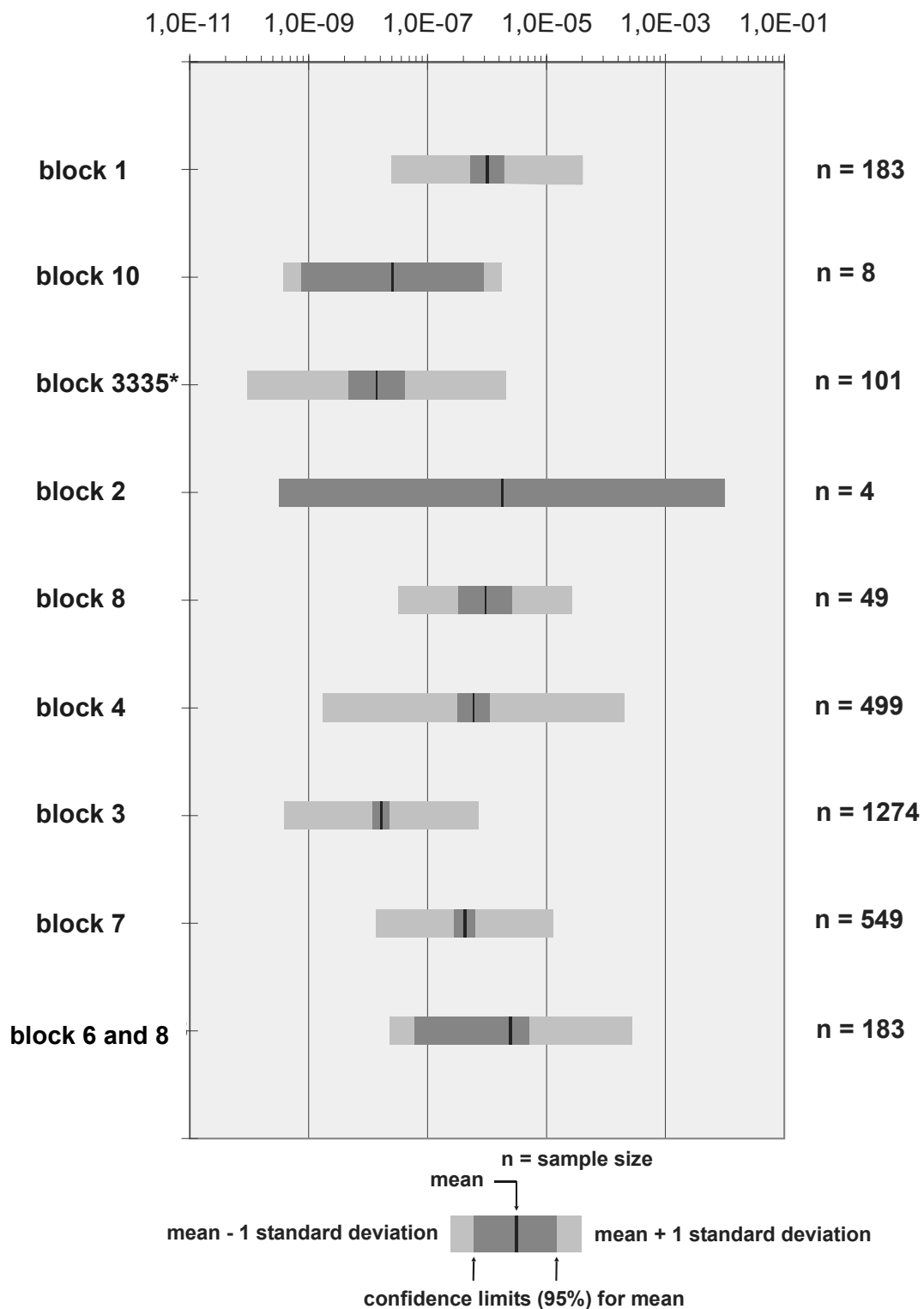


**Figure 6-3** Descriptive statistics of the hydraulic conductivity (m/s) for defined rock blocks within the Äspö02 model. The Block numbers are working names but identical with the working names used in Geology /Berglund et al., 2003/. Block 3335 has no orientated data for the fractures and have therefore not been given a name (the block belongs to the southern part of Äspö02). Block 8 has been split and also block 6 has been merged with parts of block 8. This is due to difference between base model version 1 which was used for statistical work and the final base model (version 2).

**Table 6-2 Anisotropic mean value statistics for defined rock domains within the Äspö02 model. Mean values are based on available surface and probe borehole data for each defined rock domain. Results from Äspö 96 are given for comparison.**

Rock block unit	Vertical plane, 120-140° (m/s)	Vertical plane, 20-80° (m/s)	Horizontal plane (m/s)	Ratio
Äspö96	1.1E-07	4.2E-10	4.0E-09	260:1:10
Äspö02	2.7E-07	1.6E-09	3.6E-09	170:1:2.2
1	3.2E-06	2.7E-06	4.2E-08	75:65:1
10	-	-	2.2E-09	
3335	-	-	1.3E-09	
4	1.2E-07	8.1E-12	1.0E-09	15000:1:125
3	2.8E-07	1.3E-09	1.9E-09	215:1:1.5
7	-	-	5.6E-09	
6 & 8	-	5.0E-08	-	

### 6.3.3 Correlation with geological characteristics

/Rhén & Forsmark, 2000/ performed a study on high-permeability features (HPF,  $T > 10^{-5}$  [m<sup>2</sup>/s]) occurrence in relationship to geological characteristics, such as rock type, rock contacts, rock veins, crushed rock/natural fractures, and areas of high/low (Rock Quality Design) RQD values.

It is significant that the HPFs are more than twice as frequent within the fine-grained granites compared to the other lithological units at Äspö. The fine-grained granite composes about 15% of the rock units at Äspö but contains approximately 30% of the HPFs. The High-Permeability Features are less frequent in Äspö diorites with approximately 41% in relationship to the 55% occurrence of the rock unit. The other rock units at Äspö (Smålands granite, greenstone, mylonite, and quartz veins) cannot be significantly differentiated from their normal occurrence. Additionally important is the amount of veins of fine-grained granites within test sections composed of Äspö diorite and Smålands granite. This may indicate on an even stronger importance of the fine-grained granite units as hydraulic domains.

It could not be significantly illustrated that rock contacts were an important feature for the location of HPFs. For the case of rock veins it could be concluded that the fine-grained granite frequently occur as imbedded or host rock for pegmatite veins.

High-permeability features are not significantly dominating within rock of a specific RQD. Important however is that HPFs occur either for low or high RQD values and very few HPFs occur for RQD values between 20 and 80. Similarly, the results from correlation between crushed rocks or natural fractures indicate that 43% of the HPFs occur in relationship to crushed rock regions and 57% relates to natural fractures.

### 6.3.4 Hydraulic connectivity pattern

/Gurban, 2002/ performed a visual connectivity study on a series of different surface boreholes (KAS). As a preliminary result this study indicate that there exist connectivity between all of the affected rock blocks.

Further investigations were initiated but have not been finalised due to project decisions.

### **6.3.5 Hydraulic Soil Domains**

As the soil cover is thin and often missing no hydraulic information have been established. Even though the soil being important in issues concerning deeper groundwater recharge little other than soil cover distribution accessible from Figure 4-4 and Section 4.3 is known.

## **6.4 Hydrogeological simulation approach**

SKB's systems approach to hydrogeological modelling is described in the general programme for site investigations /SKB, 2001/.

In short: A site's hydrogeological properties and states are described by a parameterisation, which details the hydraulic properties of both quaternary deposits and bedrocks, and governs the hydrological processes. The model domain is divided into Hydraulic Soil Domains (HSD), Hydraulic Conductor Domains (HCD), and Hydraulic Rock Domains (HRC) as described in Section 6.1. Each hydraulic domain with its geometric description defines a hydrogeological region that should be implemented in a numerical groundwater flow model. The size and the position of the boundaries in a numerical model depends on the purpose of the modelling, hydrological conditions, and strive to set simple and trustworthy boundary conditions on the vertical and bottom boundaries.

In this section the results from a numerical groundwater flow model is used to test how well the hydrogeological descriptive model compares to measured large-scale hydrogeological conditions. The use of a numerical groundwater flow model to integrate detailed information within a volume can increase the confidence of the descriptive model. The groundwater flow model is also used to create a spatial description of flow. However, a tested and calibrated numerical groundwater flow model also yields information of type of major uncertainties and the spatial arrangement of these areas.

It is concluded that the main features of the geological description of the Äspö96 model are essentially the same as the updated model, Äspö02. Therefore the use of a numerical groundwater flow model based on this descriptive model is ratified however the need of a more thorough discussion on uncertainties is essential.

## 6.5 Numerical code

The spatial extension and also due to that it is a recent model the Laboratory Scale analysis /Svensson, 1999/ was chosen as the most representative numerical groundwater flow model available.

The system of essential equations is solved by the general equation solver PHOENICS, /Spalding, 1981/. PHOENICS is based on a finite-volume formulation of the basic equations and embodies a wide range of coordinate systems and numerical techniques. Output parameters from the code are primary pressure, salinity, and Darcy velocities; however it is a simple task to generate additional output parameters such as hydraulic head and density.

The conceptual idea behind the geometrical description in the numerical groundwater flow model is a Discrete Fracture Network (DFN) approach. This leads to an essential transformation of the described fracture network into equivalent inter-node conductivity values prior to the solution of the flow equations. Hence, the numerical groundwater flow model is able to capture the anisotropy, possible correlation, and heterogeneity of a geological environment.

Besides the major deterministic zones (HCDs) the numerical groundwater flow model also contains random hydraulic features. These latter features are a description of the background fracturing composed of conductive fractures and minor conductive zones not modelled deterministically in the defined HRDs. Conductive features with an extension shorter than the numerical cell size cannot directly be accounted for. This is solved by the use of a background hydraulic conductivity value for the rock mass.

## 6.6 Numerical modelling approach

The numerical groundwater flow model is based on the geological model from Äspö96. The model horizontal extension is described in Figure 6-4 with a considered depth interval of 200 metres down to 560 metres. The cell size in the numerical groundwater flow model is 5 metres.

Only the geological model of Äspö96 is considered and not the updated Äspö02 version nor presented alternatives.



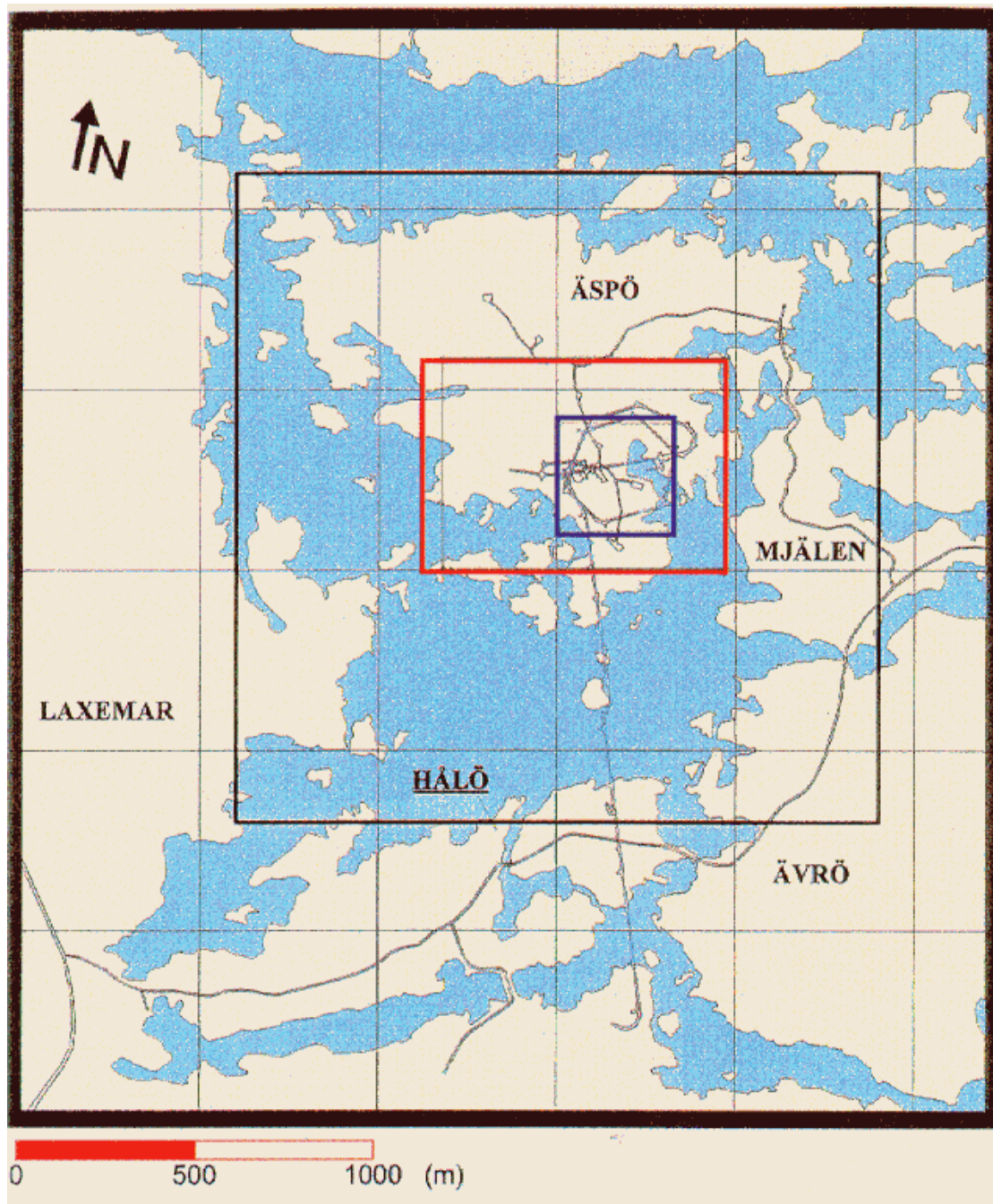


*Figure 6-4 The isle of Äspö and the Äspö HRL. The black rectangle shows the area of the Site Scale model /Svensson, 1997a/. The red rectangle shows the main computational domain considered in this study. The blue rectangle shows an area where a special study of the conductivity statistics on a 3 metre scale was performed within /Svensson, 1999/. Taken from /Svensson, 1999/.*

### **6.6.1 Hydraulic Conductor Domains (HCD)**

The properties of the HCDs are taken from the hydrogeological Äspö96 model and partly modified based on calibrations made in /Svensson, 1997a/. Property values are summarised in Table 6-3 with additional comments on diversions related to the Äspö02 properties and zones.

**Table 6-3 Used transmissivity and width of conductive structures on Äspö (based on Table 3-1 in /Svensson, 1999/).**

HCD	Transmissivity [m <sup>2</sup> /s]	Width [m]	Comments
EW1, 88°	5.2E-07	20	
EW1, 78°	1.2E-05	20	
EW3	1.2E-05	10	Modified due to calibration in /Svensson, 1997a/.
NE2	8.0E-06	10	Modified due to calibration in /Svensson, 1997a/.
NE1	3.0E-04	10	Modified due to calibration in /Svensson, 1997a/.
NNW1	3.0E-05	10	Modified due to calibration in /Svensson, 1997a/. Not a HCD in Äspö02.
NNW2	1.0E-05	10	Modified due to calibration in /Svensson, 1997a/. Not a HCD in Äspö02.
NNW3	2.0E-05	10	Not a HCD in Äspö02.
NNW4	6.5E-05	10	
NNW5	4.0E-06	10	Not a HCD in Äspö02.
NNW6	1.4E-05	10	Not a HCD in Äspö02.
NNW7	8.0E-05	10	Modified due to calibration in /Svensson, 1997a/. Not a HCD in Äspö02.

### 6.6.2 Hydraulic Rock Domains (HRD)

As far as hydraulic rock domains were considered in /Svensson, 1999/ it was as one homogeneously described background fracture volume. The background fractures were specified with respect to orientation, size distribution, fracture intensity, width, and transmissivity distributions. Where the transmissivity distribution were used as a calibration parameter.

The fracture orientation was based on field results from primary three experimental sites. These were the TRUE Block Scale volume, the ZEDEX tunnel and the TBM tunnel. Based on results from these three experiments it was decided that three major fracture sets were to be used. Namely one horizontal -, one sub-vertical north-west trending -, and one sub-vertical north-east trending fracture set. Of these three sets the horizontal set is defined as the least water conductive and the north-west the most water conductive fracture set. The treatment of the differences in hydraulic conductivity for different fracture sets was done by an intensity control; that creates most fractures in the northwestern direction and least for the horizontal fracture set. The spread within the orientation is for each fracture orientation described by a Fisher dispersion coefficient.

The amount of fractures is specified using a power law distribution, with a power exponent of  $-2.6$ . The used intensity was defined by generating a fracture length sample with comparable lengths to the deterministic fracture zones. Fracture shape is assumed square with a length (L) and for each fracture length sample a specified and constant width on the relationship of  $0.02 \cdot L$ ; however, with the restriction that the ratio between fracture width and cell size must be larger than 0.1. Statistics for one generation of the background fractures is presented in Table 6-4.

Figure 6-5 illustrates one realisation of high permeability features with a transmissivity value  $\geq 1.0E-06$  [m<sup>2</sup>/s].

**Table 6-4 One generation of background fractures presented for six different fracture length samples. Based on Table 3-2 in /Svensson, 1999/.**

Fracture length sample, #	Length interval [m]	Number of generated fractures	Mean length [m]	Specified width [m]
1	320-160	33	208	4.2
2	160-80	110	104	2.1
3	80-40	537	52	1.0
4	40-20	2830	26	0.5
5	20-10	15554	13	0.5
6	10-5	92076	6	0.5

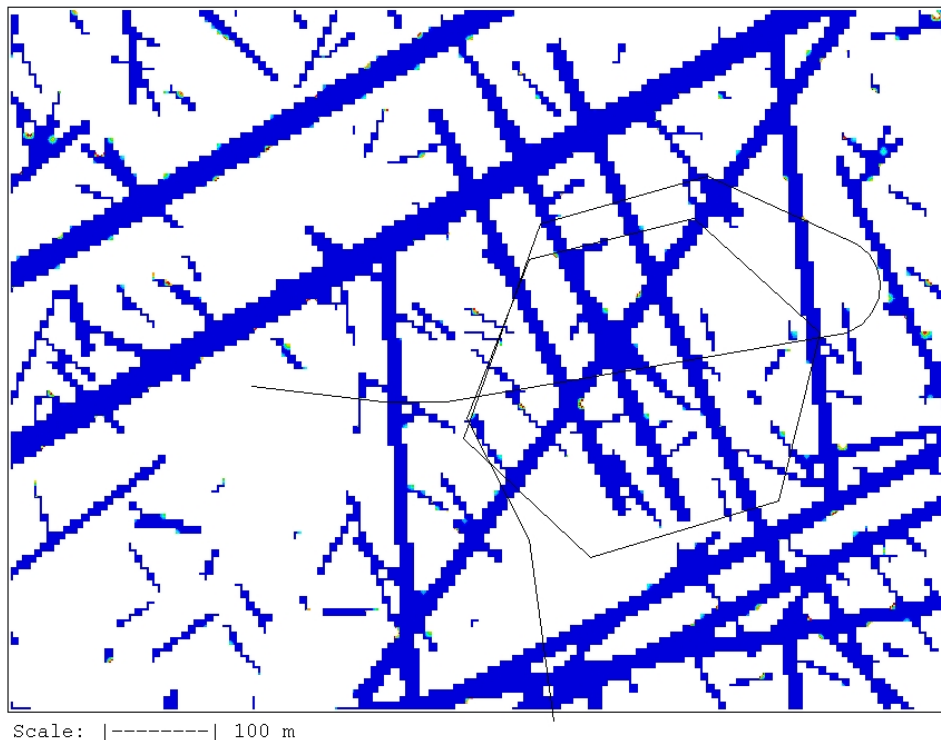


**Figure 6-5** Illustration of calculated High Permeability Features ( $T \geq 10^{-6} [m^2/s]$ ) for a depth of 450 metres. Taken from /Svensson, 1999/.

### 6.6.3 Boundary conditions

For the case in this numerical groundwater flow model the boundary conditions on all six sides are given as prescribed pressure (Figure 6-6) and salinity distributions. These are generated from the result of the Site Scale model /Svensson, 1997a/ (for extension see Figure 6-4). In this latter numerical groundwater flow model the cell size is 20 metres and therefore needed to be transformed into the smaller cell size of 5 metres used in the Laboratory Scale model. The transformation is done by linear interpolation. The boundary conditions of the Site Scale model is based on the result of the Regional Scale model /Svensson, 1997b/, which had its boundary conditions set as no flow boundaries on the mainland and as hydrostatic on the boundaries facing the Baltic Sea (eastern and parts of the southern). The salinity was specified based on the relationship found on Åspö and described in /Rhén et al., 1997a/.



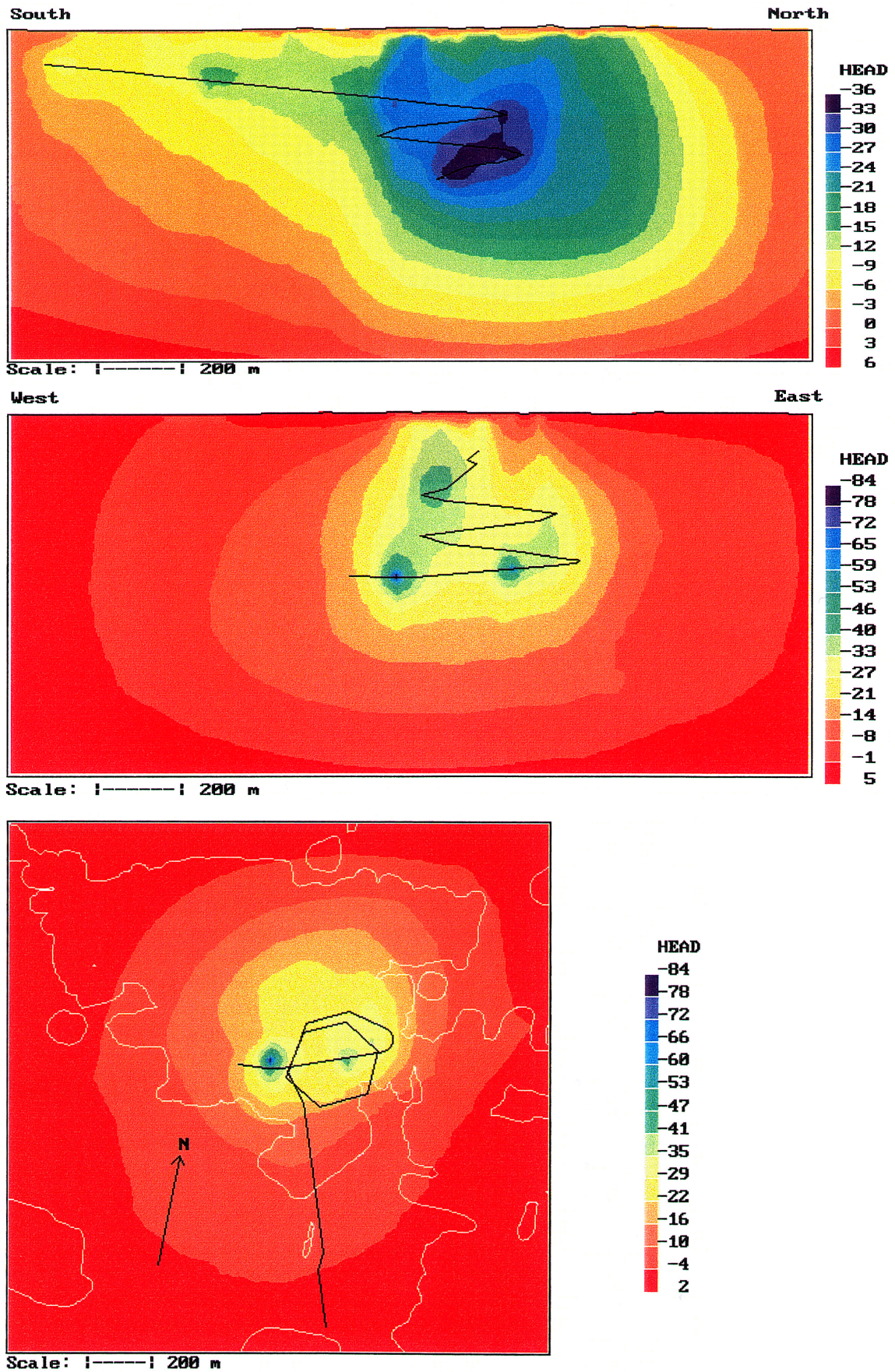
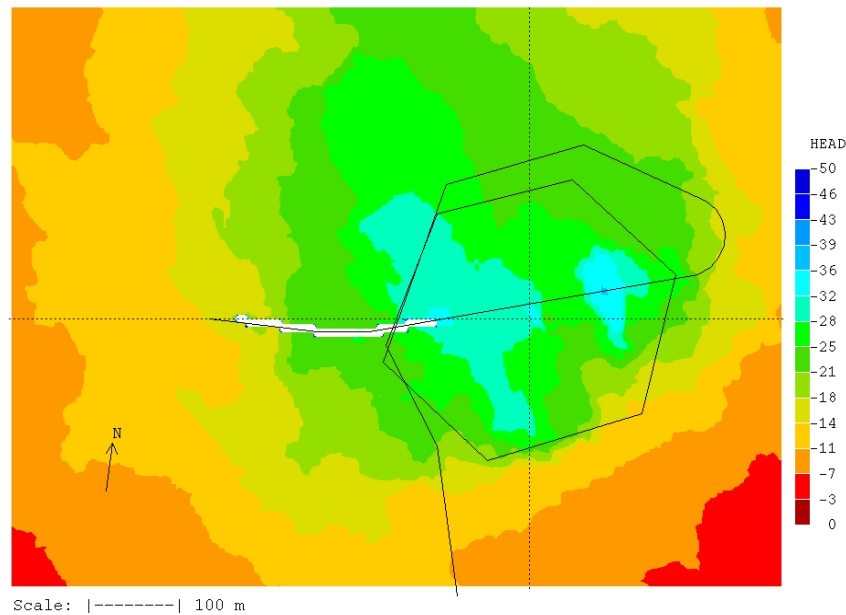


Figure 6-6 Hydraulic head (m) distribution from the Site Scale model /Svensson, 1997a/.

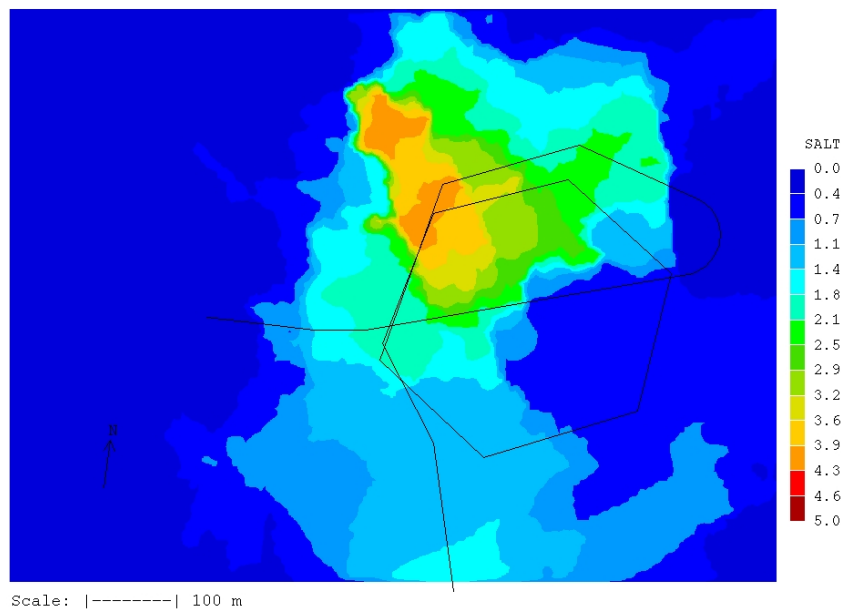
### 6.6.4 Results

/Svensson, 1999/ provides a detailed description of the numerical groundwater flow modelling and all the results. Herein the results are briefly summarised and briefly commented. Further comments may also be found in section 6.6.5.

Figure 6-7 presents the resulting hydraulic head situation in a horizontal section at 450 metres depth. The maximum drawdown corresponds well with the measured values. This maximum drawdown is essentially located in deterministic hydraulic conductors.



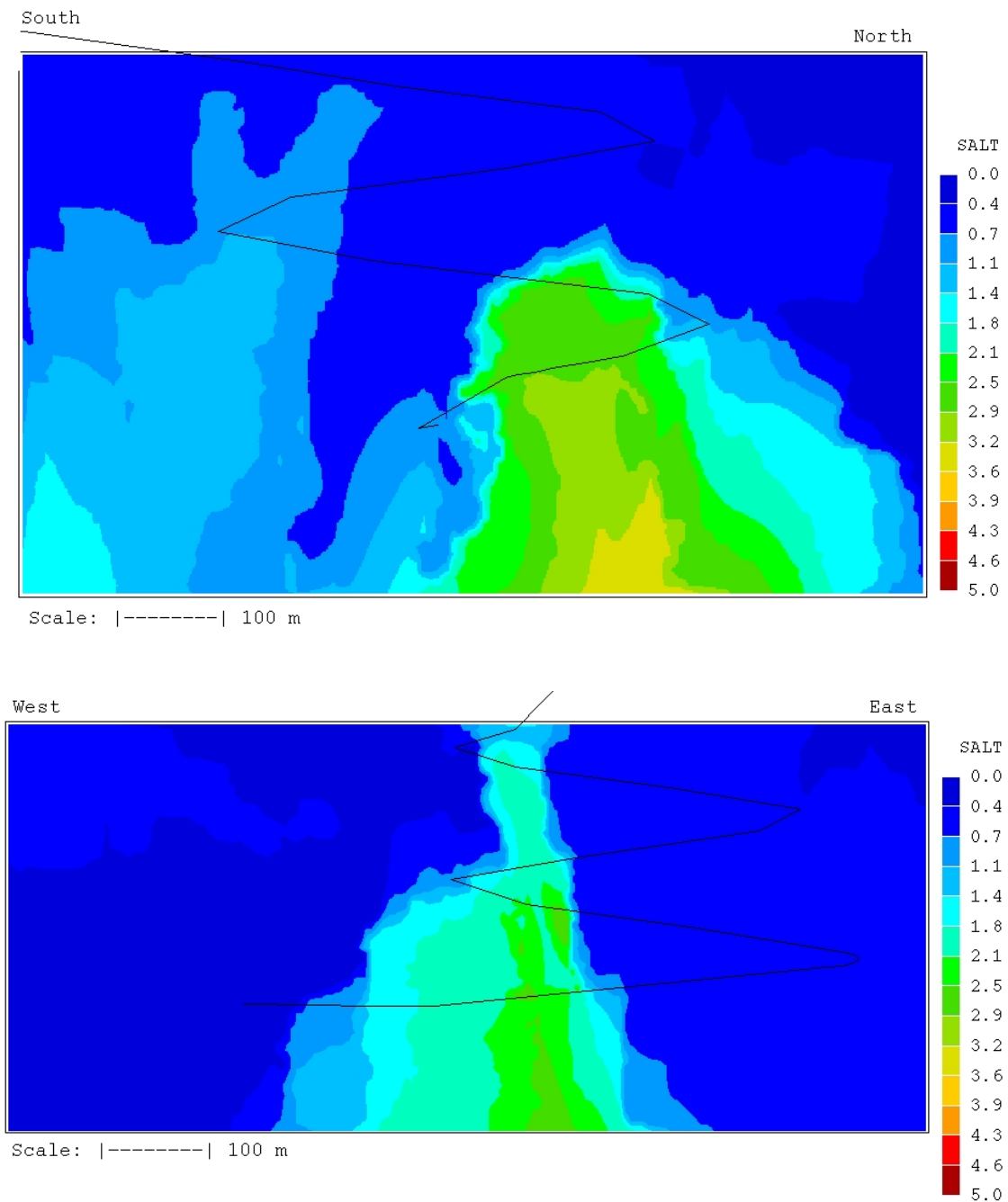
**Figure 6-7** Hydraulic head (m) distribution at a depth of 450 metres below ground level. The two dashed lines show positions for the vertical sections in Figure 6-9. White area along the tunnel mark prescribed atmospheric pressure /Svensson, 1999/.



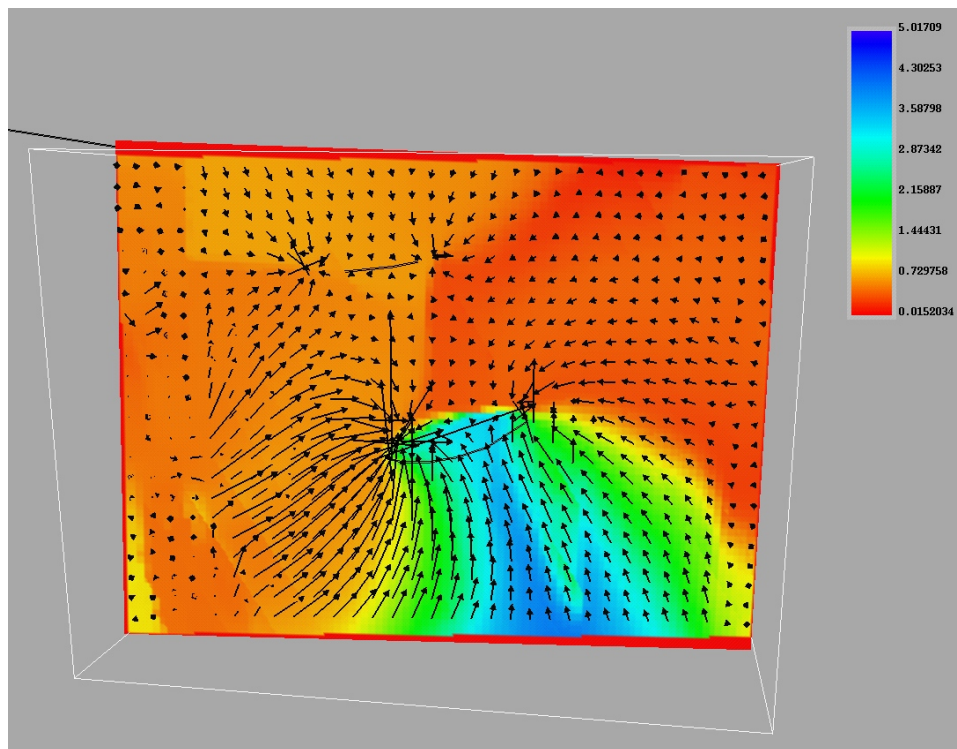
**Figure 6-8** Salinity (%) distribution at a depth of 450 metres below ground level /Svensson, 1999/.



Figure 6-8 and Figure 6-9 present the resulting salinity distribution in the model domain. Figure 6-8 presents the distribution of salinity at a horizontal plane at 450 metres depth, while Figure 6-9 presents the distribution in two cross-sections that correspond to the lines shown in Figure 6-7. The maximum salt concentration is found in deterministic structures and partly associated with the deepest drawdown. Figure 6-10 shows the salinity distribution but also the flow vectors in the deterministic structure NNW4. In this illustration it is clear that the sink, that is the lower part of the tunnel crossing the structure, creates a strong effect of upconing on the brines.



**Figure 6-9** Salinity (%) distribution in two vertical sections /Svensson, 1999/.



**Figure 6-10** Flow and salinity (%) distribution in NNW4. View from east /Svensson, 1999/.

### 6.6.5 Uncertainties

This Section is for main parts based on personal communication with /Follin, 2003/ but also /Ericsson, 2003/, /Rhén, 2003/, /Svensson, 2003/, /Berglund et al., 2003/, and /Eliasson, 2003/.

The Laboratory Scale model is the third and last groundwater flow model in a series of three /Svensson, 1997b/, /Svensson, 1997a/, and /Svensson, 1999/. The three models are clearly coupled in terms of boundary conditions but less united in terms of hydraulic properties and hydro-philosophy. Looking back at the three numerical models from the viewpoint of the Äspö02 model, however, one may wonder about the appropriateness of various assumptions made in the three model studies and, hence, the reported results.

The three models are all based on the integrated finite difference (finite volume) formulation for the solution of the governing equations (momentum and continuity), but focus on different scales. The Laboratory Scale model is a high-resolution flow model of the central part of the Äspö HRL. However, it is also an experimental model from a flow modelling approach point of view. The Laboratory Scale Model uses a new fracture network algorithm to derive grid cell hydraulic conductivity values. The algorithm consists of two parts, one statistical, which treats the generation (production) of fractures, and one hydraulic, which computes grid cell conductivity values. The correctness of the statistical part is not clear-cut from a structural geology point of view although there are no obvious reasons to be against the simplifications made in this particular case. For example, the structural analysis of trace line data suggests three fracture sets in the Äspö area, but the Laboratory Scale model only assign hydraulic parameters to the two most conductive ones.

Furthermore, the Laboratory Scale model is based on two significant assumptions, which both may be disputed, depending on the reader's own perception of hard rock hydrogeology. The two cornerstones of the laboratory model are:

- The generation of stochastic features (fractures) follows a power law distribution for the fracture size (length).
- There are positive, linear correlations between the fracture size and other geometric properties of the stochastic fractures including their transmissivity.

The following points compile the main objectives concerning the numerics of the Laboratory Scale model.

- Boundary conditions - pressure and salt concentration were specified on all surfaces, which make the system very rigid. In particular, it is very questionable if the salinity field ever will be in a steady state. The lack of contact with the water table may also be disputed.
- Calibrations - the flow into the tunnel is not calculated but specified for a tunnel front position at 2875 m, which makes the system even more rigid. Comparisons were then made between observed and calculated hydraulic heads in a number of borehole sections. The agreement was quantified in terms of two statistical performance measures, mean error and goodness of fit, none of which is explicitly defined in the report.
- Calibrations - no evaluation of the quality of the calibration at 2875 m is made by comparing with the inflow and drawdowns for a tunnel front position at 3600 m.
- Equivalent conductivity - the novel approach used in the Laboratory Scale model yields a slightly more conductive model domain as compared to the approach used in the Site Scale model. The net increase in hydraulic conductivity in the NS-direction is approximately 30% and in the vertical direction approximately 7%.

As stated the boundary conditions for the Laboratory Scale model came from the Site Scale model. The Site Scale model is an intermediate-resolution flow model, which encompasses the isle of Äspö and its close surroundings. The modelling approach for deriving grid cell conductivity values, however, is quite different in the Site Scale model as compared to that used in the Laboratory Scale model. The only feature that is common is the treatment of deterministic hydraulic conductors. Since the main body of the flow treated within the numerical models is tied to the deterministic features, it is no surprise that the two models yield approximately the same results.

The use of solely steady state solutions of flow and salinity may prohibit a good calibration of the rock mass between the major fracture zones. Further, such use is an assumption that is not necessarily warranted although the present-day shoreline displacement process is very slow. In particular, it is worrying that the flow and salinity fields around the Äspö tunnel are modelled at steady state only. It should be noted that the Site Scale model results are dependent on the used boundary conditions, for instance:

- The groundwater levels on the isle of Äspö are very sensitive to the net infiltration specified on the upper boundary.
- The flow into the tunnel affects the boundaries on all sides of the model domain of the Site Scale model.



Further, the pressures and salinities on the vertical sides and the bottom side of the Site Scale model are obtained from the steady state solution of the Regional Scale model. Hence ignoring the fact that the latter model uses twice as large net infiltration as the Site Scale model, 200 [mm/year] instead of 100 [mm/year]. Further, the mean rock mass hydraulic conductivity is on the average more than five times as conductive in the Regional Scale model,  $1.34\text{E-}07$  [m/s] vs.  $2.41\text{E-}08$  [m/s], as in the Site Scale model. One argument for this setting is that the concept of rock mass on a regional scale incorporates local fracture zones. However, since the rock mass in the Regional Scale model is assumed isotropic this means that local zones are omnidirectional, which is not the case according to the Site Scale model.

The results of the numerical groundwater flow model show a strong dependency of the deterministic structures in the conceptual model used. Especially of the deterministic hydraulic conductors NNW1, 2, and 7 from Äspö96 together with the geological zone NNW4. These features are all described as crossing the entire tunnel spiral and are therefore all directly affected by the drawdown. Since the hydraulic conductors NNW1, 2, and 7 from Äspö96 are described as 10 metre wide features, they yield a broad and site specific drawdown that may cause an uncertainty in siting less effected domain within the spiral. The main concern is that volumes in between these features are believed to be less effected domains, this especially since these hydraulic conductors have little or no geological significance. Results of this kind are worrisome since a fracture network probably dominates within the tunnel spiral domain. This fracture network is partly dominated by clusters of hydraulically fractures which have two dominant strike directions one in a west-north-westerly direction and another in a north-north-westerly direction, however little is known of the extension and connectivity pattern of these clusters of fractures.

The belief in a hydraulic dominance of the defined deterministic structures leads to a treatment of the background hydraulic conductivity field that may cause conceptual errors. The hydraulic field test have yielded a background hydraulic conductivity at a 5 metre scale that is highly anisotropic and significant large at least for structures in the north-west direction (approximately  $3.0\text{E-}07$  [m/s]). The hydraulic conductivity in this latter direction is not far from being equivalent with the transmissivity values for the deterministic structures.

Before the tunnel was constructed the hydraulic boundaries surrounding the isle of Äspö were most likely controlled by a hydrostatical behaviour yielded by the Baltic Sea. However, the strong drawdown indicates that many of the geological zones cause a drawdown that extends all the way out under the Baltic Sea. Some chemical interpretations have been presented that further indicate that the drawdown may extend all the way to surrounding land areas, such as Ävrö and the mainland at Laxemar and Simpevarp. Therefore it may for the present be a significant error to set the boundary conditions for Äspö as controlled by hydrostatic conditions yielded by the Baltic Sea.

The positions of the high salt concentrations in the presented results show a slight discrepancy in relationship to the positions of the maximum drawdowns. This may be due to the boundary conditions, however as these are hard to assess due to the fixed values from the Site Scale model, interpretations are limited. Based on the presented illustrations the salt concentrations in NNW4 the tunnel seems to yield large flows from the bottom boundary. However, since this boundary has fixed salt concentrations no increased salt upconing from deeper parts is allowed. Therefore the drawdowns and salinity within the Site Scale model at all time control the established salt concentrations and associated positions within the Laboratory Scale model.



## 7 The Äspö HRL site hydrogeological descriptive model results

The description below comprises hydraulic properties for the essential geometrical units and present day boundary conditions at Äspö valid for the Äspö02 Model domain. The geometrical units in the hydrogeological description are: Hydraulic Conductor Domains (HCD), Hydraulic Rock Domains (HRD), and Hydraulic Soil Domains (HSD) (Section 6.2).

### 7.1 Hydraulic Conductor Domains (HCD)

The hydraulic properties within the Hydraulic Conductor Domains (HCDs) are represented by constant values. No spatial models for stochastic distribution of properties within each conductor are proposed. However, the values should be treated with care, since they are highly subjected to uncertainties since the majority of these features are tested with few or even no hydraulic tests. Regional HCDs should if possible be based on the regional descriptions in /Rhén et al., 1997a/.

Geometrical descriptions of the centre line of the defined hydraulic conductors is found in /Berglund et al., 2003/. The geometry is given in Figure 6-2 and the hydraulic conductivities are summarised in Table 6-1.

### 7.2 Hydraulic Rock Domains (HRD)

The definition of hydraulic parameters for Hydraulic Rock Domains is subjected to many uncertainties due to, among other factors, the statistical significance of the available data. Therefore different approaches may be equally significant. Based on the developed geological rock block model /Berglund et al., 2003/ and scrutinised the hydraulic descriptions for the same block it is concluded that most blocks are impossible to separate but are equally well described by one statistic description.

Therefore the description of the properties is made in only two alternatives:

- One porous media statistical description (Stochastic Continuum, SC) for the entire Äspö02 Model domain.
- Statistical distributions of transmissivity and fractures in a Discrete Fracture Network (DFN) description.

#### 7.2.1 SC description of HRD

The available primary data on hydraulic conductivity are for most usage strongly biased due to experimental objectives and used methodologies. Based on a critical review /Lanyon, 2003/ suggests that the only available data sets in SICADA that are as unbiased as possible are the probe boreholes and possibly also most parts of the surface boreholes (statistics for these two datasets are presented in the Appendices 1 and 2).

The hydraulic characteristics of the bedrock in hydraulic rock domains are strongly coupled with the structural geology. The only method available to capture this kind of extreme heterogeneity is to use an anisotropic hydraulic conductivity tensor. The scale dependency of the hydraulic conductivity values is treated by the proposed regression formulas formulated in /Rhén et al., 1997a/ and presented in Table 5-2. However for small-scale cases the standard deviation should be larger than proposed by the regression formulas, approximate standard deviation values could be inferred from Figure 5-2.

Matrix rock is at Äspö reasonable permeable and a background hydraulic conductivity value of approximately  $1\text{E-}12$  [m/s] should be used. That is the effective hydraulic conductivity for a defined block, what ever the modelled scale, should not be lower than this matrix rock hydraulic conductivity.

**Table 7-1 Anisotropic hydraulic conductivity values [m/s] (scale equals 30 metres). Values based on probe hole investigations and surface borehole investigation.**

Domain	Vertical plane, 130°	Vertical plane, 40°	Horizontal plane
Äspö02	3E-07	2E-09	4E-09

The specific storage values for the rock mass are inferred from a linear regression on data presented in Figure 5-7 (Appendix 3). Both the illustrated results in Figure 5-7 and scoping theoretical calculations support a lower bound for the specific storage of approximately  $1\text{E-}09$  [1/m]. There is little support for any scale dependency in this relationship between the specific storage and the hydraulic conductivity; further the standard deviation seems constant about 1.5 for the logarithmic values.

**Table 7-2 Anisotropic specific storage values [1/m] (scale equals 30 metres). Values based on probe hole investigations and surface borehole investigation.**

Domain	Vertical plane, 130°	Vertical plane, 40°	Horizontal plane
Äspö02	7E-07	4E-08	6E-08

## 7.2.2 DFN approach for HRD description

Three hydraulically active fracture sets have been defined /Berglund et al., 2003/ within the hydraulic rock domains of the Äspö02 model. However, due to project decisions the DFN model parameters were not fully evaluated (modelled). Hence the presented statistical parameter values for orientation, spatial distribution, and intensity that are compiled and presented in Table 7-3 are taken from /Stigsson et al., 2001/ and /Follin & Hermansson, 1996/. These statistics are based on measurements in the sub-volumes (the Prototype Repository and the TBM region) of the Äspö02.

**Table 7-3 Geometrical properties for evaluated natural fractures from /Stigsson et al., 2001/ assumed representative for the hydraulic rock domains of the Äspö02 model domain.**

Fracture set	Distribution	Strike (°)	Dip (°)	$\kappa$
1	<i>Fischer</i>	213	84	4
2	<i>Fischer</i>	127	87	11
3	<i>Fischer</i>	18	8	9

**Table 7-4 Spatial properties for evaluated natural fractures from /Stigsson et al., 2001/ assumed representative for the hydraulic rock domains of the Äspö02 model domain.**

Fracture set	Location model	Conductive intensity, P32
All	Poisson distributed Enhanced Baecher	0.71

Hydraulic characteristics for the fractures within the different fracture sets should be assigned so that the equivalent continuum values matches the anisotropic values presented in Table 7-1 and Table 7-3.

### 7.3 Hydraulic Soil Domains (HSD)

The mapped Quaternary deposits are shown in Figure 4-4. Very little is known about soil depth apart from being in general thin.

At Äspö the main Quaternary deposits are located along topographical depressions, which with no known exception are composed of at least one layer of clay. The thin till and the clay layers inhibit rather than enhance the possible infiltration of ground water into the bedrock. It is therefore proposed that no HSDs are to be used in the Äspö02 model.

### 7.4 Boundary Conditions

The following sub-chapters represent a compilation of information stated in Section 1 together with additional comments and recommendations.

#### 7.4.1 Air temperatures and precipitation

The mean air temperature varies between approximately 0°C in January to approximately 16°C in July.

The corrected annual mean precipitation for Oskarshamn is 681 mm for the period 1991-2000. Approximately 20% fall as snow. The driest period is January-May with a mean around 40 mm/month. The period between June and December has a monthly mean precipitation around 65 mm.

#### 7.4.2 Drainage basins

Drainage basins at Äspö are presented in Figure 4-4.

#### 7.4.3 Recharge and discharge

Watercourses and peatlands illustrated in **Fel! Hittar inte referenskälla.** indicate discharge areas at the Äspö02 Model area; however these hydrology features are at Äspö all underlaid by low-permeable soils and represent local surficial drainage system. Therefore the rest of the available land-surface can be considered as recharge areas; but also the soil covered bedrock can be considered as recharge areas at least while the figures for deep groundwater recharge is considered.

The evaluated actual annual evapotranspiration at Äspö is approximately 450 mm/year.

Little knowledge of the deep groundwater recharge is available for Äspö. Values from northern Äspö indicate that the recharge is at least 15 mm/year (approximated over a drainage basin). These experimental values further indicate that a deep drawdown has little affect on the actual deep groundwater recharge, which in this case seems conditioned by the infiltration capacity of the bedrock.

Numerical groundwater flow models have indicated that a deep groundwater recharge with the tunnel present needs to be approximately 150 mm/year in order to reach the interpolated water table of present day. However, this figure is among other assumptions based on constant hydrostatic boundary conditions surrounding the isle of Äspö.

#### 7.4.4 Water table

Very few observations in the model area are available. These indicate that the water table, as generally found under natural conditions without the tunnel, roughly follows the topography (Figure 4-5) with a maximum elevation around 4 metres.

The same measurement locations indicate that the tunnel has caused a water table dominated by a drawdown cone at the western part of the spiral. The interpolated water table (Figure 7-1) has a minimum elevation of approximately 60 metres. Additionally, the measurements indicate that the water table is almost unaffected north of the geological EW1 structure.

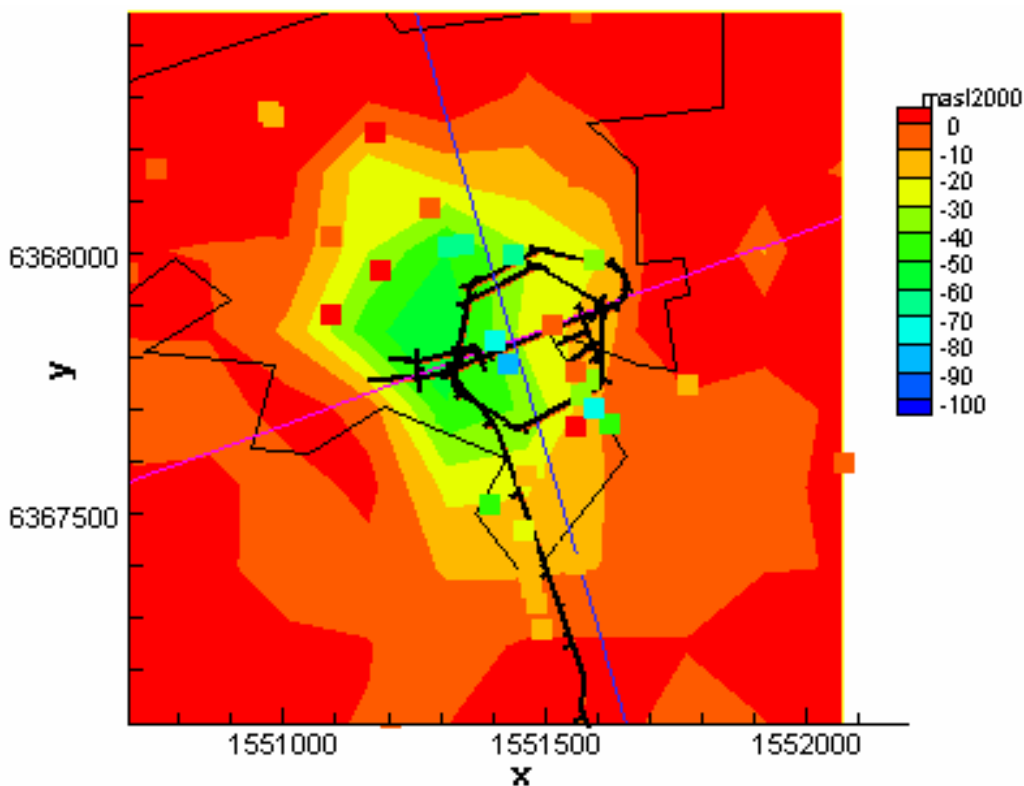


**Figure 7-1** Water table at year 2000 based on interpolated pressure measurements in surface boreholes at the isle of Äspö. Squares represent the local measurement value.

#### 7.4.5 Baltic Sea level variation and salinity

The presented monthly sea level statistics indicate that the sea level varies with  $\pm 1.0$  metre during winter and  $\pm 0.5$  metres in summer. On a shorter time scale variations on the centimetre scale are possible.

A mean value on the salinity in the Baltic Sea fringing the isle of Äspö is approximately 6 grams per litre.

#### 7.4.6 Vertical boundaries

For simulations of the natural conditions, without the tunnel, at Äspö the Baltic Sea can be used as steady hydrostatic boundary conditions. The salinity can be defined by the relationship for  $s(z)$  presented in Table 7-6.

For simulations with the tunnel present the use of nested numerical models is recommended. The boundaries for these models should be set at such distance so that no disturbance of the boundaries can be observed at and close around Äspö. The regional scale boundaries could be set to hydrostatic for Baltic Sea boundaries and no flow boundaries on the distant mainland. Salinity profiles for the regional scale can be defined by the relationship for  $s(z)$  presented in Table 7-6.

Additional information on salinity may be found in Hydrogeochemical reporting on Äspö e.g. /Laaksoharju, 2003b/.

**Table 7-5 The prescribed salinity distribution in relationship with depth based on measurements at Äspö and Laxemar. Taken from /Svensson, 1997b/ see also /Rhén et al., 1997a/.**

Salinity	Relationship, $z$ = depth
$s_1(z)$	$= 0.60 + 0.0017 \cdot z$
$s_2(z)$	$= -11.42 + 0.0121 \cdot z$
$s(z)$	$= \text{MAX}(S_1(z); S_2(z))$

#### 7.4.7 Bottom boundary

For bottom boundary a no flow situation is recommended. It is however not recommended using models with depth below 1000 metres in order to avoid significant boundary effects on flow. This figure assumes that the groundwater is subjected to salinity stratification and that the modelled time scale is such that no great climatic boundaries such as ice sheet loads are available /Svensson, 2003/. Further it is also recommended to avoid models deeper than 1500 metres, if no temperature dependence is included, in order to avoid significant viscosity effects on the flow calculations. However, it is for every different scope and objective important to validate the chosen boundaries by sensitivity studies /Follin, 2003/.

#### 7.4.8 Tidal effects

Earth tidal affects the piezometric pressure responses but generally the amplitude is confined within  $\pm 0.1$  metres.

## 7.5 Groundwater flow pattern according to numerical simulations

Extremely simplified large-scale regional groundwater flow models - on the scale of hundreds of kilometres - yield that the entire Swedish coastal area is a discharge area with an upward flowing regional groundwater flux /Voss & Provost, 2001/. However, as soon as local topography, fracture zone geometry, and chemical groundwater stratification are accounted for these kind of large-scale regional groundwater flow diminish and instead the flow regimes are dominated by smaller flow-cells on the scale of a couple to tens of kilometres /Voss & Provost, 2001/ and /SKB, 2003/.

Therefore it is concluded that the results from a regional groundwater model covering the scale of 100 square kilometres (10 · 10 km) /Svensson, 1997b/ is large enough for illustrations of the regional groundwater flow pattern around the isle of Äspö. Based on /Svensson, 1997b/ no groundwater flow generated at the mainland reaches the isle of Äspö except for a small portion distributed along the main regional fracture zones.

The groundwater flow pattern on the Äspö02 model domain scale, is exemplified with the results from the Laboratory Scale model /Svensson, 1999/. As seen in Figure 7-2 the groundwater flow pattern is controlled by the drawdown caused by the tunnel but also that the flow field is dominantly located along connected major structures, that is the predefined deterministic hydraulic conductors.

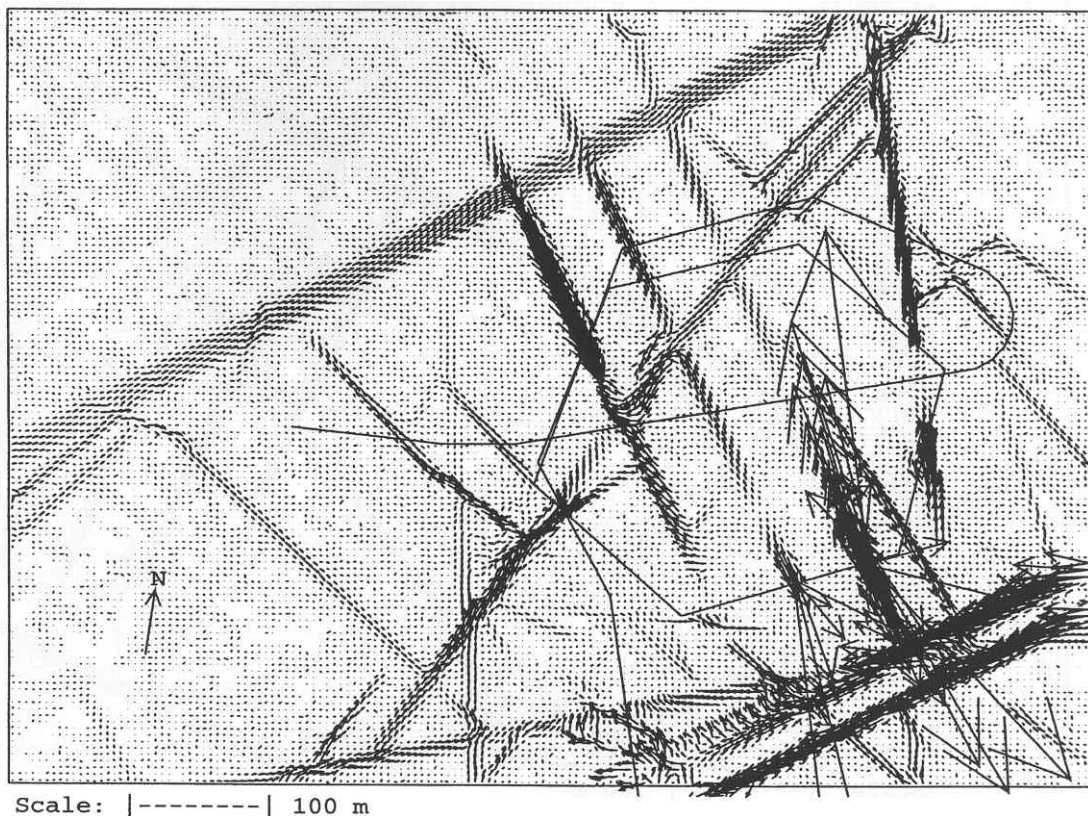


**Figure 7-2** Horizontal flow at a depth of 300 metres below ground level /Svensson, 1999/.

Darcy velocity scale:  $\longrightarrow 5 \times 10^{-7} [m/s]$ .



## **8 Concluding remarks and overall assessment of uncertainties in the hydrogeological description**

This report may be used as a stand-alone hydrogeological 3D conceptual model.

Äspö02 does in many parts differ significant from the Äspö96 model. Unfortunately many of the indications that support these differences have not been possible to validate due to project limitations. However, the indications are strong and also the suggested changes are complex developments of the conceptual model compared to the Äspö96 model. Some of the model differences come from different views of the geological model; this may of course be differences in individual interpretations but also the results of a hard-working group of geologists attempt to prove a theory right or wrong.

Some of the differences are also part of major conceptual uncertainties that are more thoroughly discussed in the following.

### **8.1 Uncertainties in the primary data**

Much of the primary data is stored in the database SICADA. SICADA contains data on transmissivity, storage, yield, etc.; however nothing on how the data has been earlier interpreted. Further it has been observed that even though the treatment and sorting of primary data were performed equal for äspö02 as for Äspö96 the results turns out different. The reason/reasons for this discrepancy is impossible to specify. However, the most likely reason is that not all data has been stored in SICADA. Also the treatment of truncation limits and similar statistical problems are not well documented in the different reports.

The site specific and experimental objectives create different biases, which all are hard to assess. Further the presence of the tunnel and hence disturbed pressure fields together with forced experiments and multiple ongoing events make most of the hydraulic tests uncertain. A rough estimate may be that all but the early core boreholes tests from the surface and hopefully the probing boreholes in the tunnel front is too biased to be used in significant analyses.

The conceptual importance of scale and its influence on evaluated parameters makes many of the small scale (~ below 10-30 metres) tests uncertain (many of the early surface boreholes are below these scales). Hence all of the scale dependant characteristics in these small-scale regions are possibly dangerous to use since it may significantly under-estimate the flow properties of the bedrock. Similar conceptual problems may result from the ignorance of saturation conditions as well as boundary condition within the tested rock volumes.

## 8.2 Uncertainties due to scale dependant descriptions

At a site such as Äspö HRL the detailed knowledge is sometimes extensive; therefore specific domains are sometimes well described. One example of this kind of domains is the True Block Scale site. The experimental objectives and the extensive time period for the True BS experiment have created a detailed knowledge of the rock mass from the site scale (of an approximately 50-metre cube) down to local characteristics within individual fractures.

The objectives of True BS experiment and the delimited site scale have allowed a discrete fracture approach for the True BS 3D site descriptive model. However, even within such a limited site scale approximations and simplifications have been allowed within the interpolated volume and extrapolated knowledge is only briefly performed and does implicitly contain uncertainties. Therefore, a detailed knowledge such as for the True BS site does not imply a detailed knowledge over other domains of similar scale. But, a detailed knowledge over a smaller scale does support both larger scale knowledge and uncertainties of fracture geometry and characteristics.

Additional problems in site descriptions come from the scale dependent definitions of a structure. For a larger scale model such as Äspö96 and Äspö02 a deterministic structure is of the scale of tenths to hundreds of metres, while a smaller scale model such as the True BS site model defines structures of the scale metres to tenths of metres. Similarly the larger scale structures are normally defined by hydraulic characteristics of the order of  $1E-05$  [ $m^2/s$ ] for the transmissivity while the smaller scale models contain structures with transmissivity values around  $1E-08$  [ $m^2/s$ ].

## 8.3 Over-all dependence in the result on conceptual boundary conditions

The older conceptual model, Äspö96, is presented with hydrostatic boundary conditions under the Baltic Sea. However, there are now at least some indications that a hydrostatic boundary condition, caused by the present of the Baltic Sea, is not a realistic assumption and this kind of assumptions need further investigation, primary in the areas presented below.

- Studies on hydrochemical signatures of the tunnel inflow waters have concluded that more meteoric water is discharged from the tunnel than what would be possible from purely Äspö surface recharge. It was a project wish that the hydrogeochemical report should produce results on water characteristics along the tunnel chainage, so that it would be possible to define amounts of the different water types coming into the tunnel at different locations and especially from fracture zones. However, this far, these types of hydrogeochemical results have not been presented. Therefore, the role of fracture zones in transporting meteoric waters from fringing mainland and isles must unfortunately stand untested.
- Due to the probable behaviour with meteoric water transportation within the fracture zones extending away from the isle of Äspö. The hydrogeological characteristics of the Baltic Sea seabed materials, which at least conceptual previously have been assumed more or less impermeable, must be put into a more rigid investigation.

The important hydrological output from a surface boundary is the deep groundwater recharge. This variable is governed by factors such as precipitation and specific discharge but also important are topography and surficial hydrogeological characteristics, both unsaturated and saturated. For most purposes the precipitation is well enough known but the unknowns in a defined specific discharge are many. The specific discharge often varies locally and therefore the deep groundwater recharge is hard to assess. Further the effect on the deep groundwater recharge from variations in the suction created by the distance to the groundwater table is mostly unknown.

Probing investigations on the effect on deep groundwater recharge due to an artificial drawdown are being performed /Graffner, 2003/ however the results are still few and in parts hard to validate. However, it is in general assumed that an extensive drawdown causes an increased deep groundwater recharge. This assumption may however be erroneous since for much of the bedrocks the infiltration capacity is already used; and regions where more water could infiltrate are often sealed with a tight material such as clays.

In the older model, Äspö96, figures on deep groundwater recharge from 0.5 [mm/year] (natural) to approximate 130 [mm/year] are presented. Both these figures seem to be at the extreme bounds for the recharge. Even though the deep groundwater recharge puts a significant constraint on the numerical groundwater model results, it is in most an unknown variable. The knowledge on spatial patterns as well the actual amount of recharge need further attendance before local understanding on flow patterns and pressure distribution could be drawn from the results of numerical groundwater models.

Salinity profiles also put a significant constrain on the numerical groundwater model results. Prescribed salinity profiles are conserved at the boundary even if the flow and pressure situations at the boundary are such that a change in salinity is to be expected. This places a great conceptual uncertainty in understanding numerical results if not the boundaries are validated and tested for stabile conditions. This kind of salinity conservation may for instance create a discrepancy between hydraulic and salinity anomalies (sinks).

#### **8.4 Over-all dependence in results on conceptual deterministic structures**

A 3D site descriptive hydrogeological model is for most parts a continuous porous media description; defined by domains of either rock masses or conductors. In many perspectives it could be useful to view a 3D descriptive model from a discrete fracture approach. However, this latter approach has its drawbacks as well as the former porous media approach has its drawbacks. Not least from the necessity of 3D visual understanding the porous media approach is preferable; this may change with time since more and more hydrogeologists being trained in a discrete approach.

However, at present, both a porous media as well as a discrete fracture approach demand certain decisions to be made. Within the GeoMod project one of the decisions was based on the integrated necessity that a deterministic hydrogeological conductor must coincide with a geological feature. Therefore if a preliminary feature could not be significantly verified within one subject it could not be viewed as a final feature within the model.

In the Äspö96 model /Rhén et al., 1997a/ a NNW trending drawdown behaviour were concluded as the results of NNW hydraulic conductors crossing over the tunnel spiral. In Äspö02 these structures are recognised along local tunnel sections within the spiral as clusters of hydraulic fractures. However, the extension and also the direction of the individual fractures within these clusters could not be vindicated as belonging to NNW hydraulic conductors but are instead viewed as a part of the dominant hydraulic NW fracture set. This fracture set may be interconnected by either splays within the set or by a less dominant fracture set trending NE. Either way the NW trending fracture set, together with inter-connective structures would create drawdown behaviour much like the one recognised in both the Äspö96 model, as well as in the new Äspö02 model.

The above described individual treatment of some of the fractures and structures causes an antropogenic introduced uncertainty in prognoses of both flow and concentrations as well as in many other areas of interest. This is clearly illustrated by the importance of these deterministic structures in the flow descriptions that are results from individual numerical groundwater flow models. Therefore if these kinds of models are used for predictions of e.g. hydraulic pressures at an unknown location in the bedrock; it is crucial to the results if this region of the bedrock coincide with a deterministic structure or not.

## 9 References

**Alm P., 1999.** Hydro-Mechanical behaviour of a pressurised single fracture, An in-situ experiment. Doctorial Thesis, Chalmers University of Technology, Göteborg, Sweden.

**Andersson J., Berglund J., Follin S., Hakami E., Halvarson J., Hermanson J., Laaksoharju M., Rhén I., Wahlgren C-H., 2002a.** Testing the methodology for site descriptive modelling, Application for the Laxemar area. SKB TR-02-19, Svensk Kärnbränslehantering AB.

**Andersson P., Dershowitz B., Doe T., Hermanson J., Meier P., Tullborg E-L., Winberg A. (ed), 2002b.** Final report of the TRUE Block Scale project, 1. Characterisation and model development. SKB TR-02-13, Svensk Kärnbränslehantering AB.

**Berglund J., Curtis P., Eliasson T., Olsson T., Starzec P., Tullborg E-L., 2003.** Äspö HRL Update of the geological model 2002. SKB IPR-03-34, Svensk Kärnbränslehantering AB. (Draft versions and personal communication)

**Carlsson A., Olsson T., 1993.** The analysis of fractures, stress and water flow for rock engineering projects. *In: Hudson J.A. (ed) Comprehensive engineering, principles, practice & projects. Vol. 2. Pergamon Press, Oxford, pp. 415-437.*

**Eliasson T., 2003.** Personal communication.

**Emsley S., Olsson O., Stenberg L., Alheid H-J., Falls S., 1997.** ZEDEX - A study of damage and disturbance from tunnel excavation by blasting and tunnel boring. SKB TR-97-30. Svensk Kärnbränslehantering AB.

**Ericsson L. O., 2003.** Personal communication.

**Follin S., Hermansson J., 1996.** A discrete fracture network model of the Äspö TBM Tunnel Rock mass, SKB AR D-97-001, Svensk Kärnbränslehantering AB.

**Follin S., Årebäck M., Axelsson C-L., Stigsson M., Jacks G., 1998.** Förstudie Oskarshamn, Grundvattnets rörelse, kemi och långsiktiga förändringar. SKB R-98-55, Svensk Kärnbränslehantering AB (in Swedish).

**Follin S., 2003.** Personal communication.

**Graffner O., 2003.** Groundwater recharge in crystalline bedrock. Licentiate Thesis, Chalmers University of Technology, Göteborg, Sweden (in preparation).

**Gurban I., 2002.** Personal communication.

**Gustafson G., Liedholm M., Lindblom B., Lundblad K., 1989.** Groundwater flow calculations on a regional scale at the Swedish Hard Rock Laboratory. SKB SHRL PR 25-88-17. Svensk Kärnbränslehantering AB.

- Gustafsson E., 2001.** Äspö Hard Rock Laboratory, matrix fluid chemistry experiment, Hydraulic character of the rock matrix. ITD-01-07, Svensk Kärnbränslehantering AB.
- Hakami E., 1995.** Aperture distribution of rock fractures. Doctorial Thesis, Royal Institute of Technology, Stockholm, Sweden.
- Holmén J., 1997.** On the flow of groundwater in closed tunnels. Generic hydrogeological modelling of nuclear waste repository, SFL 3-5. SKB TR 97-10, Svensk Kärnbränslehantering AB.
- Jarsjö J., Gale J., 2001.** Groundwater degassing and two-phase flow in fractured rock: Summary of results and conclusions achieved during the period 1994-2000. SKB TR-01-13. Svensk Kärnbränslehantering AB.
- Laaksoharju M., 2003.** Personal communication.
- Laaksoharju M., 2003b.** Äspö HRL Update of the geological model 2002. SKB IPR-03-36, Svensk Kärnbränslehantering AB. (Draft versions and personal communication)
- Landström O., Aggeryd I., Mathiasson L., Sundblad B., 1994.** Chemical composition of sediments from the Äspö area and interaction between biosphere and geosphere. Arbetsrapport 94-13, Svensk Kärnbränslehantering AB.
- Lanyon G.W., 2003.** Personal communication.
- La Pointe P.R., Wallmann P., Follin S., 1995.** Estimation of effective block conductivities based on discrete network analyses using data from the Äspö site. SKB TR-95-15. Svensk Kärnbränslehantering AB.
- Larsson-McCann S., Karlsson A., Nord M., Sjögren J., Johansson L., Ivarsson M., Kindell S., 2002.** Meteorological, hydrological and oceanographical information and data for the site investigation program in the community of Oskarshamn. SKB TR-02-03, Svensk Kärnbränslehantering AB.
- Maaranen J., Lehtioksa J., Timonen J., Pre-print.** Characterisation of Äspö rock samples with the helium gas method. (Department of physics, University of Jyväskylä, Finland)
- Morén L., Påsse T., 2001.** Climate and shoreline in Sweden during Weichsel and the next 150,000 years. SKB TR-01-19, Svensk Kärnbränslehantering AB.
- Munier R., Follin S., Rhén I., Gustafson G., Pusch R., 2001.** Projekt JADE, Geovetenskapliga studier. SKB R-01-32, Svensk Kärnbränslehantering AB (in Swedish).
- Oda M., Saitoo T., Kamemura K., 1989.** Permeability of rock masses at great depth. *In: Maury & Fourmaintraux (eds), Rock at great depth, 449-455, Balkema.*
- Påsse T., 1997.** A mathematical model of past, present and future shore level displacements in Fennoscandia. SKB TR 97-28, Svensk Kärnbränslehantering AB.

- Påsse T., 2001.** An empirical model of glacio-isostatic movements and shore-level displacement in Fennoscandia. SKB R-01-41, Svensk Kärnbränslehantering AB.
- Rhén I. (ed), Gustafson G., Stanfors R., Wikberg P., 1997a.** Äspö HRL - Geoscientific evaluation 1997/2 Results from pre-investigations and detailed site characterization. Summary report. SKB TR 97-03, Svensk Kärnbränslehantering AB.
- Rhén I. (ed), Bäckblom G. (ed), Gustafson G., Stanfors R., Wikberg P., 1997b.** Äspö HRL - Geoscientific evaluation 1997/5. Model based on site characterization 1986-1995. SKB TR 97-06, Svensk Kärnbränslehantering AB.
- Rhén I., Forsmark T., 2000.** Äspö Hard Rock Laboratory, High-permeability features (HPF). SKB IPR-00-02, Svensk Kärnbränslehantering AB.
- Rhén I., Forsmark T., 2001.** Äspö Hard Rock Laboratory, Prototype Repository, Hydrogeology, Summary report of investigations before the operation phase. SKB IPR-01-65, Svensk Kärnbränslehantering AB.
- Rhén I., 2003.** Personal communication.
- Rutqvist J., 1995.** Coupled stress-flow properties of rock joints from hydraulic field testing. Doctorial Thesis, Royal Institute of Technology, Stockholm, Sweden.
- SKB, 2001.** Site investigations: Characterisation methods and general execution programme. SKB TR-01-29, Svensk Kärnbränslehantering AB.
- SKB, 2003.** Grundvattnets regionala flödesmönster och sammansättning - betydelser för lokalisering av djupförvaret. R-03-01, Svensk Kärnbränslehantering AB.
- Sundblad B., Mathiasson L., Holby O., Landström O., Lampe S., 1991.** Chemistry of soil and sediments, hydrology and natural exposure rate measurements at the Äspö Hard Rock Laboratory. SKB PR 25-91-08, Svensk Kärnbränslehantering AB.
- Svensson U., 1987.** Hydrological conditions in the Simpevarp area. SKB PR 25-87-09, Svensk Kärnbränslehantering AB.
- Svensson U., 1997a.** A site scale analysis of groundwater flow and salinity distribution in the Äspö area. SKB TR 97-17, Svensk Kärnbränslehantering AB.
- Svensson U., 1997b.** A regional analysis of groundwater flow and salinity distribution in the Äspö area. SKB TR 97-09, Svensk Kärnbränslehantering AB.
- Svensson U., 1999.** A laboratory scale analysis of groundwater flow and salinity distribution in the Äspö area. SKB TR-99-24, Svensk Kärnbränslehantering AB.
- Svensson U., 2003.** Personal communication.
- Stigsson M., Outters N., Hermansson J., 2001.** Äspö Hard Rock Laboratory Prototype Repository Hydraulic DFN model no:2. SKB IPR-01-039, Svensk Kärnbränslehantering AB.

- Uchida M., Doe T., Derschowitz W., Wallmann A.T.P., Sawada A., 1994.** Discrete-fracture modelling of the Äspö LPT-2, Large-scale pumping and tracer test. SKB ICR-94-09. Svensk Kärnbränslehantering AB.
- Vidstrand P., 1998.** Previously unpublished field data from the La Scala experiment. Äspö HRL in the spring 1998.
- Vidstrand P., 1999.** Hydrogeological scale effects in crystalline rocks, Comparison of field data from Äspö HRL with data from predictive upscaling methods. Licentiate Thesis, Chalmers University of Technology, Göteborg, Sweden.
- Voss C.I., Provost A.M., 2001.** Recharge-area Nuclear Waste Repository in Southeastern Sweden, Demonstration of Hydrogeologic Siting Concepts and Techniques. SKI Report 01:44. Statens Kärnkraftsinspektion.
- Wei Z.Q., Egger P., Descoeurdes F., 1995.** Permeability predictions for jointed rock masses. Int. J. Rock Mech. Min. Sci. & geomech. Abstr., Vol. 32, No. 3, 251-261.



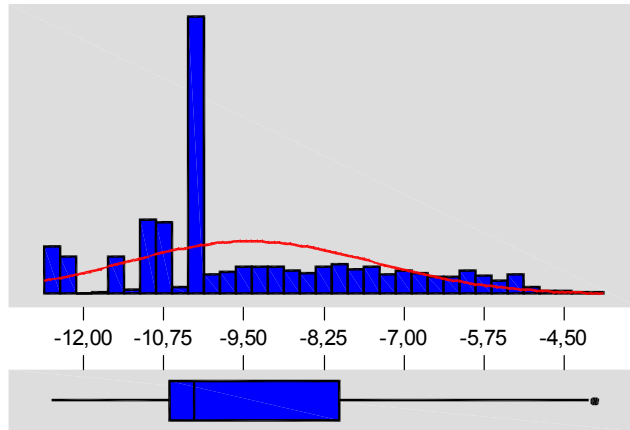
# Appendices

<b>Appendix 1</b>	<b>Statistics for KAS boreholes from the SICADA database, 3 metres sections</b>	<b>93</b>
<b>Appendix 2</b>	<b>Statistics for probe boreholes from the SICADA database</b>	<b>95</b>
<b>Appendix 3</b>	<b>Linear regression: Specific storage-hydraulic conductivity</b>	<b>97</b>

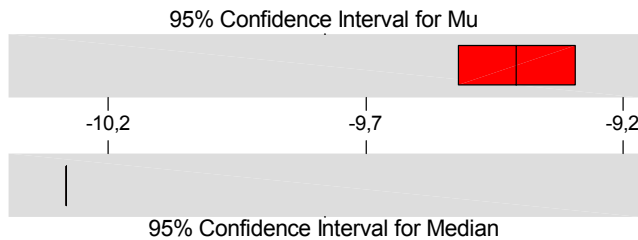


# Appendix 1

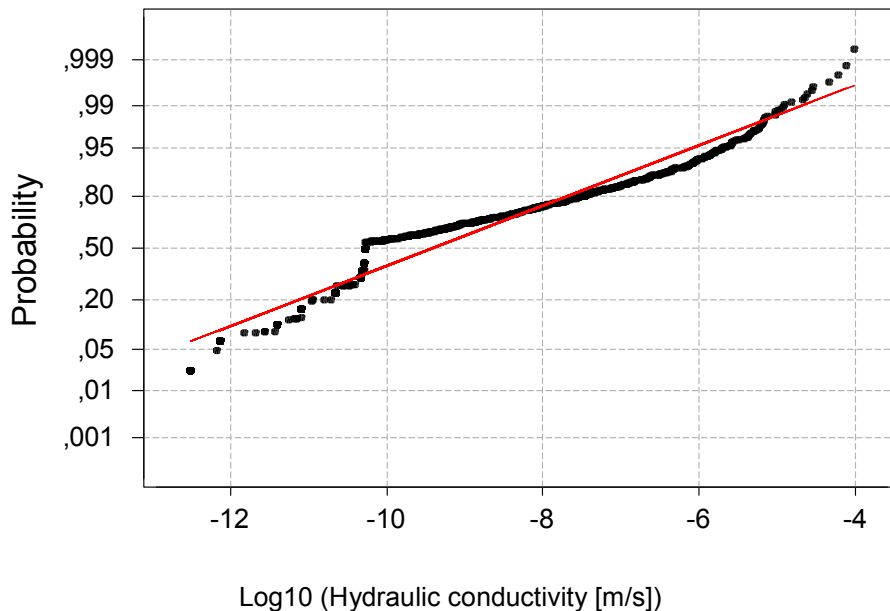
## Statistics for KAS boreholes from the SICADA database, 3 metres sections



Mean	-9,40671
StDev	1,94060
Variance	3,76594
Skewness	0,640106
Kurtosis	-4,2E-01
N	1113
Minimum	-12,5086
1st Quartile	-10,6576
Median	-10,2798
3rd Quartile	-8,0193
Maximum	-4,0088
95% Confidence Interval for Mu	-9,5208 -9,2926
95% Confidence Interval for Sigma	1,8632 2,0248
95% Confidence Interval for Median	-10,2798 -10,2798



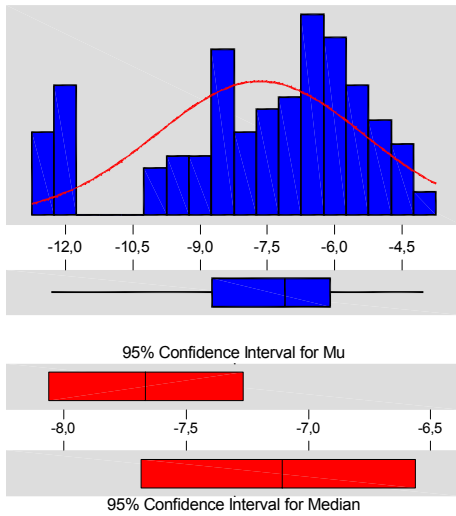
Descriptive statistics, Log10 (Hydraulic conductivity [m/s]), for reported KAS boreholes excluding measurement limit values.



Normal probability plot for reported KAS boreholes excluding measurement limit values. Kolmogorov-Smirnov normality test, approximate P-value: < 0.01.



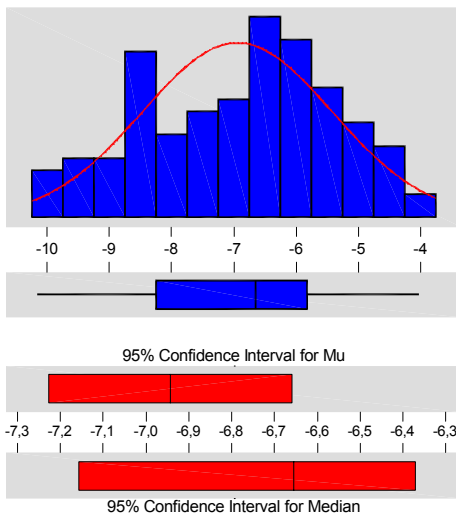
### Statistics for probe boreholes from the SICADA database



Mean	-7,66680
StDev	2,30381
Variance	5,30753
Skewness	-7,4E-01
Kurtosis	-3,4E-01
N	131

Minimum	-12,3118
1st Quartile	-8,7404
Median	-7,1078
3rd Quartile	-6,1024
Maximum	-4,0280

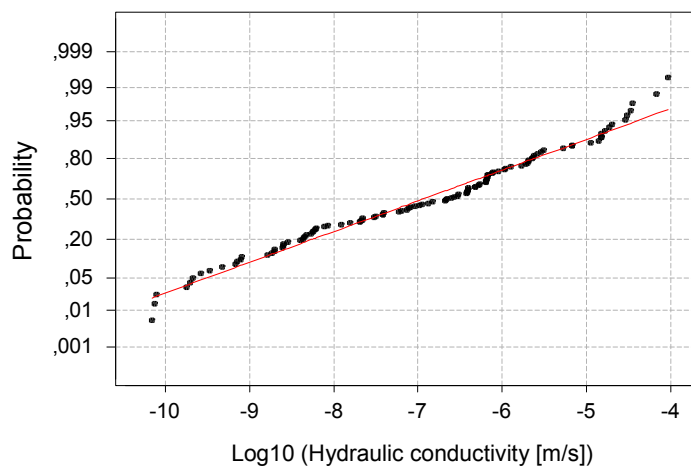
Descriptive statistics, Log10 (Hydraulic conductivity [m/s]), for reported probe boreholes.



Mean	-6,94413
StDev	1,52473
Variance	2,32482
Skewness	-2,3E-01
Kurtosis	-7,8E-01
N	113

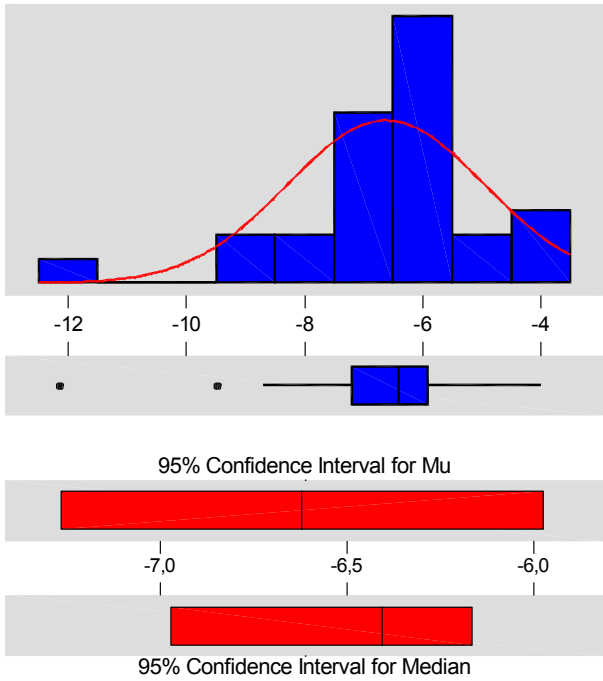
Minimum	-10,1567
1st Quartile	-8,2455
Median	-6,6548
3rd Quartile	-5,8290
Maximum	-4,0280

Descriptive statistics, Log10 (Hydraulic conductivity [m/s]), for reported probe boreholes excluding measurement limit values.



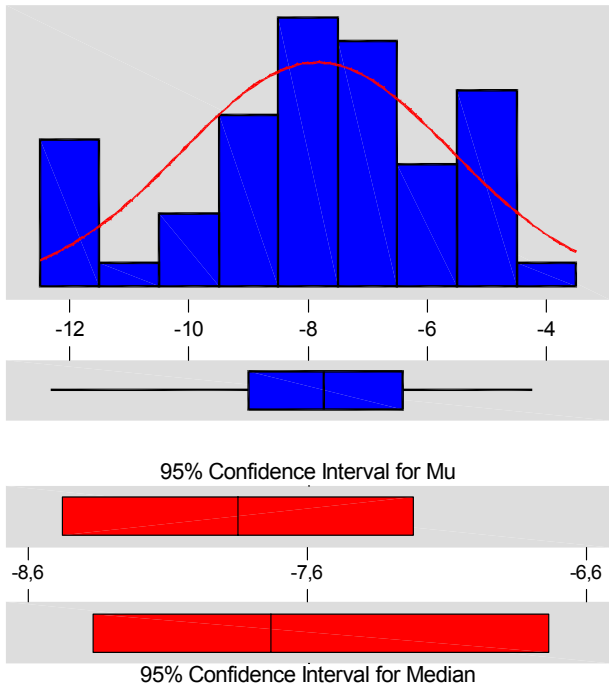
Normal probability plot for reported probe boreholes excluding measurement limit values.  
Kolmogorov-Smirnov normality test, approximate P-value: 0.019.

**Probe boreholes, sorted for structures with a strike between 120 and 140.**



Mean	-6,62004
StDev	1,66626
Variance	2,77643
Skewness	-1,24806
Kurtosis	3,57962
N	28
Minimum	-12,1303
1st Quartile	-7,2024
Median	-6,4058
3rd Quartile	-5,9079
Maximum	-4,0000
95% Confidence Interval for Mu	-7,2662 -5,9739
95% Confidence Interval for Sigma	1,3174 2,2680
95% Confidence Interval for Median	-6,9721 -6,1669

**Probe boreholes, sorted for structures with a strike between 20 and 80.**



Mean	-7,84954
StDev	2,26245
Variance	5,11867
Skewness	-4,9E-01
Kurtosis	-4,0E-01
N	52
Minimum	-12,3096
1st Quartile	-9,0029
Median	-7,7297
3rd Quartile	-6,4148
Maximum	-4,2441
95% Confidence Interval for Mu	-8,4794 -7,2197
95% Confidence Interval for Sigma	1,8960 2,8057
95% Confidence Interval for Median	-8,3676 -6,7345

Linear regression: Specific storage-hydraulic conductivity

$$S_s = -2.374 + 0.79 K$$

Values taken from hydraulic investigations during the Prototype Repository Experiment.

